

Development of a nano-adjuvant cancer vaccine and its evaluation for melanoma in combination with radiotherapy

THÈSE N° 8844 (2018)

PRÉSENTÉE LE 31 AOÛT 2018

À LA FACULTÉ DES SCIENCES DE LA VIE

LABORATOIRE DE RECHERCHE INTÉGRATIVE DU SYSTÈME LYMPHATIQUE ET DU CANCER
PROGRAMME DOCTORAL EN CHIMIE ET GÉNIE CHIMIQUE

ÉCOLE POLYTECHNIQUE FÉDÉRALE DE LAUSANNE

POUR L'OBTENTION DU GRADE DE DOCTEUR ÈS SCIENCES

PAR

Sylvie HAUERT

acceptée sur proposition du jury:

Prof. K. Severin, président du jury
Prof. M. Swartz, Prof. V. Hatzimanikatis, directeurs de thèse
Prof. P. Romero, rapporteur
Prof. A. Esser Kahn, rapporteur
Prof. H. A. Klok, rapporteur



ÉCOLE POLYTECHNIQUE
FÉDÉRALE DE LAUSANNE

Suisse
2018

Acknowledgements

I would like to start by saying that this thesis would not have been made possible and enjoyable without the support and help of the following people:

Prof. Melody A. Swartz for accepting me in your research group during my master project, although my background is in chemistry, and giving me the opportunity to study a subject in which I have always been interested. I truly believe you are a great mentor, always helping us when we need, and at the same time giving us the liberty to advance our project the way we want to.

Prof. Vassily Hatzimanikatis, for accepting to co-advise me and thus making it possible for me to be able to do research in the laboratory of Prof. Swartz.

My thesis jury, Prof. Pedro Romero, Prof. Aaron Esser-Kahn, Prof. Harm-Anton Klok and Prof. Kay Severin, for accepting to be part of my committee and taking the time to read my thesis, as well as giving feedbacks on it.

Shann, for teaching me how to do research during my master project and having fun while doing it. Moreover, you were always ready to help me in the lab or outside.

Priscilla, although we did not talk so much in Lausanne, the end of my thesis in Chicago was awesome thanks to you. You helped me enormously with my experiments, presentations and the day-to-day life. It was great working with you.

The people in LLCB, thanks for creating such a fun and interesting environment that made me love coming to work every day without having the impression of working. In addition, our outing was always exciting.

The people in Chicago, especially Katharina, Mariastella and Peyman, for always helping me in the lab, creating a welcoming environment and making me laugh.

My husband, Valentin, for being so supportive and understanding when I had to work late, move to Chicago, and who fed me when I didn't have time to cook for myself. This journey would have been impossible without you.

Finally, my family for always being there for me and supporting me in everything I do. I know for certain that I would not be here without the help of Sabine all along my thesis.

Thesis abstract

Cancer is the second leading cause of death in the world and melanoma is the deadliest type of skin cancer. Although surgery, radiotherapy and chemotherapy are still standard treatments, the discovery of the role played by the immune system in cancer has allowed the development of new treatments, called immunotherapies. The goal of these treatments is to help the immune system eradicate cancerous cells, for example by increasing the anti-tumor response of the patient.

In this particular case, the treatment has to activate cytotoxic CD8⁺ and CD4⁺ helper T cells against the cancer cells. This can be done by using subunit vaccines composed of tumor antigens, adjuvants and a delivery system, which will be internalized by dendritic cells (DCs). The vaccine induces the activation of DCs followed by their migration to the lymph nodes, where they will educate T cells against specific antigens. Our laboratory has developed two different delivery systems, nanoparticles (NPs) and polymersomes (PSs) that can enhance the vaccine's immune response by efficiently entering the lymphatic system, due to their size, and drain to the lymph node. Once they reach that location, they will be internalized by DCs and induce an anti-tumor response.

In this thesis, we used these two nanocarriers to create a vaccine composed of different nano-adjuvants capable of activating several toll-like receptors simultaneously and test their efficacy at inducing an anti-tumor response in melanoma. We have developed and characterized the different nano-adjuvants, PS-MPLA, PS-CL075 and NP-CpG-B, and demonstrated, *in vitro*, synergistic effects on DC activation when PS-MPLA + PS-CL075 and PS-MPLA + NP-CpG-B were combined. *In vivo*, we showed the enhanced immune response with the different nano-adjuvant combinations, but only PS-MPLA + NP-CpG-B was able to delay tumor growth in melanoma. We then tested this vaccine in combination with radiotherapy, mimicking a clinical situation. We first demonstrated an enhanced immune response when combining a high irradiation dose, 15 Gy, with the nano-adjuvant vaccine draining the tumor-draining lymph node. Moreover, the vaccination of NP-CpG-B + PS-MPLA and radiotherapy increased mice survival by 17 days compared to mice only receiving radiotherapy.

Overall, we have demonstrated that combining different nano-adjuvants targeting the tumor-draining lymph node, with radiotherapy, enhanced significantly the survival in a melanoma model. This approach is particularly promising since ionizing radiation is a standard treatment in cancer and our vaccine could be applied to a multitude of cancers since it does not contain any antigen and its composition can easily be modified.

Keywords: Cancer, radiotherapy, vaccine, nanoparticles, polymersomes, T cells, dendritic cells, lymph node, toll-like receptors

Résumé de thèse

Le cancer est la deuxième cause de mortalité dans le monde à ce jour, et le mélanome est la première cause de décès pour les cancers de la peau. Bien que la chirurgie, la radiothérapie et la chimiothérapie restent les traitements standards contre le cancer, la découverte du rôle central que joue le système immunitaire dans le cancer a permis le développement de nouveaux traitements, appelés immunothérapies. Ainsi, les immunothérapies ont pour but d'aider le système immunitaire du patient à détruire la tumeur, par exemple en améliorant la réponse immunitaire anti-tumorale du patient.

Dans ce cas particulièrement, le traitement immunothérapeutique doit parvenir à activer des lymphocytes cytotoxiques CD8⁺ et auxiliaires CD4⁺ de type 1 spécifiquement contre les cellules tumorales. Ceci peut se faire entre autres par la création d'un vaccin sous-unité composé d'antigènes du cancer, d'adjuvants et d'un système de distribution adéquat. Suite à l'injection, ce vaccin serait internalisé par les cellules dendritiques (DCs), entraînant leur maturation, leur migration dans les ganglions lymphatiques et l'éducation par les DCs des lymphocytes contre les antigènes. Notre laboratoire a développé deux types de système de distribution visant à améliorer ces vaccins anti-cancer, des nanoparticules (NPs) et des polymersomes (PS), qui grâce à leurs tailles, sont capables d'entrer efficacement dans le système lymphatique et d'être drainées jusqu'aux ganglions où elles sont internalisées par des DCs.

Dans cette thèse, nous utilisons ces deux technologies en combinaison pour créer des vaccins composés de différents nano-adjuvants, capable d'activer conjointement différents récepteurs de type Toll, et testons leur efficacité à induire une réponse anti-tumorale contre le mélanome. Ainsi, nous avons commencé par développer et caractériser les différents nano-adjuvants, PS-MPLA, PS-CL075 et NP-CpG-B, avant de montrer, *in vitro*, l'utilisation combinée des différents nano-adjuvants, notamment de PS-MPLA + NP-CpG-B et PS-MPLA + PS-CL075, pour augmenter la sécrétion de cytokines inflammatoires de façon synergique par les DCs. *In vivo*, nous avons montré que les combinaisons des nano-adjuvants amélioreraient la réponse immunitaire, mais que seulement PS-MPLA + NP-CpG-B permettait de ralentir la croissance de mélanomes. Nous avons ensuite testé ces vaccins en combinaison avec de la radiothérapie, mimant ainsi une situation clinique. Nous avons démontré que la réponse immunitaire pouvait être augmentée lorsqu'une haute dose de radiation, 15 Gy, était combinée avec les nano-adjuvants drainant dans le même ganglion lymphatique que celui du mélanome. De plus, la vaccination de NP-CpG-B et PS-MPLA combinée

à l'irradiation a prolongé la vie des souris de 17 jours par rapport aux souris n'ayant reçu que la radiothérapie.

Globalement, nous avons démontré que la combinaison des différents nano-adjuvants, ciblant le même ganglion lymphatique que la tumeur, avec la radiothérapie, prolonge de façon significative la durée de vie dans un modèle de mélanome. Cette approche est particulièrement prometteuse puisque l'irradiation est un traitement clinique standard et que notre vaccin peut être appliqué à une multitude de cancers du fait de sa composition et de l'absence d'antigène.

Mots-cléfs : Cancer, radiothérapie, vaccin, nanoparticules, polymersomes, lymphocytes T, cellule dendritique, ganglion lymphatique, récepteur de type Toll

Table of Contents

List of abbreviations.....	xi
List of figures	xii
Chapter 1: Motivation, Background and Aims	1
1.1. Motivation	2
1.2. Background	4
Subunit cancer vaccines development	4
Radiotherapy	7
1.3. Thesis aims	9
1.4. Accomplishments	10
Chapter 2: Formulation and Characterization of Adjuvant-based Nanocarriers.....	11
2.1. Abstract	12
2.2. Introduction	13
2.3. Materials and Methods	15
Animals	15
Reagents	15
F127-COOH synthesis	15
Pyridyl disulfide cysteamine • HCl (PDC) synthesis	15
Nanoparticle formation	16
Proteins or molecules conjugation to NPs	16
PEG-b-PPS diblock copolymer synthesis	17
Polymersome formation.....	18
Generation of Bone marrow-derived dendritic cells (BMDCs).....	18
In vitro experiments	18
Flow cytometry	19
ELISA	19
Diffusion coefficient calculation.....	19
Data collection	20

2.4. Results	21
Synthesis and formation of the different nanocarriers	21
Encapsulation of Poly(I:C) was not successful in either nanocarrier	23
MPLA adsorption on nanoparticles and polymersomes	24
Polymersomes encapsulation of the TLR-7/8 agonist, CL075	26
CpG-B adjuvant, TLR-9 agonist, was chemically conjugated to nanoparticles	27
The different diffusion coefficients were not influencing the cell uptake speed and both nanocarriers are endocytosed by macropinocytosis.....	28
2.5. Discussion	30
Chapter 3: Combinatorial in vitro and in vivo screening of adjuvanted-nanoparticulates	33
3.1. Abstract	34
3.2. Introduction	35
3.3. Materials and Methods	37
Animals	37
Cell line	37
Materials, Reagents, and Antibodies.....	37
Generation of Bone marrow-derived dendritic cells (BMDCs).....	37
BMDC activation experiments.....	38
BMDC-CD4 ⁺ or CD8 ⁺ T cell co-culture experiments	38
Tumor inoculation and immunizations	38
Whole organ/tumor processing into single-cell suspensions	39
Ex vivo restimulation	39
Flow cytometry	40
ELISA	40
Data collection	40
3.4. Results	41
Combining PS-MPLA with PS-CL075 promotes synergistic effects on BMDC activation and cytokine production by CD4 ⁺ T cells in vitro	41
The addition of PS-CL075 to PS-MPLA slightly increased the percentage of polyfunctional CD4 ⁺ & CD8 ⁺ T cells but did not reduce tumor growth	44

Combining PS-CL075 with NP-CpG-B induced synergistic effects for TNF α secretion in BMDCs activation as well as CD4 ⁺ T cell cytokine expression, in vitro.....	47
At the dose tested, no enhance in the immune response was observed for the combination of PS-CL075 with NP-CpG-B, in tumor bearing mice.....	50
Although synergistic effects were observed for several PS-MPLA and NP-CpG-B combination in BMDCs activation, it did not translate in a strong T cell activation, in vitro.....	54
A decrease in tumor growth was observed when both adjuvants were co-injected although the T cell immune response was similar.....	57
3.5. Discussion.....	61
Chapter 4: Radiotherapy in combination with an adjuvant-based vaccine delays tumor growth.....	65
4.1. Abstract.....	66
4.2. Introduction.....	67
4.3. Materials and Methods.....	69
Mice.....	69
Cell line.....	69
Materials, reagents and antibodies.....	69
Tumor inoculation and immunizations.....	69
In vivo tumor irradiation.....	70
Whole organ/tumor processing into single-cell suspensions.....	70
Blood processing.....	71
Ex vivo restimulation.....	71
Flow cytometry.....	71
ELISA.....	71
Flow cytometry.....	71
4.4. Results.....	73
The combination of adjuvant vaccination with radiotherapy enhance the T cell immune response and delayed tumor growth.....	73
A decrease in tumor growth and increase in polyfunctional CD8 ⁺ T cells was observed when targeting the non-TdLN.....	76

Intradermal and intratumoral injection induced similar tumor growth and survival	79
Increased production of IL2 in the TdLN was detected when PS-MPLA & NP-CpG-B were co-injected but similar tumor growth was observed for all vaccinated groups	81
Co-injection of PS-MPLA & NP-CpG-B reduced tumor growth and increased overall survival compared to radiotherapy only or NP-CpG-B.	84
4.5. Discussion	86
Chapter 5: Conclusion, Implication and Future prospect	91
5.1. Conclusion.....	92
5.2. Implication and future directions	94
Development of an adjuvanted-cancer vaccine	94
Radiotherapy combination with adjuvanted vaccine	95
References.....	96
Curriculum Vitae.....	104

List of abbreviations

Ar	Argon
APC	Antigen-presenting cells
BMDC	Bone marrow derived dendritic cells
CTL	Cytotoxic T cells
DBU	1,8-Diazabicyclo[5.4.0]undec-7-ene
DC	Dendritic cells
DCM	Dichloromethane
DLS	Dynamic Light scattering
EDC	1-ethyl-3-(3-dimethylaminopropyl) carbodiimide
FDA	Food and drug administration
GPC	Gel Permeation chromatography
HPLC	High Performance Liquid Chromatography
ICD	Immunogenic cell death
i.d.	Intradermal
i.t.	Intratumoral
LN	Lymph node
MHC-I/II	Major Histocompatibility complex class I/II
MPLA	Monophosphoryl lipid A
NK	Natural killer
NKT	Natural killer T cells
NPs	Nanoparticles
PDC	Pyridyl disulfide cysteamine hydrochloride
PEG	Polyethylene glycol
PEG-OMs	Mesylated polyethylene glycol
PEI	Polyethylenimine
PPS	Polypropylene sulfide
PSs	Polymersomes
Sulfo-NHS	N-hydroxysulfosuccinimide
TAA	Tumor-associated antigen
TdLN	Tumor-draining lymph node
TLR	Toll-like receptor
TSA	Tumor-specific antigen

List of figures

Figure 1.1	Generation of an anti-tumor response using cancer vaccines or immunostimulatory molecules	5
Figure 1.2	Radiotherapy and the induction of an anti-tumor immune response.....	8
Figure 2.1	Nanocarrier structures and characteristics.....	13
Figure 2.2	Types of Toll-Like receptors agonist used for the adjuvanted-particle formulation.	14
Figure 2.3	Synthesis and formation of nanoparticles, polymersomes and their components.....	22
Figure 2.4	Low molecular weight poly(I:C) encapsulation, and purification, in polymersomes.....	23
Figure 2.5	MPLA, TLR-4 agonist, adsorption to nanocarriers and activation of BMDCs in vitro	25
Figure 2.6	CL075, TLR-7/8 agonist, purification and BMDC activation comparison between encapsulated vs free adjuvant	26
Figure 2.7	CpG-B, TLR-9 agonist, loading efficiency and BMDC activation, in vitro, with either encapsulated or free adjuvant.....	27
Figure 2.8	Influence of the particle size on BMDCs uptake	29
Figure 3.1	Pattern recognition receptors activating innate immune response and their subcellular location.....	36
Figure 3.2	BMDCs activation with different PS-MPLA and PS-CL075 combinations showed synergistic effect for proinflammatory cytokines and CD40 expression.....	42
Figure 3.3	An increase in cytokine positive CD4 ⁺ T _{Eff/EM} but not CD8 ⁺ T _{Eff/EM} cells were observed.....	43
Figure 3.4	The addition of PS-CL075 to PS-MPLA did not delay tumor growth or increase antigen specific CD8 ⁺ T cells.....	45
Figure 3.5	A decrease in granzyme B and IFN γ secretion were observed for co-administered adjuvant compared to PS-MPLA only.....	46
Figure 3.6	Only TNF α production was synergistically increased when 0.1 μ M NP-CpG-B was incubated with PS-CL075	47
Figure 3.7	Synergistic effect for IL2 secretion in CD8 ⁺ T cells activation and a small increase in IFN γ + CD4 ⁺ T cells was detected when combining adjuvants.....	49
Figure 3.8	PS-CL075 addition to NP-CpG-B vaccine did not delay tumor growth or increase the T cell immune response.....	51

Figure 3.9	The addition of PS-CL075 to NP-CpG-B did not improve the T cells immune response in the spleen or TdLN.....	53
Figure 3.10	Synergistic effect was observed in cytokines secretion for several different adjuvant combinations.....	54
Figure 3.11	No synergistic effects were observed in CD8 ⁺ or CD4 ⁺ T cells co-cultures with the different adjuvant combinations tested.....	56
Figure 3.12	PS-MPLA addition to NP-CpG-B vaccine delayed tumor growth but did not increase SIINFEKL-specific CD8 ⁺ T cells.....	58
Figure 3.13	The addition of PS-MPLA to NP-CpG-B did not increase the T cells immune response	60
Figure 4.1	The T cell population was similar in the tumor microenvironment between both schedules	74
Figure 4.2	A trend in favor of an increased immune activation was detected when mice were vaccinated	75
Figure 4.3	Targeting the non-TdLN results in a more marked delay of tumor growth compared to the TdLN, without significant changes in T cell frequencies.....	77
Figure 4.4	A significant increase in polyfunctional CD8 ⁺ T cells, in the spleen but not in the TdLN was observed when the non-TdLN was targeted.....	78
Figure 4.5	Intratumoral and intradermal NP-CpG-B injection have similar effects on tumor growth and mouse survival	80
Figure 4.6	Vaccination with single or combined adjuvants resulted in a delayed tumor growth and an increased T cell response.....	82
Figure 4.7	NP-CPG-B, alone or in combination, induced a slightly higher T cell activation in the TdLN	83
Figure 4.8	Survival was increased when mice were co-injected with both adjuvants.....	85

Chapter 1

Motivation, Background and Aims

1.1. Motivation

Cancer ranks as the second leading cause of global deaths, according to the World Health Organization, with nearly 15% of people dying from it¹. More alarming, cancer incidence rate is increasing, and is expected to reach more than 20 million newly diagnosed cases per year as well as 13 million cancer-related deaths in 2030^{1,2}. The causes of cancer are multiple and range from genetic predisposition to the life style (smoking, diet, ...), through viral infections (e.g. Human papilloma viruses)². Cancer can primarily develop in any part of the body, and often metastases to distant sites and organs, which dramatically increases its associated mortality³. Among the various types of cancer, melanoma cancer remains the deadliest skin cancer, and is currently listed as the fifth and sixth most incident cancer in men and women respectively, in the United States of America².

While cancer is highly heterogeneous among patients, malignant tumors share some biological similarities – categorized as “the hallmarks of cancer” – that help researchers to break down the complexity of this disease and subsequently guide the development of novel anti-cancer therapies. As a well-known example, cancer cells are prone to genetic mutations and dysregulations, allowing them to extensively proliferate independently of environmental signals or internal cell cycle regulation mechanisms⁴. Another hallmark that has been recently adopted is the capability of tumor cells to evade immune destruction. Indeed, it has been demonstrated that the immune system is capable of both recognizing cancerous cells and mounting an anti-tumor response against them⁵. However, this anti-cancer immune response is not sufficient to eradicate all tumor cells, which actively evade immune attack through different mechanisms such as the induction of an immunosuppressive environment with the expression of PD-L1 or CTLA-4, the secretion of anti-inflammatory cytokines, the reduction of antigen presentation on their surface or the mutation of the antigen presented^{6,7}. This process by which cancerous cells evade the immune system is caused by the anti-tumor response and is called cancer immunoediting⁸.

First-line treatments against cancer are mainly focused on removing the primary tumor by surgery, radiotherapy and chemotherapy, often used in combination with one another, with the goal of removing or killing as many cancer cells as possible, if not all. Radiation and chemotherapy are particularly prescribed to treat inoperable tumors and potential nonvisible metastasis. Over the past decades, an increasing number of studies showed the ability of most of these treatments to also re-activate the immune system against cancer cells^{9,10,11}. By themselves, the induced anti-tumor responses are not strong enough to completely eradicate the remaining cancer cells and so, to increase their efficiency, immunotherapies have been added as a second-line treatment¹².

Therefore, the role of an immunotherapy is to help the immune system eradicate cancer cells by decreasing the tumor immunosuppressive environment or increasing the anti-tumor response^{13, 14}. The current strategies used in patients to activate the immune system are to extract either dendritic cells or T cells from the patient and expand and activate them *ex vivo* before re-injecting them intravenously^{15, 16}. Another possibility, extensively studied in research as well as in clinical trials, is to activate the patient's immune system *in situ* using cancer vaccines^{17, 18}. The main factors to consider in the development of effective cancer vaccines are the choice of antigens, adjuvants and the delivery system, which will influence and tune the type of anti-cancer immune response induced.

1.2. Background

Over the past decade, cancer research has made a great progress in understanding the disease and its interactions with the immune system. From what we have learned, the success of a treatment will not only depend on the type of cancer, but also on the patient themselves. Indeed, since all tumors are different in their tumor microenvironment, cancerous cell heterogeneity and the immune response, the most efficient way to treat them would be through the use of personalized treatment. However, to understand the interplay between each patient's immune system and their tumor, the discovery of tumor-specific antigens and the development of the vaccine (which safety has to be assessed), personalized treatment is not a viable option for the moment^{19,20}. In the meantime, the discovery of the interaction between the tumor and the immune system opened a whole new field of possible cancer treatments based on the immunomodulation of the tumor, so-called immunotherapy, that aims at either decreasing the immunosuppressive tumor microenvironment or helping and educating the immune response to better fight the tumor²¹. In this last case, an interesting approach to generate an anti-tumor response *in vivo* is the use of subunit cancer vaccines that would induce a potent immune response to eradicate tumor cells and metastasis. Such vaccines are often designed with three different components, namely the antigen, the adjuvant and the delivery system.

Subunit cancer vaccines development

Because cancer cells are derived from the self, the first obstacle in the development of a cancer vaccine is the choice of antigen. Indeed, antigens are either tumor-specific antigens (TSA), which arise from point mutation, or tumor-associated antigens (TAA), which are specifically overexpressed in cancerous cells but also expressed in healthy cells^{22,23}. TSAs have the advantage of being specific to the tumor, which makes it easier to induce a specific immune response against it but, unfortunately, are patient-dependent and thus the identification is more troublesome²⁴. On the other hand, TAAs are self-antigens and so, most reactive T cells against them have been deleted during the tolerance clonal selection²⁵. A final approach is to not define the antigen, by either using whole tumor lysate²⁶ or by inducing immunogenic cancer cell death *in situ*, upon radiotherapy²⁷ or chemotherapy^{28,29}.

Nevertheless, the development of a potent cancer vaccine does not only have to induce an immune response against the right tumor antigens, it also has to overcome the immunosuppressive environment induced by the tumor. Hence, the second parameter in the development of a cancer vaccine is the choice of immunomodulatory molecules, which are defined by any substance capable

of inducing, enhancing or suppressing an immune response, notably by influencing the signaling requirement between antigen-presenting cells (APCs) and T cells leading to T cell activation. Indeed, three signals are needed to induce the activation of T cells (Fig 1.1)^{30,31}. The first one being the presentation of the antigen on the major-histocompatibility complex and its interaction with the T cell receptor on T cells³². The second and third signals are the expression of co-stimulatory molecules and the secretion of inflammatory molecules by APCs, respectively. The purpose of the last two signals is to educate T cells on the type of behavior they have to adopt against that specific antigen; those signals are induced by immunomodulatory molecules or adjuvants (i.e. *any substance capable of enhancing an immune response*).

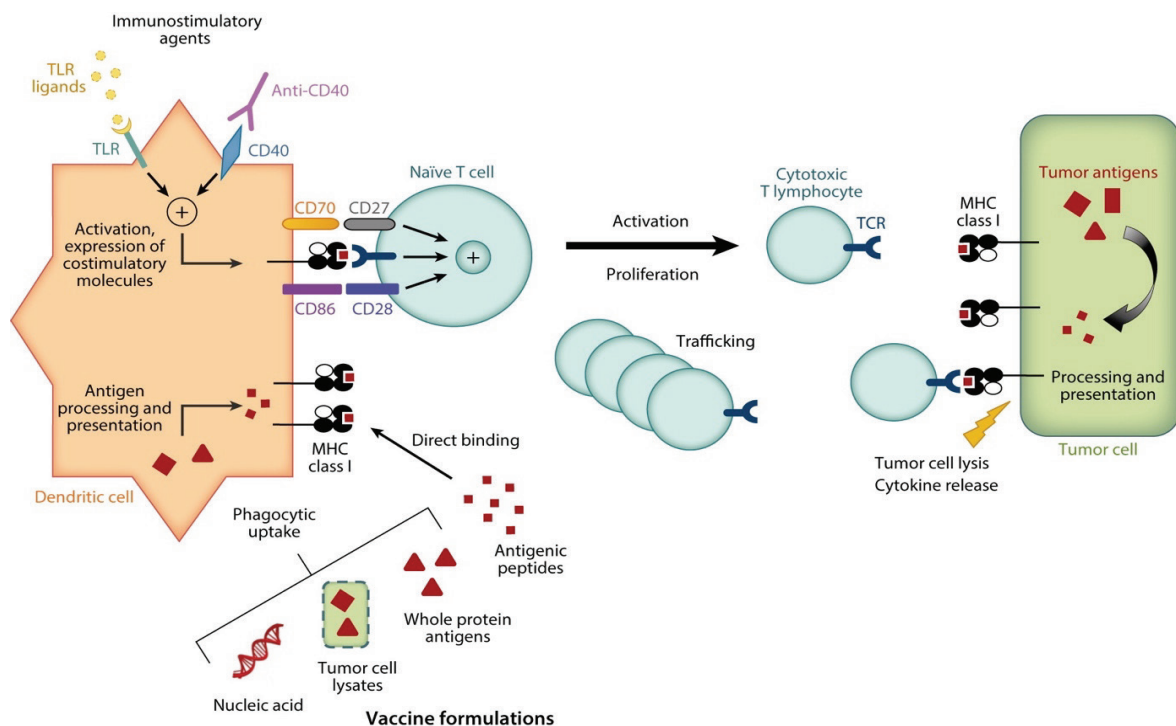


Figure 1.1 Generation of an anti-tumor response using cancer vaccines or immunostimulatory molecules. Toll-Like receptors agonists induce the expression of co-stimulatory molecules, in addition of cytokine secretion (not shown), which in combination with a tumor antigen presentation on the MHC-I, induce a T cell anti-tumor response. Figure adapted from Lizée et al.³³

Currently, most of the adjuvants tested in cancer vaccines are from the Toll-Like receptors (TLR) family, which recognize highly conserved structural motifs, known as pathogen-associated microbial patterns or danger-associated molecular patterns³⁴. The activation of the different TLRs will not induce the same type of immune responses, which are often classified by the phenotype of CD4⁺ T helper (Th) cells, CD8⁺ T cells and humoral response it induces. In the case of cancer, it is thought that Th1 response, with the presence of activated cytotoxic CD8⁺ T lymphocytes (CTL), are among the most effective responses for an anti-tumor immunity³⁵. As a consequence, all adjuvants known to induce this type of response have been tested in clinical trials against cancer³⁶. Among

them, the TLR-3 is an endosomal receptor that recognizes double-stranded RNA, and in the context of cancer, the use of synthetic agonists, Poly(I:C) and Poly (ICLC), was able to induce a potent tumor specific CTL, natural killers (NK) and natural killer T cells (NKT) responses³⁷. The TLR-4 is present on the cell surface as well as in endosomes and is activated with lipopolysaccharides structures from Gram-negative bacteria and their less toxic derivatives, such as monophosphoryl lipid A (MPLA) or glucopyranosyl lipid A. MPLA is already approved in a prophylactic cancer vaccine against human papillomavirus (HPV)³⁸, and it is also able to induce a tumor-specific humoral and cellular immune response in colorectal cancer^{39,40}. The third TLR targeted in cancer vaccines is TLR-7/8 agonist. It recognizes viral single-stranded RNA in addition to imidazoquinoline derivatives and its activation leads to a humoral and cellular response. A topical cream containing imiquimod, a small molecule, is already approved by the FDA as a therapeutic agent for basal carcinoma and, in addition to having a low toxicity, it is able to promote a pro-immunogenic tumor microenvironment⁴¹. The final TLR agonist tested for cancer vaccine in clinical trials activates the TLR-9 pathway when it recognizes a single-stranded DNA. It was able to induce an NK cell-mediated anti-tumor response in melanoma⁴² and an increase in CD8⁺ T cells⁴³.

Other immunostimulant molecules that do not stimulate TLRs, currently tested in clinical trials are anti-CD40 and IL2. The interaction of CD40, expressed by dendritic cells (DCs) with its ligand, is critical to induce the full activation of DCs and effective priming of T cells. Monotherapy of CD40-targeting antibodies in melanoma patients showed a partial response in 27% of patients⁴⁴. A clinical trial testing IL2 alone or in combination with an antigen, gp100, demonstrated an overall increase in survival in patients with melanoma⁴⁵. Interestingly, most of the clinical trials described above are done without using a delivery system, although it is known to be able to increase the immune response and decrease the risk of adverse effects.

The last parameter in the development of a subunit cancer vaccine is the delivery system, which is as important as the other two parameters. Indeed, it can act as an immunostimulant, target specific organs, or cells, modify the pharmacokinetic properties of the delivered-molecule or simply allow the delivery of several molecules to the same location, which in other terms help tune the desired immune response while reducing the possible side effects. For instance, nanocarriers such as emulsions (MF59, Montanide), saponin based, mineral salt and virosomes particles are able to act *per se* as immunostimulatory compound. Indeed, the first three create a depot in a specific location whereas virosomes encapsulate the molecules of interest in an influenza virus envelope⁴⁶. Other types of nanocarriers such as virus-like particles, liposomes and synthetic polymeric nanoparticles will enhance the immune system, but not by directly interacting with it. For example, the size of the carrier influences their retention time in the body, where they drain and how they are internalized

by cells. More precisely, it was demonstrated that intradermal injection of nanoparticles ranging from 20-200 nm are able enter the lymphatic system and drain to the lymph with a preference for particles ranging around 40 nm^{47, 48} whereas large ones will be retained longer at the injection site. In the blood stream, carriers smaller than 5 nm will be filtered by the kidney in less than 5 min or escape the vessel and diffuse in the local tissue, in contrast to larger nanoparticles that tend to have a longer circulating time but lower tissue penetration once they enter solid tumors⁴⁹. In addition, the uptake of the carrier by the cells through phagocytosis, macropinocytosis and receptor mediated endocytosis is influenced by the size, shape, surface charge and coating of the carrier⁵⁰. Briefly, 50 nm particles are taken up quicker than larger particles but at similar size, spherical particles are internalized faster than nanorods, or other shape⁵¹. The chemical structure and the approach used to deliver the molecule can influence the immune response by favoring different endosomal pathways; for instance, the molecule of interest can escape the endosomal compartment and enter the cytosol when coupled to the particle through a reduction, or acid, sensitive bond⁵². Consequently, the choice of the delivery system, as well as its composition, size and shape, have to be carefully chosen during the development of cancer vaccines in order to induce the desired immune activation.

Radiotherapy

A majority of patients with solid cancer are treated with radiotherapy, alone or in combination with chemotherapy, making it one of the most common cancer treatments currently used⁵³. Although it is now accepted that ionizing radiation is able to induce an immune response against cancer cells, studies are trying to understand the effect of the dose and frequency of ionizing radiations on cancerous cells, the tumor microenvironment and the immune system. Currently, three different radiotherapy approaches are used to treat cancer: the conventional treatments are done with 1.8-2 Gy per fraction administered five times a week of a period of 3-7 weeks; the hyperfractionation treatment is delivering 0.5-2.2 Gy twice a day, 2-5 days a week and 2-4 weeks; and finally, the hypofractionation uses doses between 3-20 Gy administered once a day for 1-3 days⁵⁴. Depending on the dose and the cancer, radiotherapy is able to promote immunogenic cell death (ICD), which massively release dead-cell associated antigens and activate the immune response against them, through several mechanisms (Fig.1.2)⁵⁵.

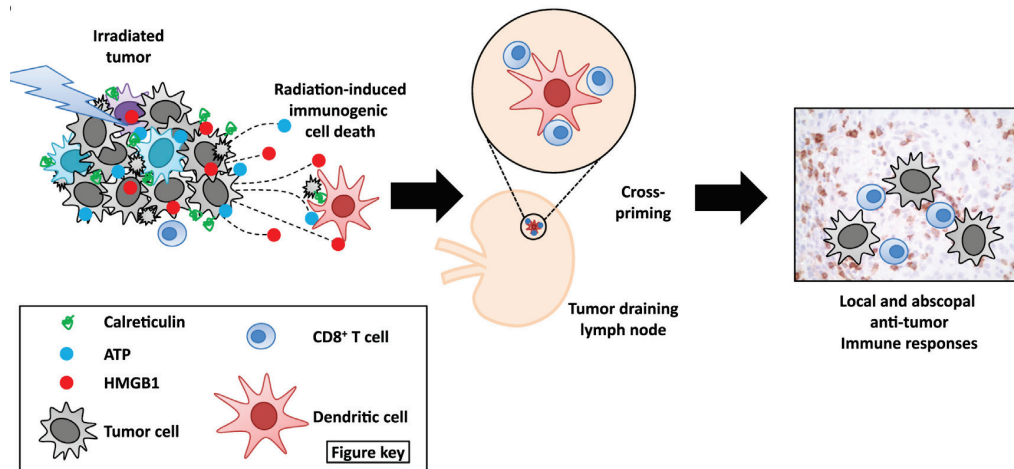


Figure 1.2 Radiotherapy and the induction of an anti-tumor immune response. Ionizing radiation induce immunogenic cell death resulting in the release of ATP and HMGB1 as well as cell surface translocation. Figure adapted from Golden et al.⁵⁶

Particularly, radiotherapy treatment induces the exposure of endoplasmic reticulum chaperone calreticulin on the cell surface, an “Eat-me” molecule that will increase its phagocytosis by DCs⁵⁷. Once the DCs get activated, they enter the lymphatic system in a CCR7-dependent manner and drain to the tumor-draining lymph node to prime the immune response^{58, 59}. In addition, an increase in antigen-specific CTL-mediated cells lysis occurs due to an increased secretion of ATP and HMGB1 proteins, in the tumor⁶⁰. Although these mechanisms are not always present, T cell priming seems to occur in the tumor-draining lymph node when they are taking place; thus, the delivery of adjuvants to that location seems promising to enhance the anti-tumor response.

1.3. Thesis aims

Over the past decade, our laboratory has developed different nanocarriers for cancer vaccines and demonstrated the advantage obtained when antigens or adjuvants were delivered by them. As a first carrier, nanoparticles (NPs), made of a polypropylene sulfide (PPS) solid core coated with a polyethylene glycol polymer (PEG) and ranging from 30-50 nm, were developed and conjugated to CpG-B⁶¹. It was demonstrated that 5 consecutive daily injections of NP-CpG-B in the forelimb draining the tumor-draining lymph node decreased tumor growth compared to targeting the contralateral lymph node⁶². Similar results were observed when NP-CpG-B was co-injected with NPs conjugated to tumor antigens⁶³. In addition, it was shown that the dose required to induce a strong CD8⁺ T cell response was lower when the vaccine was delivered by NPs compared to carrier-free⁶⁴. As a second material, polymersomes (PSs), formed with a bilayer of PEG-PPS polymer and ranging from 140-170 nm, were able to activate DCs when loaded with an adjuvant and an antigen⁶⁵. Interestingly, antigen delivery mediated by PSs enhanced CD4⁺ T cell whereas a stronger CD8⁺ T cells was detected when the antigen was loaded on NPs⁶⁶. All these studies successfully showed the possibility to enhance the immune response against cancer, while decreasing the dose. In addition, induced immune responses could be specifically tuned toward more CD8⁺ or CD4⁺ T cells polarized responses by the nanocarriers.

However, none of these studies focused on the combined delivery of these adjuvant-conjugated nanocarriers, although it is rationally expected that the targeting of multiple TLRs would increase the efficacy of the cancer vaccine⁶⁷. Moreover, we were interested in this thesis in testing the different vaccine formulations as a co-treatment with radiotherapy, to better mimic a clinical situation wherein the patient is given a standard-of-care anti-cancer treatment.

Therefore, and taking advantage of the tumor-draining lymph node targeting properties previously demonstrated, we started this thesis by the development and characterization the different adjuvanted-nanocarriers (1). We then tested them in combination with one another to determine if synergistic effects were detected on dendritic cells activation *in vitro* and if this translated into an increase T cell immune response *in vitro* and *in vivo*, in a model of melanoma cancer (2). Finally, we evaluated the most promising adjuvant formulation *in vivo* in combination with radiotherapy (3). Overall, this thesis aims at developing an effective nano-adjuvant cancer vaccine against melanoma cancer.

1.4. Accomplishments

The focus of the second chapter was to test the loading of four different TLR agonists to nanoparticles, and polymersomes, and characterize them. After synthesizing the different nanocarriers and polymers, MPLA or CL075 was successfully encapsulated in polymersomes whereas CpG-B was conjugated to nanoparticles, through a disulfide bond. The activation of bone marrow-derived dendritic cells (BMDCs), *in vitro*, was similar for NP-CpG-B compared to free CpG-B, as well as PS-CL075 with free CL075. A small decrease in activation was detected when PS-MPLA activated BMDC in comparison with MPLA only.

The third chapter was focused on determining the presence of synergistic effects when our nano-adjuvant formulations were combined together, and if the adjuvant ratio was important for an enhance activation. *In vitro*, we observed an increase in pro-inflammatory cytokines, notably IL12p70 and TNF α , when combining PS-MPLA with NP-CpG-B or with PS-CL075 whereas only TNF α was increased for the combination of NP-CpG-B with PS-CL075. Intriguingly, the effects observed on BMDCs activation did not translate to the same extent on T cell activation, *in vitro*. However, *in vivo*, the combination of PS-MPLA with NP-CpG-B was the most efficient to reduce tumor growth, in the B16 model of melanoma cancer in mice.

In the fourth chapter, we demonstrated an enhance T cell response after targeting the lymph node when combined with radiotherapy. In addition, we did not observe any difference in tumor growth or survival when the NP-CpG-B was injected intratumorally or intradermally, targeting the tumor-draining lymph node. Finally, we tested the combination of PS-MPLA + NP-CpG-B with radiotherapy and demonstrated an increase in survival as well as a decrease in tumor growth when both nano-adjuvants were co-injected. However, the T cell immune response quantification did not reveal any significant differences between the different vaccine formulations tested except for an increase in IL2 secretion after reactivation of the tumor-draining lymph node.

In the final chapter, we summarized the key results of this thesis and comment on their implication. We also discussed the future prospect for our vaccine developed.

Chapter 2

Formulation and Characterization of Adjuvant-based Nanocarriers

2.1. Abstract

During the development of a vaccine, several factors are considered in order to reach a fine balance between its efficacy to induce a strong immune response and its safety. In the case of subunit vaccines, they are usually considered safe but, unfortunately, less potent at inducing an immune response against the antigen of interest compared to live-attenuated vaccines. Our laboratory has engineered two different nanocarriers capable of enhancing the immune response against an antigen compared to the soluble protein, which is very interesting in the case of subunit vaccines. Nanoparticles (NPs) have a solid hydrophobic core coated with a polyethylene glycol (PEG) polymer whereas polymersomes (PSs) are vesicles formed with a polymer bilayer. At first, it was important to understand the properties of the two nanocarriers to determine all possible interactions between the molecules of interest, adjuvants, and the particle. NPs either adsorb the molecule on its surface or covalently conjugating it by a disulfide exchange reaction. PSs, on the other hand, could encapsulate molecules in their vesicle or adsorb it on the polymer bilayer. We have demonstrated that, out of the four molecules of interest tested (Poly(I:C), MPLA, CL075, CpG-B), three could be successfully delivered by both nanocarriers and used for our vaccine formulation. In addition, they were all able to activate dendritic cells, *in vitro*, and induce similar levels of cytokine productions compared to its free counterpart. Finally, we demonstrated that both nanocarriers were internalized by macropinocytosis.

2.2. Introduction

The discovery of prophylactic vaccination against infectious diseases, with live-attenuated or inactivated vectors, is considered one of the most groundbreaking findings in medicine⁶⁸. These vaccines are extremely efficient at inducing an immune response but are considered less safe than subunit vaccines due to the possibility for them to regain their virulence⁶⁹. In addition, in the case of cancer, only a few of them originate from a known pathogen and therefore subunit vaccines are the only possible option. Furthermore, current cancer vaccines are therapeutic rather than prophylactic since the antigen varies among patients, cell type and locations. Three main factors, such as antigens, immunomodulator compounds and delivery system, are taken into account for the development of an efficient CD8⁺ T cell subunit vaccine⁷⁰. The focus of this study was to take advantage of the nanocarriers developed in our laboratory to create an adjuvant-based vaccine that could be delivered to the tumor-draining lymph node to induce an immune response.

The two different nanocarriers used for the vaccine formulation are both primarily composed of polyethylene glycol (PEG) and propylene sulfide but have different structures and properties (Fig. 2.1). The first nanocarrier, called ‘nanoparticle’ throughout this thesis, is a 30-50 nm polypropylene sulfide (PPS) solid core covered in an ABA pluronic F-127 triblock polymer. Due to their small size, they have the ability to enter the lymphatic system and go to the skin draining lymph node^{48, 71}. In addition, an enhanced delivery to dendritic cells and an increase in CD8⁺ T cell response is observed if antigens, or adjuvants, are conjugated to them^{72, 73, 64}. The second nanocarrier, called ‘polymersome’ throughout this thesis, is a 140-170 nm vesicle with a polymer bilayer composed of PEG₁₇-PPS₃₀ polymer. Although both particles are composed of the same components, antigens will be processed differently, inducing an increase in humoral and CD4⁺ T cell response when delivered by polymersomes versus a CD8⁺ T cell response for NPs^{74, 66, 75}.

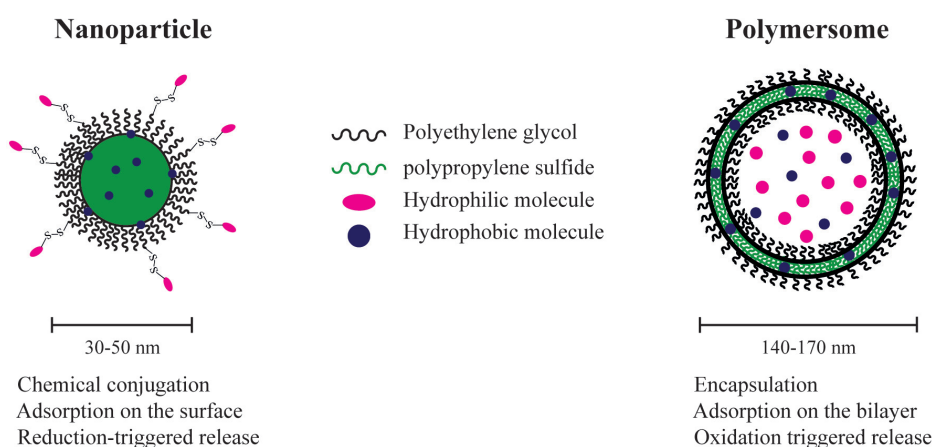


Figure 2.1 Nanocarrier structures and characteristics. Image adapted from *Stano et al*¹⁰.

The choice of adjuvants for the vaccine was based on the feasibility to deliver them with nanoparticles or polymersomes and their efficacy in cancer vaccine. Toll-like receptors (TLR) are a subset of the pattern-recognition receptors family, which can strongly activate dendritic cells (DCs). They have been well studied for cancer vaccines and, in some cases, used in clinical trials. Four different TLR agonists, Poly(I:C), MPLA, CL075 and CpG-B, were chosen due to their properties to either be conjugated, adsorbed or encapsulated in particles. Poly(I:C), a double-stranded RNA, which is recognized by endosomal TLR-3 is present on myeloid DCs and macrophages, as well as cancer cells, such as colorectal, ovarian, melanoma and many others⁷⁶. The principal mechanism by which it produces an anti-tumor activity is by enhancing both the innate and adaptive immune responses³⁷. Many of the clinical trials involving a TLR-3 agonist are used in combination with pulsed peptide to treat pancreatic cancer and were able to generate antigen-specific T cells^{77, 78, 79}. The second adjuvant, MPLA, a TLR-4 agonist, is the only one signaling through the MyD88 and the TRIF pathways, whereas other TLRs activate either one or the other. It is mainly expressed on dendritic cells, macrophages, granulocyte and monocytes, as well as some cancer cells⁸⁰. MPLA is found in several vaccines such as a prophylactic vaccine for human papillomavirus^{81, 82}, allergic rhinitis⁸³, HBV^{84, 85} and metastatic melanoma. The third adjuvant is a TLR-7/8, CL075, which signals through the MyD88 pathway and stimulates inflammatory monocyte-derived DCs⁸⁶. Colorectal cancer cells treated with this adjuvant showed a reduction in IL-6 production, *in vitro*, which may prevent recurrence, in addition to reducing IL-8 cytokine production in various cancer cell lines⁸⁷. The last adjuvant chosen (CpG-B), a TLR-9 agonist, is expressed in many different immune cells and activates the MyD88 pathway. In addition, our laboratory demonstrated the efficacy of nanoparticle conjugated CpG-B to reduce tumor growth and prolong mice survival⁶³. This adjuvant is used in several clinical trials for diseases such as HBV, Anthrax, Malaria, cancer and many others^{88, 89}. As said previously, this chapter is focused on the characterization of the different adjuvanted-particles and their effect on BMDC activation compared to free adjuvants.

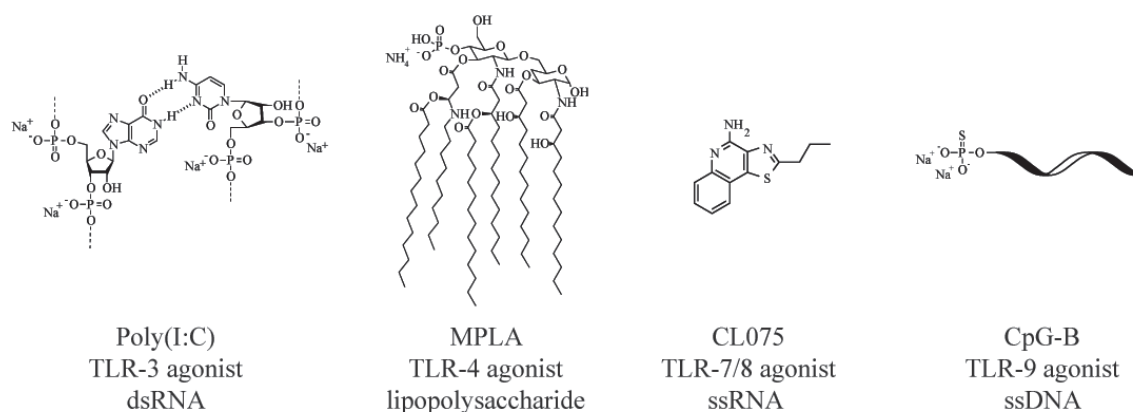


Figure 2.2 Types of Toll-Like receptors agonist used for the adjuvanted-particle formulation.

2.3. Materials and Methods

Animals

All mice used for experiments were C57BL/6 female ranging from 8-12 weeks old, purchased from Harlan (France) or Jax (USA). All procedures were performed in compliance with the Veterinary Authority of the Canton of Vaud (Switzerland) according to Swiss laws and the Institutional Animal Care and Use Committee at the University of Chicago (USA).

Reagents

Reagent grade chemicals were purchased from Sigma-Aldrich (Saint Louis, MO, USA) unless noted otherwise. All adjuvants, except for CpG-B, were purchased from InvivoGen (San Diego, CA, USA). The modified 5'SPO₃-CpG-B (5'-TCCATGACGTTCCCTGACGTT-3') was purchased from Microsynth (Balgach, Switzerland) or TriLink Biotechnologies (San Diego, CA, USA).

F127-COOH synthesis

An adapted version of the protocol described by Liu et al⁹⁰ was used to synthesize the carboxylated F-127 from the commercially available F-127 hydroxyl polymer. Due to the hygroscopic nature of the pluronic, water had to be removed before starting the reaction. This was done by dissolving 5 g of polymer in dichloromethane (DCM) and precipitating it in diethyl ether. The precipitate was collected and dried overnight. The following day, 2.5 g of F-127-OH (0.2 mmol) and 193 mg maleic anhydride (1.95 mmol) were dissolved in anhydrous toluene (10 mL). The solution was thoroughly degassed and the system was put under inert conditions before 500 μ L of anhydrous pyridine (6 mmol) was added. The reaction was stirred at room temperature for 8 h, after which it was precipitated in cold ether and dried. A reaction yield of 64% was obtained and a conversion yield of 80 % was determined by ¹H NMR in CDCl₃. ¹H NMR: δ = 1.1 (*m*, -CHCH₃, PPO), 3.3 (*m*, -CHCH₃, PPO), 3.4 (*m*, -CHCH₂O, PPO), 3.5 (*m*, -CH₂CH₂, PEO), 4.4 (*m*, -COOH), 6.3-6.5 (*m*, -CH=CH).

Pyridyl disulfide cysteamine • HCl (PDC) synthesis

PDC synthesis was done following the protocol from Van Der Vlies et al⁶¹. Shortly, 3.3 g of Aldrithiol-2 (15 mmol) was dissolved in 10 mL of methanol before adding 570 mg of cysteamine •HCl (0.5 mmol) and reacting it overnight. The solution was purified twice by precipitation in diethyl ether before lyophilizing it and performing a ¹H NMR (DMSO-d₆). δ = 8.54-8.48 (*m*, 1H), 8.26 (*bs*, 3H), 7.86-7.81 (*m*, 1H), 7.75 (*d*, 1H), 7.33-7.23 (*m*, 1H), 3.12-3.03 (*m*, 4H). The reaction and conversion yield obtained were 80% and 100%, respectively.

Nanoparticle formation

The synthesis was adapted from the protocol described by Rehor et al.⁹¹. Briefly, 500 mg, at a 3:1 ratio of hydroxyl to carboxyl polymer, F-127 pluronic, was dissolved in 10 mL mQ H₂O before purging and degassing the system with argon (Ar). Afterwards, 400 µL of propylene sulfide (5 mmol) was added to the reaction and stirred for 30 min to create the emulsion. In the meantime, 14.8 mg of four-arm initiator (0.024 mmol, synthesized in the laboratory) was dissolved, and activated with a solution of 0.5 M NaOCH₃, in MeOH, before adding it to the reaction flask. After stirring for 15 min, 60 µL of 1,8-Diazabicyclo[5.4.0]undec-7-ene (DBU) was added before flushing the reaction with Ar and leaving the polymerization go overnight. The following day, the solution was exposed to air for 2 h in order to cross-link the nanoparticle core before quenching the remaining surface thiolates with 47.5 mg iodoacetamide (0.26 mmol) for 30 minutes. An Ellman's assay was performed to determine the presence of thiolates in the solution, following the manufacturer's indications (ThermoFisher scientific, Waltham, MA, USA). Nanoparticles were then functionalized by reacting the carboxyl groups with pyridyl disulfide cysteamine. Briefly, 2-(N-morpholino)ethanesulfonic acid was added to the solution at a concentration of 100 mM and the pH was adjusted to 4 – 4.5. PDC, N-hydroxysulfosuccinimide (sulfo-NHS, Thermofisher, Waltham, MA, USA) and 1-ethyl-3-(3-dimethylaminopropyl) carbodiimide (EDC) were added to the nanoparticle solution at an excess of 20 equivalent relative to the amount of pluronic carboxyl present. The reaction was then stirred overnight before dialyzing it using a MWCO = 100 kDa for 2 days. After filtering the solution (0.22 µm filter, Millipore Corporation, Burlington, MA, USA), the size was determined by dynamic light scattering (DLS, Nano Zs Zetasizer, Malvern, UK) and a small volume was lyophilized to obtain the concentration in mg/mL of material. The concentration of PDC was quantified by reducing a small volume with TCEP•HCl (Thermofisher, Waltham, MA, USA) and measuring the absorbance at 340 nm.

Proteins or molecules conjugation to NPs

Due to the properties of NPs, the molecule of interest can either be adsorbed on the surface of the nanocarrier, if it is hydrophobic, or it can react with the pyridyl disulfide group, if it has a thiol. In the case of OVA, the protein was dissolved at a concentration of 20 mg/mL in mQ H₂O before adding 100 µL of it to 400 µL of NPs solution containing 6 M guanidine hydrochloride. The reaction was left overnight at room temperature before purifying it by size exclusion chromatography through sepharose CL-6B column in 1x PBS. The concentration was quantified by BCA assay following the manufacture's instruction (Thermofisher, Waltham, MA, USA). Since the CpG-B, 5' SPO₃-CpG-B, already had a free thiol, the adjuvant was directly mixed to the NP solution and reacted overnight at room temperature before purifying it similarly to the OVA

conjugation. The quantification of the adjuvant was performed by GelRed assay (Brunschwig, Basel, Switzerland). Finally, due to the hydrophobicity property of MPLA, it was dissolved in DMSO at a concentration of 7 mg/mL before 500 μ g of adjuvant was added to 400 μ L nanoparticle solution and thoroughly vortexed. The following day, the solution was purified by size exclusion and quantified by HEK-BlueTM TLR-4 following the manufacturer's protocol (Invivogen, San Diego, CA, USA) or by fluorescence if the adjuvant was fluorescently labeled (adjuvant was labeled in the laboratory).

PEG-b-PPS diblock copolymer synthesis

The synthesis of PEG-b-PPS polymer was adapted from Velluto et al⁹², where the reaction was done by anionic ring opening polymerization of propylene sulfide and stopped with the addition of mesylated-PEG (PEG-OMs). Before starting the polymer synthesis, polyethylene glycol monomethyl ether (Mn 750, PEG-OH) was chemically modified with a mesylate group on the terminal hydroxyl group. Briefly, 15 g of PEG-OH (0.03mol) was dissolved in 200 mL of toluene and heated at reflux for 3 hours to remove the water using a Dean-Stark trap under inert atmosphere. The solution was then cooled down at 0°C before adding 11.15 mL triethylamine (80 mmol). Afterwards, 6.2 mL methanesulfonyl chloride (82.4 mmol), diluted in toluene ($V_{\text{final}} = 20$ mL), was added dropwise to the reaction under inert atmosphere. The solution was reacted for 3 h before removing the toluene and re-dissolving the polymer in 60 mL dichloromethane. 5 g of activated charcoal was added and the solution was stirred for 30 min before filtering it and collecting the filtrate. The polymer was then precipitated in diethyl ether at room temperature before adding 40 mL n-hexane and cooled at 0°C for 30 minutes. The precipitate was collected and dried overnight before repeating the purification step a second time. The ¹H NMR in CDCl₃ showed a 100% conversion yield and the amount recovered was 6 g (40%). ¹H NMR (CDCl₃): $\delta = 4.39\text{-}4.36$ (*t*, -OCH₂CH₂S, mesylate), $3.84\text{-}3.44$ (*m*, -OCH₂CH₂, PEG), $3.38\text{-}3.36$ (*s*, -OCH₃, PEG), $3.09\text{-}3.07$ (*s*, -SCH₃, mesylate).

Once the purity of PEG-OMs was confirmed, the polymer synthesis was performed. 67.8 μ L of benzyl mercaptan (0.58 mmol, initiator) was diluted in 6.3 mL DMF under inert atmosphere. The initiator was then activated with 1.3 mL of NaOMe and stirred for 15 min. The flask was then submerged in a water bath at room temperature before adding 1 mL propylene sulfide (12.76 mmol). After 45 min, 940 mg PEG-OMs, dissolved in 2 mL DMF, was added to the reaction, to stop the polymerization, and stirred overnight. The solution was purified by precipitating twice in MeOH and dried before storing it at -20°C. The recovery yield obtained was 85% and the number of propylene sulfide monomeric unit was determined by ¹H NMR. ¹H NMR (CDCl₃): $\delta = 1.26\text{-}1.32$

(*m*, -CH₃, PPS), 2.58-2.69(*m*, CH, PPS), 2.82-3.01 (*m*, -CH₂, PPS), 3.24-4.26 (-OCH₃, PEG), 3.49-3.54 (-CH₂, PEG), 7.16-7.19 (d, -CH_{aromat}, benzyl).

Polymersome formation

Depending on the property of the molecule of interest, hydrophilic or hydrophobic, the adjuvant was added at different time points during the formulation process. If the molecule was hydrophobic, it was dissolved and dried with the polymer during the first step of PSs formation whereas if it was hydrophilic it was added during the re-hydration process. Briefly, 30-50 mg of PEG₁₇-b-PPS₃₀ was dissolved in DCM and dried in a piranha-etched HPLC glass vial overnight. The thin-film formed on the vial was then re-hydrated in 50 mM phosphate buffer and rotated for 3-5 days at 4°C. The solution was extruded 5 times through a 0.2 µm nucleopore track-etched membranes (Whatman, Maidstone, UK). The particle size was determined by DLS, ranging between 140-170 nm, and a polydispersity index lower than 0.2 was obtained. Once the size was within the correct range, a size exclusion chromatography with Sepharose CL-6B beads was performed in order to separate polymersomes from unloaded molecules. The molecule of interest was quantified and endotoxin levels were tested by HEK-Blue™ TLR4 cells (Invivogen, San Diego, CA, USA) before storing the solution at 4°C for further use.

Generation of Bone marrow-derived dendritic cells (BMDCs)

An adapted version of the protocol described by Lutz et al⁹³ was used to generate CD11c+ BMDCs. Briefly, bone marrow cells were isolated from a C57BL/6 mouse and cultured for 9 days with 20 ng/mL of GM-CSF. The media was replaced with fresh media every 3 days until day 6 after isolation. At day 9, because 70-85% of the non-adherent cell population expresses the signature dendritic cell marker CD11c⁺, the bulk unsorted non-adherent cells were used in downstream studies detailed below.

In vitro experiments

All BMDCs activation experiments were performed in a tissue culture U-bottom 96-well plate and cells were used on day 9 after harvesting. All the experiments were done with 200'000 cells per well, plated before the different treatments were added. The adjuvant dose response experiments were incubated for 24 h at 37°C in a 5% CO₂ incubator before collecting the supernatant and performing the different ELISAs.

The diffusion experiment under static or dynamic condition was performed as follows. BMDCs were incubated with either free, NP conjugated or PS encapsulated fluorescently labeled OVA or FITC at 37°C in a 5% CO₂ incubator. At different time point, cells were collected and washed before quantifying the fluorescence using a plate reader spectrophotometer (Tecan, Männedorf, Switzerland). The plate was not mixed or moved for the static condition whereas it was slowly shaken for the dynamic condition.

For the uptake inhibition experiments, serial dilution of filipin III (50 µg/mL), Dynasore (62.5 µM), both in DMSO, and amiloride (500 µM), in ethanol, were prepared before cells were pre-incubated with them for 45 min at 37°C in a 5% CO₂ incubator. Afterwards, nanoparticles or polymersomes were added to the wells and incubated an additional 6 h at 37°C in a 5% CO₂ incubator. BMDCs were then stained and analyzed by flow cytometry.

Flow cytometry

Before starting the antibody staining for flow cytometry, cells were centrifuged and washed with 1x PBS. Afterwards, samples were incubated with a fixable live/dead stain at 4°C for 15 min and washed once with PBS. For surface staining, a cocktail of antibody was diluted in staining buffer and incubated at 4°C for 15 min, in the dark. Finally, the cells were fixed with 2% paraformaldehyde, washed with staining buffer and stored in the same buffer for data collection. Anti-mouse antibodies CD11c and MHC-II were purchased from biolegend (San Diego, CA, USA) whereas CD86 and live/dead fixable were from ThermoFisher Scientific (Waltham, MA, USA).

ELISA

Cytokine detection and quantification was performed with Ready-SET-Go! ELISA kits purchased from ThermoFisher Scientific and used according to the manufacturer's instructions.

Diffusion coefficient calculation

The diffusion coefficients were obtained by using the Stokes - Einstein equation.

$$D = \frac{k_B T}{6\pi \eta r} = \frac{1.38 \times 10^{-23} \times 296}{6\pi \times 0.0007 \times r}$$

Where k_B is the Boltzman constant ($\frac{N \times m}{K}$), T is the temperature (K), η the viscosity ($\frac{N \times s}{m^2}$) and r the radius of the particle (m).

Data collection

Flow cytometry was performed using either a CyAnTM ADP (Beckman Coulter, Brea, CA USA) or a BD LSRFortessaTM (BD Biosciences, San Jose, CA, USA). The data obtained were analyzed with FowJo (v.10, Tree Star, Ashland, OR, USA). Graphs and statistical analysis were done using the GraphPad Prism 7 Software (GraphPad Software Inc, La Jolla, CA, USA).

2.4. Results

Synthesis and formation of the different nanocarriers

In order to determine if the different TLR agonists could be delivered to the targeted organ thanks to the vehicles developed in the laboratory, it was important to characterize their properties. Nanoparticles were composed of a solid hydrophobic core coated with a F-127 pluronic, at a 1:3 ratio of F-127-COOH to F-127-OH. The synthesis of the carboxylated pluronic was performed under inert conditions without the presence of water and since the polymer was hygroscopic, it was necessary to dry it beforehand (Fig.2.3.A). The reaction and conversion yields obtained were 64% and 80%, respectively. Nanoparticles were formed by performing an oil-in-water emulsion at a high stirring speed to decrease the size of particles before polymerizing the hydrophobic core (Fig.2.3.B). Once NPs were formed and free thiols blocked, the carboxyl groups were functionalized with a pyridyl cysteamine group to be able to conjugate any thiol-containing molecule of interest to it. NPs ranged between 30-40 nm and the concentration of PDC varied between batches from 100 μ M to 300 μ M. The polymer synthesis, for the polymersomes formation, was also done under inert conditions, but since the reaction is an anionic chain reaction, several factors can influence the length of the polymer (Fig.2.3.C). The polymersome formation was done by drying a thin layer of PEG₁₇-PPS₃₀ on a glass surface before adding 50 mM PBS solution and slowly rotating the solution for 3-4 days. The solution was extruded several times under high pressure through a 0.2 nm pore membrane until the size ranged between 140-170 nm (Fig.2.3.D).

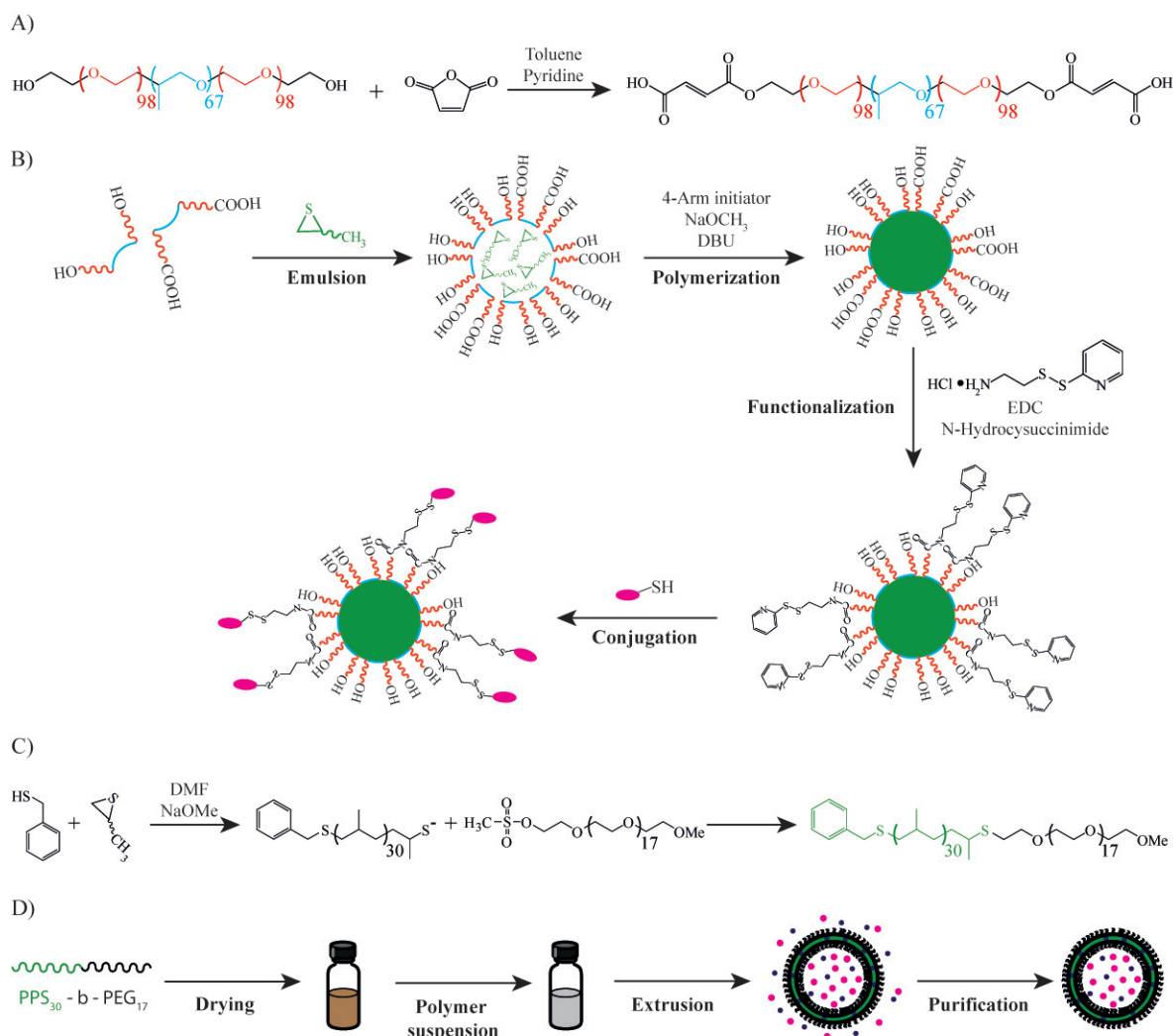


Figure 2.3 Synthesis and formation of nanoparticles, polymersomes and their components. (A) F-127-COOH synthesis reaction. F-127-OH was reacted with maleic anhydride for 8 h under inert conditions in toluene before purifying the polymer by precipitation in ether. (B) Formation of nanoparticles and adjuvanted-nanoparticle conjugation. The first step of NP formation was an oil-in-water emulsions, where a 3:1 ratio of F-127-OH : F-127-COOH was dissolved in mQ H₂O before adding propylene sulfide and polymerizing the core with the activated 4-Arm initiator. After blocking the free thiols with iodoacetamide, NPs were functionalized by reacting carboxyl groups with pyridyl disulfide cysteamine. Finally, a disulfide exchange reaction was performed to conjugate any thiol containing molecules. (C) PEG₁₇-b-PPS₃₀ block-copolymer synthesis. Under inert condition, benzyl mercaptan initiate an anionic chain reaction with propylene sulfide before stopping the reaction by adding PEG-OMs. (D) Polymersomes formation. The polymer, dissolved in DCM, was dried in piranha-etched vial before re-suspending it with 50 mM PBS and rotating it for 4 days. Afterwards, the solution was extruded and purified to remove free molecules.

Encapsulation of Poly(I:C) was not successful in either nanocarrier

Poly(I:C) is a double-stranded RNA composed of a polyinosinic strand annealed with a polycytidylic strand. A high molecular weight (HMW) and a low molecular weight (LMW) can be purchased with a size range of 1.5-8 kb and 0.2-1 kb, respectively. We hypothesized that due to its properties (hydrophilic and the absence of thiols), the only possibility to deliver it, using our nanocarriers, was to encapsulate it in polymersomes. To determine the loading efficiency, the free adjuvant had to be removed from the solutions and the first method tested was a size exclusion chromatography with sepharose CL6-B beads (Fig.2.4.A, *left*). Unfortunately, the separation was not possible by size exclusion and so an anion exchange chromatography was performed. The free poly(I:C), negatively charged, was blocked in the column whereas polymersomes went through it without being disturbed by the charged column (Fig.2.4.A, *middle*). To confirm the removal of the free adjuvant from the solution, the anion exchange column was regenerated with 2 M NaOH or 150 mM NaCl solvents, which released it (Fig. 2.4.A, *right*). Unfortunately, the quantification of the adjuvant by GelRed assay did not show any encapsulation and no further experiments were done with this adjuvant.

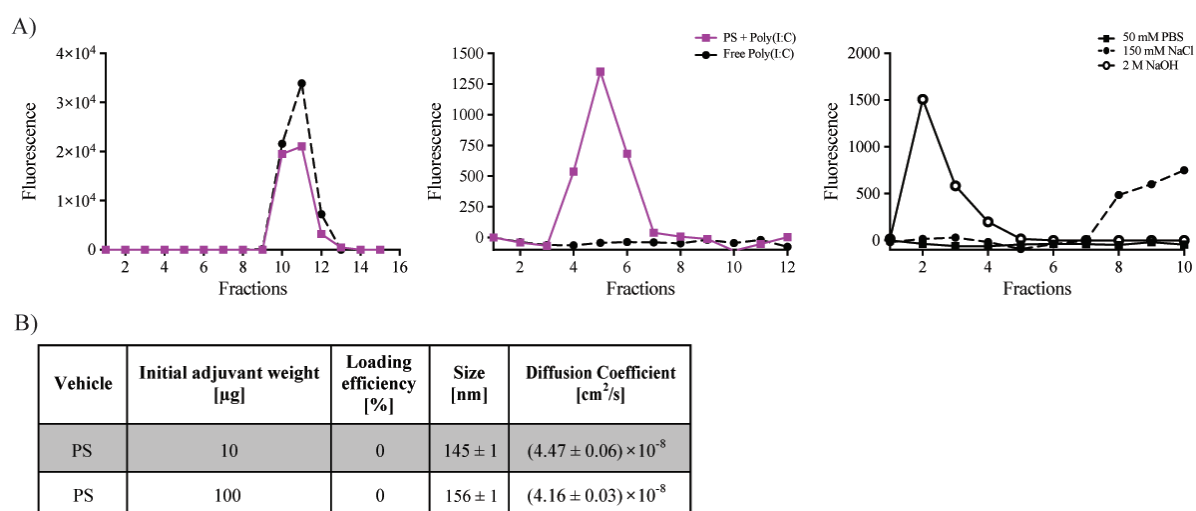


Figure 2.4 Low molecular weight poly(I:C) encapsulation, and purification, in polymersomes. (A) Purification method of free poly(I:C) from encapsulated adjuvant. *Left graph*, separation between the two populations by size exclusion chromatography, with sepharose CL-6B beads, was not successful. *Middle graph*, the purification done by anionic exchange chromatography removed free adjuvant and the column could be regenerated with 2 M NaOH or 150 mM NaCl, *right graph*. (B) PS-Poly(I:C) encapsulation summary. The loading efficiency and particles sizes were obtained by GelRed assay and dynamic light scattering, respectively. The diffusion coefficient was calculated using Stokes-Einstein equation.

MPLA adsorption on nanoparticles and polymersomes

The adsorption of the TLR-4 agonist on nanoparticles was done by dissolving it in DMSO, at a concentration of 7 mg/mL, and added dropwise to 400 μ L of NPs. To increase the loading efficiency, the solution was strongly stirred during the addition. The following day, the mixture was purified by size exclusion chromatography using sepharose CL-6B beads (Fig.2.5.A, *left*). As a control, free MPLA was run through the column and since the presence of the free adjuvant was in later fractions than NPs, the purification was successful (Fig.2.5.A, *middle*). The quantification of MPLA was performed by HEK-blue TLR-4 assay and by fluorescently labeling the adjuvant. Unfortunately, the loading efficiency obtained by both methods varied significantly. The same sample showed 20% loading efficiency by fluorescence whereas 60% was obtained for HEK TLR-4 assay. To determine if the adsorption influenced the interaction of MPLA with the TLR-4 receptor, BMDCs were incubated for 24 hours at different concentrations of free MPLA or NP-MPLA. The concentration of IL12p70, TNF α and IL6 cytokines showed similar trends between the two treatments with a small decrease when MPLA was adsorbed on nanoparticles (Fig.2.5.B). For the adsorption on the polymersome bilayer, the adjuvant was dissolved at the same time as the polymer in dichloromethane to form the thin layer on the HPLC glass vial. After extruding the polymersomes, the solution was purified by the same size exclusion chromatography as the nanoparticles solution (Fig.2.5.A, *right*). Polymersomes were detected between 3.5-4.5 mL, which correlates with the detection of MPLA whereas the free adjuvant exited after 7 mL. The quantification of the TLR-4 agonist was done again by fluorescence and HEK TLR-4 assay, which both gave a loading efficiency between 20-30%. The same activation experiment as the NP-MPLA was performed and, compared to free MPLA, a higher dose of PS-MPLA was needed to induce similar levels of IL12p70, TNF α and IL6. At 570 nM of MPLA, the levels of cytokines are identical independently of the presence, or not, of nanocarrier. The loading efficiency in polymersomes was always similar independently to the amount of starting material whereas the nanoparticle results varied strongly from batch to batch, and between quantification assays (Fig.2.5.D). Although MPLA could be adsorbed on both particles, the reproducibility of PS-MPLA compared to NP-MPLA made it a more viable option for the following experiments.

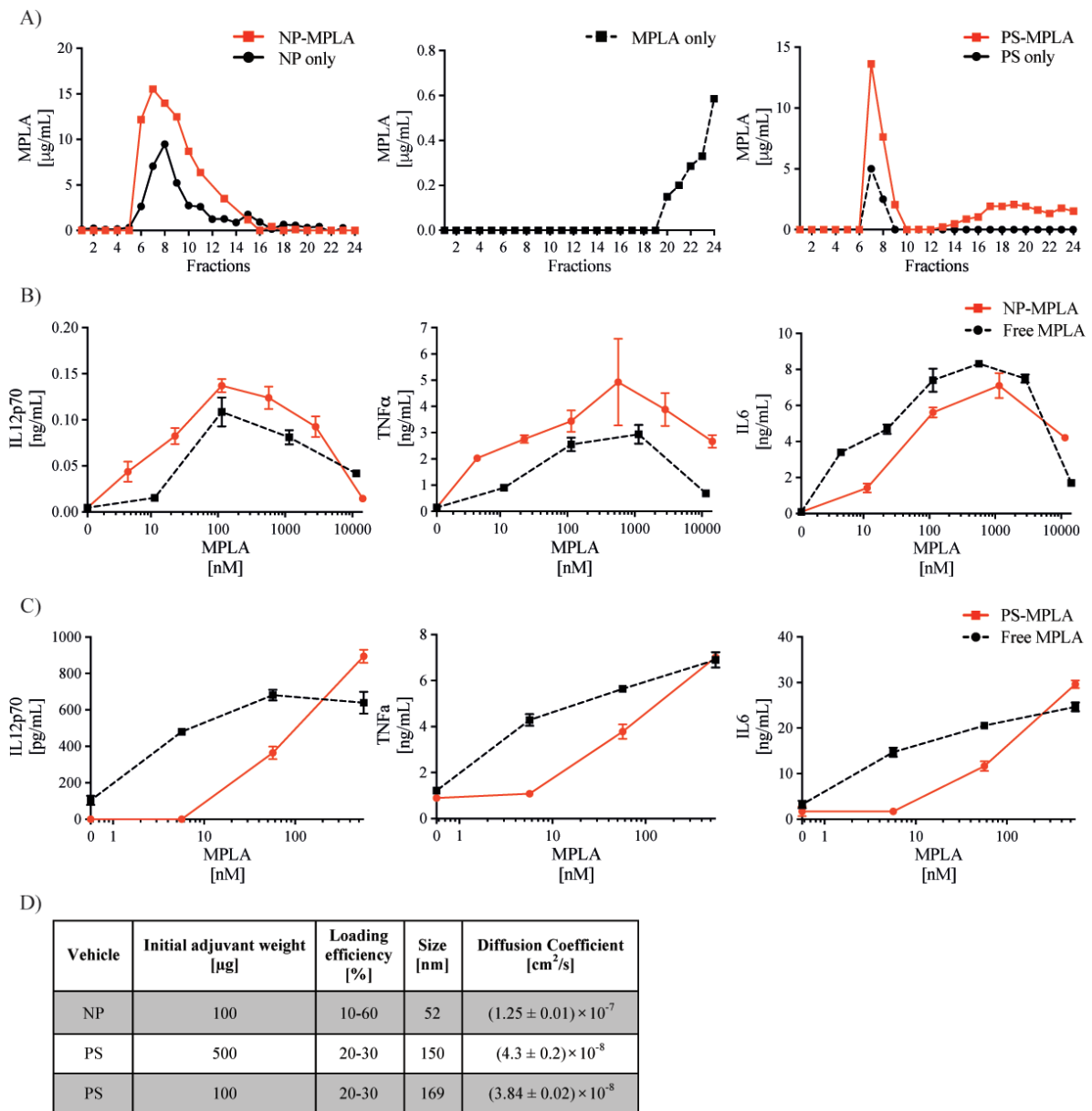


Figure 2.5 MPLA, TLR-4 agonist, adsorption to nanocarriers and activation of BMDCs in vitro. (A) Size exclusion chromatography by sepharose CL-6B of NP-MPLA (*left graph*), Free MPLA (*middle graph*) and PS-MPLA (*right graph*). MPLA quantification was performed by HEK TLR-4 endotoxin assay, as well as by fluorescence, NP and PS detection was done with an iodine assay and HPLC in DMF, respectively. (B) BMDCs were incubated for 24h with different concentration of free MPLA or NP-MPLA before collecting the supernatant and performing IL12p70, TNF α and IL6 ELISAs. (C) A similar experiment was performed as in (B) but this time with free MPLA or PS-MPLA, with identical readouts. (D) A summary of the adsorption efficiency with the different particles, their size obtained by DLS and diffusion coefficient calculated using the Stokes-Einstein equation. All Experiments were repeated three times in triplicate.

Polymersomes encapsulation of the TLR-7/8 agonist, CL075

The delivery of CL075 was not possible with nanoparticles due to its chemical structure, which does not contain any thiols or any hydrophobic chains. Fortunately, the adjuvant is a small molecule, much smaller than poly(I:C) or even MPLA, making it possible to encapsulate it in polymersomes. The TLR-7/8 agonist was dissolved in a 50 mM PBS solution before adding it to the thin polymer layer and rotated for 4 days before extruding the solution. The separation of the encapsulated vs free adjuvant was done by a size exclusion chromatography, with sepharose CL-6B beads (Fig.2.6.A, left). The loading efficiency was calculated by quantifying the adjuvant concentration by HPLC with a gel permeation column in DMF (Fig.2.6.A, right). BMDC activation with free CL075, or encapsulated, induced similar concentration of IL12p70, TNF α and IL6 (Fig.2.6.B). In addition, the highest dose tested had lower cytokine levels than a lower dose, which could indicate toxicity of the adjuvant for cells.

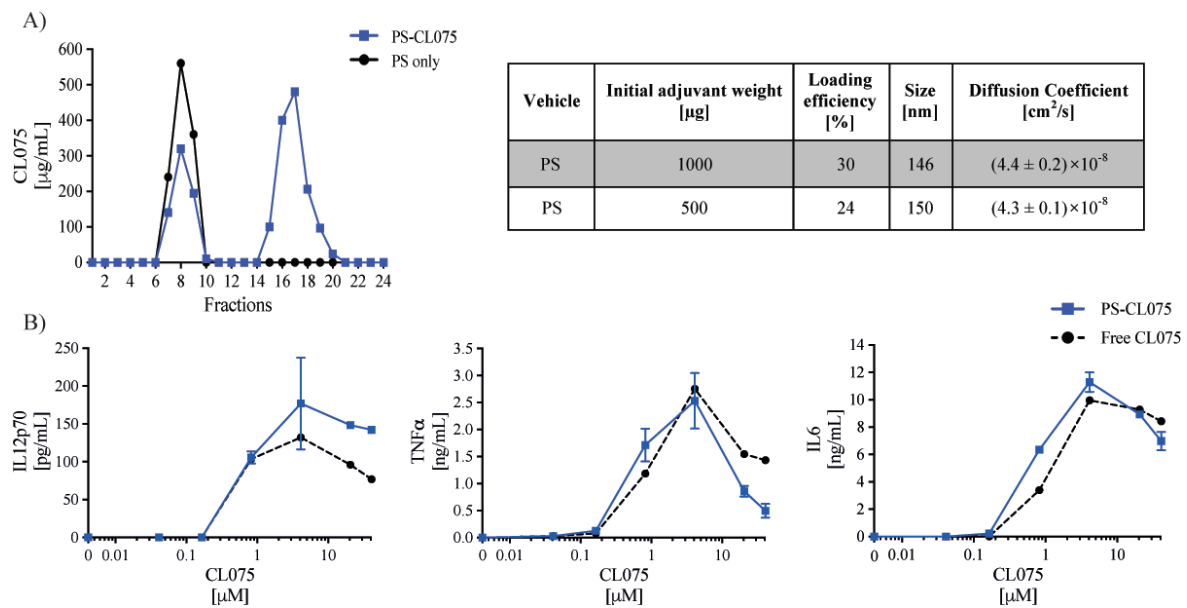


Figure 2.6 CL075, TLR-7/8 agonist, purification and BMDC activation comparison between encapsulated vs free adjuvant. (A) Size exclusion chromatography with sepharose CL-6B beads (*left graph*) and adjuvanted-particles characteristics (*right table*). Quantification of CL075 and PSs were done by HPLC with a gpc column in DMF. BMDCs were incubated for 24h with different concentrations of free, or encapsulated, CL075 before collecting the supernatant and performing IL12p70, TNF α and IL6 ELISAs. All experiments were repeated three times.

CpG-B adjuvant, TLR-9 agonist, was chemically conjugated to nanoparticles

CpG-B is a hydrophilic single stranded DNA, which does not naturally contain any thiols. To deliver it with nanoparticles, the adjuvant was purchased with a modification on the 5' end, where a thiol was added to the phosphate. Due to some difficulties conjugating the adjuvant to nanoparticles, different ratio of pyridyl disulfide cysteamine to CpG-B were tested to determine if the conjugation efficiency could be increased (Fig.2.7.A). The optimal ratio was when there was 2.5x more PDC than CpG-B, whereas small changes in the ratio reduced the conjugation. Interestingly, the production of IL12p70 by BMDCs follows similar trends for low concentration of adjuvant whereas at higher doses, NP-CpG-B had higher levels of cytokines (Fig.2.7.B, left). TNF α production is also not influenced by the addition of nanoparticles (Fig.2.7.B, middle) whereas a decrease in IL10 was observed at all doses except the highest dose tested (Fig.2.7.B, right). Overall, the peak of cytokine production for the free adjuvant was at 0.41 μ M and higher dose was toxic for the cells but the conjugated version induced higher concentration of cytokine at the 4.1 μ M. Since CpG-B is hydrophilic, the encapsulation in polymersomes was tested, but the loading efficiency was below 1% and so was not further tested (Fig.2.7.C).

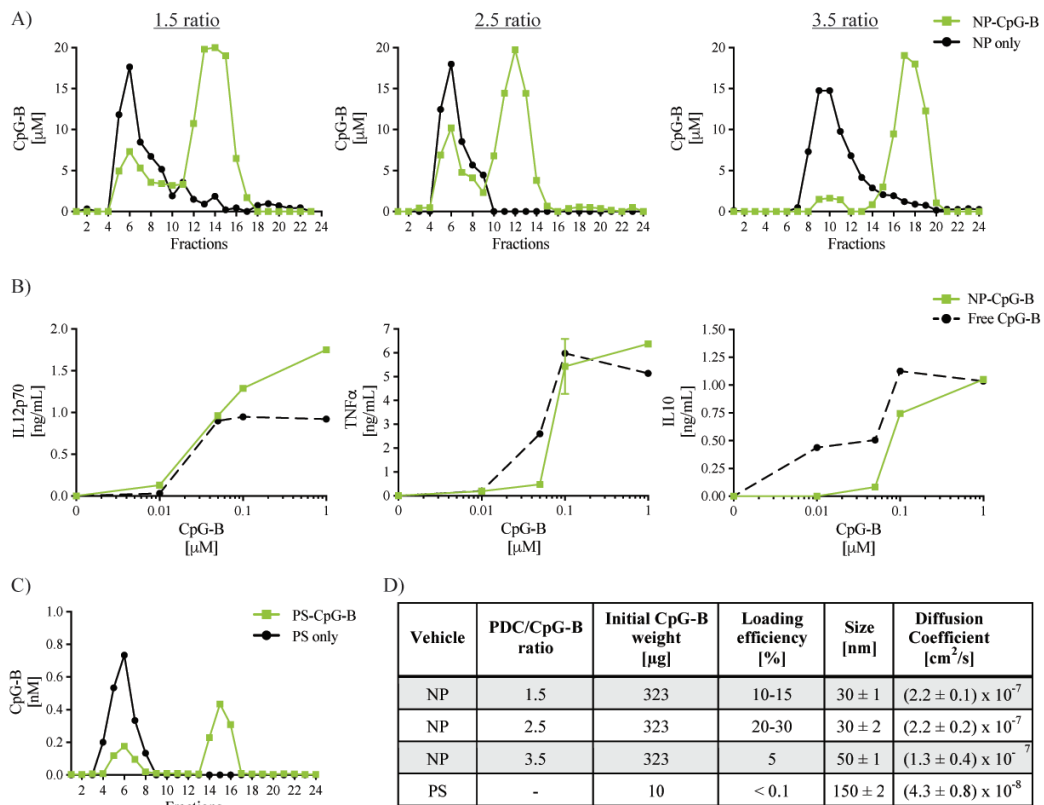


Figure 2.7 CpG-B loading efficiency and BMDC activation, *in vitro*. (A) Size exclusion chromatography performed with sepharose CL-6B beads. From left to right, the ratio of PDC to CpG-B was 1.5, 2.5 and 3.5, respectively. (B) BMDCs were incubated for 24h with different concentration of free, or encapsulated, CpG-B before collecting the supernatant and performing IL12p70, TNF α and IL10 ELISAs. (C) size exclusion chromatography, similar as for NP-CpG-B, with PS-CpG-B. Adjuvant was quantified by GelRed assay and NPs by iodine assay. (D) Summary of the loading efficiency with the different particles, their size obtained by DLS and diffusion coefficient calculated using the Stokes-Einstein equation. All experiments were repeated three times.

The different diffusion coefficients were not influencing the cell uptake speed and both nanocarriers are endocytosed by macropinocytosis

Since most of the *in vitro* experiments are done under static conditions and particles have different sizes, thus different diffusion coefficient, uptake experiments were performed to determine if there was an influence due to the size and the uptake route between particles. Fluorescently labeled OVA conjugated to NPs were incubated with BMDCs and the plate was either static or gently shaken. No difference in cell uptake was observed, since both conditions follow the same trends (Fig.2.8.A, *left*). Afterwards, the uptake of free OVA was compared to NP-OVA in static and shaken conditions, to determine if the differences in some cytokine concentration (Fig.2.5.C or Fig.2.6.B) were due to the delay in cell uptake caused by diffusion. Again, no significant difference for static and dynamic conditions was observed (Fig.2.8.A, *middle & right*). A similar experiment as in point A was performed but with free fluorescein (FITC) and PS-FITC. Again, no difference was observed in the cell uptake, when cells are incubated with PS-FITC under static conditions or dynamic mixing condition (Fig.2.8.B, *left*). The uptake of free or encapsulated FITC by BMDCs, under static or dynamic conditions, showed similar trends between the two treatments (Fig.2.8.B, *middle & right*). We were also interested in the uptake mechanism used by BMDCs for nanoparticles and polymersomes. A lower dose of amiloride, a macropinocytosis inhibitor, was needed to reduce the uptake of NPs than dynasore, a clathrin-mediated uptake inhibitor, and filipin III, a caveolae uptake inhibitor, but all three inhibitors were able to decrease to a certain extent uptake (Fig.2.8.C). Polymersomes also had a reduced uptake when cells were treated with amiloride and dynasore but not at all by filipin III (Fig.2.8.D).

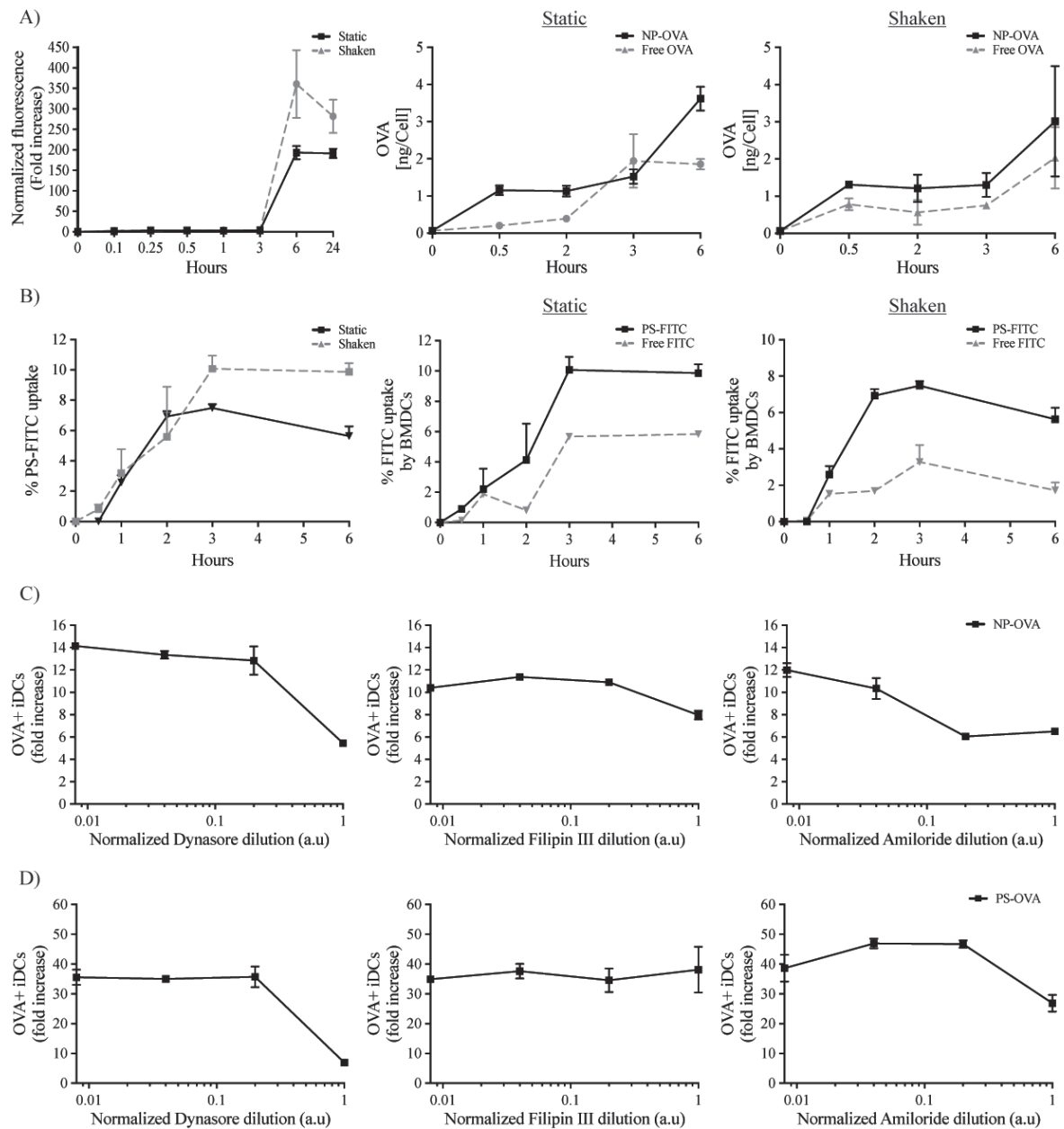


Figure 2.8 Influence of the particle size on BMDCs uptake. (A) BMDCs were incubated with only NP-OVA-AF647 under static or dynamic conditions (*left graph*) and with free OVA-AF647, or conjugated, under either condition (*middle & right graph*). *Left*, BMDCs were incubated with NP-OVA-AF647 under static or shaken conditions before collecting the cells at different time point, washing them and quantifying their fluorescence. *Middle & Right*, BMDCs were incubated with free or NP conjugated OVA-AF647 under static or dynamic condition, respectively, before collecting cells and quantifying fluorescence in cells. (B) BMDCs were incubated with only PS-FITC under static or dynamic conditions (*left graph*) and with free FITC or encapsulated, under either conditions (*middle & right graph*). *Left*, BMDCs were incubated with PS-FITC under static or shaken conditions before collecting the cells at different time point, washing them and quantifying their fluorescence. *Middle & Right*, BMDCs were incubated with free or PS conjugated FITC under static or dynamic condition, respectively, before collecting cells and quantifying fluorescence in cells. (C-D) BMDCs are treated with NP-OVA-AF647 or PS-OVA-AF647 for 4 h with three different cell uptake inhibitors, dynasore, filipin III and amiloride. All experiments were repeated twice.

2.5. Discussion

The first goals of the study were to synthesis and understand the properties of the different nanocarriers, before attempting to formulate the different types of adjuvanted-particles. The first problem encountered with the synthesis of F-127-COOH was to remove the water molecules from the polymer. Initially, F-127-OH was dissolved in toluene and heated to reflux to remove the water using a Dean-Stark trap technique but, unfortunately, the temperature needed was too high and caused the polymer to crash out of the solution. Thankfully, this issue was solved by dissolving the polymer in dichloromethane before precipitating it in methanol and drying it overnight. The formation of the nanoparticle and its size was reproducible but the functionalization would vary between reactions. To determine if it was possible to decrease the variation between batches, the reaction was repeated a second time and only a 2x increase was observed, which was not enough for it to be incorporated in the protocol. Indeed, the only molecule influenced by the concentration of PDC was CpG-B and the value obtained with the 2nd reaction was still too low to induce a good conjugation. In the case of the PEG₁₇-b-PPS₃₀ polymer used for the formation of polymersomes, it was an obligation to have a number of propylene sulfide monomeric units between 28-30 since the vesicles would not form with higher values. The most important factors controlling the chain length were the purity of PEG-OMs and the accidental incorporation of oxygen when transferring the mesylated-PEG in the reaction flask. Overall, if the molecule of interest was hydrophobic, three options were possible to deliver it with either vehicle. It could be encapsulated in the nanoparticle core during its formation or adsorbed on its surface once NPs were already formed. The surface adsorption was possible only if the molecule contained one, or several, hydrophobic tails. For polymersomes, it could either be dissolved with the polymer before the formation of a thin layer or once particles were already form. A hydrophilic molecule containing a thiol could be conjugated to nanoparticle thanks to a disulfide exchange reaction with the PDC groups and finally, any hydrophilic molecule, if not too big, could be encapsulated in polymersomes.

Unfortunately, the TLR-3 agonist tested could not be encapsulated in polymersomes, due to its size and so another vehicle should be developed in order to be able to deliver it. Currently, in vaccines using Poly(I:C) as adjuvant, Poly(I:C) is complexed to a positively charged particle such as chitosan polymer, PLGA or polyethylenimine (PEI)^{94,95,96}. All articles mentioned previously took advantage of the negatively charged adjuvant to deliver it by electrostatic interaction. *Velutto et al*⁹⁷ synthesized and used a PEG₄₄-PPS₄₀-PEI₁₂₀ polymer to deliver plasmid OVA in B16-F10 melanoma and increased the immune response against the tumor. A solution for this adjuvant would be to either use the same construct mentioned previously or add PEI to the polymer used for our polymersomes.

Inversely to poly(I:C), the second adjuvant, MPLA, could be adsorbed on both nanocarriers thanks to its hydrophobic property. Since the quantification by HEK-blue TLR-4 assay determines the effective concentration of MPLA, which could underestimate the correct concentration, MPLA was also fluorescently labeled and quantified. Values obtained for PSs, were exactly the same independently of the assay, whereas the concentration of adjuvant when adsorbed on nanoparticles varied between 20-60% between assays. In addition, the result of HEK-blue TLR-4 endotoxin assay had several false positives, indicating an overestimation of the concentration and a possibility of aggregation of nanoparticles. A dose of MPLA higher than 570 nM, for BMDCs activation, induced lower cytokine levels compared to a lower dose, indicating either toxicity or exhaustion of cells due to an over activation. Although the same dose of MPLA, either free or adsorbed on PSs, was added to BMDCs, lower levels of cytokines were detected for the PS-MPLA conditions. An explanation would be that several adjuvants are adsorbed on one particle and thus the overall number of cells activated would be lower.

The TLR-7/8 agonist was adsorbed in polymersomes, as was MPLA, and purified by size exclusion chromatography. The activation of BMDCs with different concentrations of adjuvant showed exactly the same levels of cytokines independently of the presence of nanocarrier and, again, the higher dose induced exhaustion or cell death. The adjuvant could also be incorporated in the nanoparticle hydrophobic core but, due to technical reasons, it was not tested. Indeed, the quantification of CL075 was done by HPLC in an organic GPC column after lyophilizing a sample and resuspending it in an organic solvent. This approach would not release the adjuvant from the nanoparticle due to the cross-linking of the core and so another solution should be found to quantify it.

Different ratios of pyridyl disulfide cysteamine to CpG-B were tested to determine the best conjugation efficiency. The optimal ratio found was 2.5 and the conjugation decreased drastically if the ratio changes of ± 1 . Concerning the activation of BMDCs, *in vitro*, IL12p70 concentration followed the same trends as the free adjuvant but, at high doses, higher cytokine levels were present when CpG-B was conjugated. An explanation for this result would be a reduced toxicity of the adjuvant when delivered by nanoparticles since the highest dose tested, 1 μ M, had similar, or lower, cytokine levels when treated with free CpG-B. A slight decrease in IL10 cytokine was also observed when cells were treated with NP-CpG-B, which would be an advantage for the vaccine since this cytokine is known to downregulate the expression of T_H1 cytokines, MHC-II antigens and co-stimulatory molecules. The encapsulation in polymersomes was not successful because there

was no interaction driving the ssDNA to enter the vesicle. The same polymer structure discussed for the poly(I:C) adjuvant could be used for CpG-B since it is also negatively charged.

Finally, to verify that the difference observed in BMDC activation experiments was not due to the different sizes and diffusion coefficients, uptake experiments were performed. Indeed, since all the *in vitro* experiments are done under static condition, it was important to verify if the uptake speed varied between free OVA or particulated OVA. First of all, cells were taking up NP-OVA at the same speed independently of the conditions, static or shaken. The small difference observed under static conditions between NP-OVA and free OVA protein could be explained by the fact that one nanoparticle had several proteins conjugated to it and so, as soon as the cell endocytoses a particle, the concentration of OVA will increase more rapidly than in the case of the free OVA conditions. This effect was also observed under dynamic conditions, but both conditions follow exactly the same trends. Similar results as for NP-OVA were observed when cells were incubated with free FITC or encapsulated, PS-FITC. The uptake of nanoparticles by BMDCs was inhibited when cells were incubated with dynasore or amiloride but not as strongly with filipin III, indicating a preferential macropinocytosis and clathring-mediated uptake rather than a caveolae mechanism. Polymersomes were also engulfed by BMDCs through the same mechanism but they were not influenced by Filipin III inhibitor indicating no uptake by caveolae-mediated pathway. Indeed, the vesicle size formed by caveolae-mediated ranges around 60 nm making it impossible for PSs, 140-170 nm, to use this pathway to enter the cells.

Overall, three different adjuvants could be successfully encapsulated, conjugated or adsorbed on either nanocarriers without strongly affecting their activations on BMDCs. In addition, the different diffusion coefficient did not influence their uptake by BMDCs. The next study was to test the different adjuvanted-particles in combination to determine if synergistic activation could be observed.

Chapter 3

Combinatorial *in vitro* and *in vivo* screening of adjuvanted-nanoparticulates

3.1. Abstract

One essential aspect in the development of an efficient therapeutic cancer vaccine is the delivery of immunostimulatory molecules that rationally target appropriate molecular pathways with the purpose of optimally inducing strong T cell immune responses. Their dose, physicochemical properties, toxicity, and the delivery system can all directly impact the magnitude and characteristics of the resulting immune response. One of the most common adjuvants used in vaccines nowadays are Toll-like receptor agonists but the toxicity associated with the dose needed to induce a strong immune response is still an issue. Several studies showed synergistic effects when co-targeting multiple TLRs, leading to a decrease in the required dose for a meaningful response, but such approaches also required the adjuvants to be co-delivered on the same delivery platform. In this section, we asked if combinatorial delivery of multiple nanoparticles, each harboring a different adjuvant, can produce similar synergistic effects in terms of BMDC activation *in vitro*, and further, if such *in vitro* screens may translate to optimal T cell immune responses *in vitro* or *in vivo*.

The combination of PS-CL075 with NP-CpG-B induced the least synergistic effect in cytokine secretion after activating BMDCs, *in vitro*. On the other hand, strong effects were obtained when combining PS-MPLA with either PS-CL075 or NP-CpG-B. In addition, the secretion of IL10 was induced by DCs due to the too strong activation occurring with certain adjuvant combinations. However, the formulations that performed the best in the *in vitro* BMDC screen did not translate to enhance T cell immune responses, *in vitro* and *in vivo*. Finally, the most promising adjuvant combination obtained was when a 1:5 ratio of NP-CpG-B with PS-MPLA were co-injected since a clear decrease in tumor growth was observed and it is worth noting that this combination did not increase T cell immune response. First of all, these results suggest that although synergistic effects were observed when activating two different TLR pathways, BMDCs activation *in vitro* did not allow to fully understand its activation potential since IL10 secretion was induced for certain adjuvant combinations, which can be due to the experimental limitations. In addition, the mechanism by which adjuvant-mediated lymphocyte immune response is not a straightforward process, and several other parameters, as well as the environment, come into account for their activation.

3.2. Introduction

One of the reasons for the safety of subunit vaccines is because they are not composed of the entire pathogen but only the most dominant antigens, thereby focusing the education of the adaptive immune response to the components of the pathogen⁹⁸. In addition, live-attenuated or inactivated viruses used in vaccines have a broad range of immunostimulatory molecules, creating a good combination of signals to induce a strong and protective immune response against the disease⁹⁹. Usually, adjuvants are incorporated into vaccines to increase their efficacy, but in spite of this, the most effective form of it is still not comparable to vaccination with entire pathogens. Because this is obviously a non-ideal solution due to biosafety concerns, building effective and safe vaccines requires improving the immunogenicity of subunit vaccine formulations. The simplest way of accomplishing this was to increase the amount of adjuvants used, but this approach also increases the risk of side effects, which can range from a simple rash to the development of autoimmune disease or worse¹⁰⁰. This illustrates that the optimization of subunit vaccine efficacy and immunogenicity requires a fine equilibrium between toxicity and strength of the immune activation.

An alternative approach to this problem would be to increase the organ or cellular targeting efficiency, either by direct injection of vaccine formulations in the correct anatomic location or using methods to increase retention time in the targeted organ. Such an approach would decrease the risk of side effects, while potentially decreasing the amount of adjuvants needed to induce the same response as a higher dose administered systemically¹⁰¹. Following the same logic, others have achieved the same ends through adjuvant delivery with nanocarriers specifically designed to target specific anatomic locations^{102, 103}, or adding targeting molecules to the vaccine to interact only with the cell/organ of interest^{104, 105}. Our laboratory has used such approaches by delivering CpG-B with NPs to induce a similar response at a lower dose than the free TLR-9 agonist due to a higher drainage efficacy to the lymph node and an increased uptake by APCs⁴⁸.

Another strategy to improve adaptive immune responses at lower doses of adjuvant would be to combine adjuvants targeted to multiple immune activation pathways, with the goals of inducing synergistic effects¹⁰⁵. The most common and well-studied adjuvants are a subset of the pattern recognition receptors family, called Toll-like receptors. The stimulation of TLRs induce a conformational change, which in turn initiate a cascade of events resulting in the production of cytokines, chemokines and co-stimulatory molecules, depending on the type of agonist used (Fig.3.1).

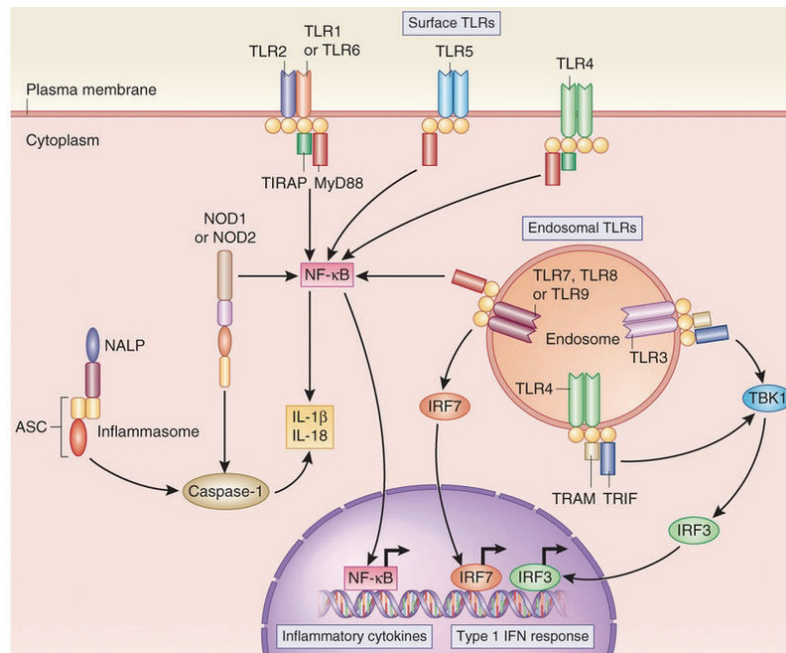


Figure 3.1 Pattern recognition receptors activating innate immune response and their subcellular location. Image adapted from Reed et al ¹⁰⁶

The rationale in targeting different immune activation pathways is the potential to induce a broader range of cytokines secreted by the cell, thereby increasing the diversity and magnitude of the resulting immune response. Kasturi et al. showed an increase in antigen-specific neutralizing antibodies when the antigen, a TLR-9 and a TLR-7/8 agonist were co-delivered in PLGA nanoparticles, versus when single TLR agonists were co-administered with the antigen ¹⁰⁷. Another group showed a synergistic effect when the TLR-4 and TLR-7/8 agonists were co-delivered within a liposome, magnifying the activation of the adaptive immune response ^{108, 109}. Finally, co-targeting the TLR-4 and TLR-9 has also been shown to improve the inflammatory activation of macrophages ¹⁰⁹. In all of these cases, the adjuvant combinations were co-delivered on the same delivery system, with the potential of activating different pathways within the same cell. The adjuvant concentrations, within these studies, are never varied and so an open question remains as if there was an optimal adjuvant ratio combination to further increase even more the synergistic effect.

For this purpose, we performed a combinatorial screening of our adjuvanted-particles *in vitro* to determine synergistic effects, even though the adjuvants are no longer on the same delivery system and to determine if the adjuvant ratio influences the immune response. Finally, we determined if the synergistic effects translated in an increased T cell immune response *in vitro* and *in vivo*

3.3. Materials and Methods

Animals

All mice used in experiments were C57BL/6 female 8-12 weeks old, purchased from Harlan (France) or Jackson Laboratory (Bar Harbor, Maine, USA). OT-I and OT-II mice, C57BL/6-Tg(TcraTcrb)1100Mjb/J and B6.Cg-Tg(TcraTcrb)425Cbn/J, respectively, were purchased from Jackson Laboratory. All procedures were performed in compliance with the Veterinary Authority of the Canton of Vaud (Switzerland) according to Swiss laws and the Institutional Animal Care and Use Committee at the University of Chicago (USA).

Cell line

The melanoma B16-F10 expressing ovalbumin (B16-OVA) cells line was gifted from Bertrand Huard (University of Geneva, Switzerland) and was maintained in high glucose DMEM (Gibco, Waltham, Massachusetts, USA; Catalog # 11995) supplemented with 10% FBS.

Materials, Reagents, and Antibodies

Reagent grade chemicals were purchased from Sigma-Aldrich (Saint Louis, MO, USA) unless noted otherwise. All adjuvants, except for CpG-B, were purchased from InvivoGen (San Diego, CA, USA). The modified 5'SPO₃-CpG-B (5'-TCCATGACGTTCCCTGACGTT-3') was purchased from Microsynth (Balgach, Switzerland) or TriLink Biotechnologies (San Diego, CA, USA). All materials for cell culture were purchased from Invitrogen/Gibco (Waltham, Massachusetts, USA) unless otherwise noted.

Anti-mouse antibodies CD11c (clone N418), MHC-II (clone M5/114.15.2) were purchased from BioLegend (San Diego, CA, USA) whereas live/dead fixable, CD80 (clone 16-10A1), CD86 (clone GL1), CD40 (clone 3/23), CD8 (clone 53-6.7), CD4 (clone RM4-5), IFN γ (XMG1.2), CD25 (clone PC61), IL2 (clone JES6-5H4), CD45 (clone 30-F11), CD3 (clone 145-2C11), FoxP3 (clone MF23), TNF α (MP6-XT22), CD62L (clone MEL-14) and CD44 (clone IM7) were from ThermoFisher Scientific (Waltham, MA, USA). The SIINFELK-specific pentamer, PE-labeled H-2Kb/OVA₂₅₇₋₂₆₄ was purchased from Proimmune (Oxford, UK).

Generation of Bone marrow-derived dendritic cells (BMDCs)

An adapted version of the protocol described by Lutz et al⁹³ was used to generate CD11c⁺ BMDCs. Briefly, bone marrow cells were isolated from a C57BL/6 mouse and cultured for 9 days with 20 ng/mL of GM-CSF. The media was replaced with fresh media every 3 days until day 6 after isolation. At day 9, because 70-85% of the non-adherent cell population expresses the signature

dendritic cell marker CD11c⁺, the bulk unsorted non-adherent cells were used in downstream studies detailed below.

BMDC activation experiments

All BMDC activation experiments were performed in a tissue culture-treated U-bottom 96-well polystyrene plates. They were done with 200'000 cells per well and incubated at 37°C in a 5% CO₂ incubator. Cytokine quantification in the cell culture supernatant was performed following 24 h of incubation, whereas cell phenotype analysis by flow cytometry was performed after 6 h.

BMDC-CD4⁺ or CD8⁺ T cell co-culture experiments

To link BMDC phenotype to T cell activation, BMDCs were co-cultured with CD4⁺ or CD8⁺ T cells. BMDCs were pre-activated overnight with combinatorial adjuvant formulations and 5 μM ovalbumin (OVA), after which the supernatant was collected (stored at -20°C) for further analysis via ELISAs. The BMDCs were washed once with PBS. OVA-specific CD4⁺ or CD8⁺ T cells were isolated from the spleen of OT-II or OT-I transgenic mice, respectively, and purified using the EasySep™ Mouse T cell isolation kit (Stemcell Technologies, Vancouver, CA) following the manufacturer's protocol. T cells were then fluorescently labeled with CFSE (eBioscience, Waltham, MA, USA), and added to the BMDCs at a 1:10 DC:T ratio. Co-culture media (Iscove's Modified Dulbecco's Medium; IMDM, supplemented with 10% FBS, 10² U/mL penicillin and 10² μg/mL streptomycin) was supplemented with OVA for the entirety of the experiment. Co-cultures were incubated for 3 days, after which cell secretion of cytokine was halted through the addition of brefeldin A (final concentration of 5 μg/mL), enabling facile detection of cytokine production at a single-cell level through flow cytometry. After 3h, cells were stained for flow cytometry analysis.

Tumor inoculation and immunizations

An orthotopic injectable melanoma model was employed through the intradermal (i.d.) injection of B16-OVA tumor cells. To expose the injection site, healthy adult wild-type C57BL/6 mice were anesthetized with isoflurane (3.5%), and the dorsal scapular skin on the mouse's right side was shaved and disinfected. 2.5 x 10⁵ B16-OVA tumor cells in 30-45 μL of 0.9% saline solution were delivered intradermally at this site. All nanoparticle adjuvants were prepared as explained in the previous chapter, and conformed for low endotoxins levels by HEK-blue™ TLR-4 assay. The formulations were mixed right before the vaccination, which was administered i.d. in the forelimb, draining the same lymph node as the tumor. The maximum volume injected was 30 μL.

Starting on day 4 post-inoculation, tumors were measured every other day with digital calipers and the volume was calculated using an ellipsoidal equation: $V = \frac{4}{3}\pi \times \frac{L}{2} \times \frac{W}{2} \times \frac{H}{2}$, where L is the length, W is the width and H is the height.

Whole organ/tumor processing into single-cell suspensions

To analyze immune responses within specific anatomic compartments, the tumor-draining lymph node (TdLN), the spleen and the tumor were harvested and processed into single-cell suspensions for flow cytometry. For the TdLN and the spleen, cell suspensions were obtained by mechanically disrupting the organ and rinsing with PBS, or IMDM, through a 0.7 μm cell strainer (CorningTM, NY, USA), and then centrifuging the resulting cell suspension at 1500 rpm for 5 min. The TdLN was then resuspended in IMDM supplemented with 10% FBS, 10^2 U/mL penicillin, 10^2 $\mu\text{g}/\text{mL}$ streptomycin and 20 μM 2-mercaptoethanol (Full media) and counted. Splenocytes were first washed in a hypotonic solution of ammonium chloride-potassium bicarbonate (ACK) for 2 min to remove red blood cells, prior to centrifugation at 1500 rpm for 5 min, resuspension in full media and counting. The tumor cell suspension was obtained by adapting a protocol from Broggi et al ¹¹⁰. Briefly, the tumor was minced, and then digested in digestion media (DMEM + 2% FBS + 1.2 mM CaCl_2 + 10^2 U/mL penicillin + 10^2 $\mu\text{g}/\text{mL}$ streptomycin) supplemented with 1 mg/mL Collagenase IV and 40 $\mu\text{g}/\text{mL}$ DNase I (Worthington Biochemical Corp, Lakewood, New Jersey, USA). This suspension was gently stirred at 37°C for 30 min, further disrupted by repetitively pipetting 100x, and then filtered through a 70 μm strainer. The remaining undigested tumor fragments were further digested at 37°C for 1 h in a second digestion mix consisting of digestion buffer supplemented with 3.5 mg/mL Collagenase D and 40 $\mu\text{g}/\text{mL}$ DNase I. The tumor fragments were further mechanically disrupted through repetitive pipetting them 100x. The enzymes were quenched through the addition of EDTA to a final concentration of 2.5 mM, and then the cell suspensions were filtered through a 70 μm strainer and combined with the cells from the first digestion step. As tumors may contain a significant amount of blood, the resulting cell suspensions were treated similarly to the splenocytes described above before they were resuspended in full media and counted.

Ex vivo restimulation

For the reactivation of antigen-specific T cells in TdLNs and spleens, these organs were processed into single-cell suspensions as described above, and then plated in U-bottom 96-well plates at up to 2×10^6 cells/well. The cells were incubated at 37°C in a 5% CO_2 incubator with 2 $\mu\text{g}/\text{mL}$ of antigenic peptide in full medium. For cytokine quantification by ELISA, supernatants were collected following 4 days of incubation, whereas for flow cytometry analysis, cells were incubated for 3 h prior to halting cytokine export through the addition of brefeldin A to a final

concentration of 5 µg/mL, followed by incubation for an additional 3 h before harvest. To re-stimulate antigen-specific CD8⁺ T cells, the MHC-I-dominant peptides OVA₂₅₇₋₂₆₄ (SIINFEKL), TRP-2₁₈₁₋₁₈₈ or gp100₂₅₋₃₃ were used, whereas CD4⁺ T cells were reactivated with OVA₃₂₃₋₃₃₉.

Flow cytometry

Cell suspensions were centrifuged and washed with 1x PBS, and then incubated with a fixable live/dead at 4°C for 15 min (eBioscience) and washed once with PBS. Antigen-specific T cells were detected via pentamer staining, which was performed by incubating cells at room temperature in a solution of 1x PBS supplemented with 2% FBS (staining buffer), for 20-30 min. For surface staining, a cocktail of antibody was diluted in staining buffer and incubated at 4°C for 15 min in the dark. Intracellular staining and intranuclear staining were performed with the BD cytofix/cytopermTM Kit or FoxP3 staining kit, respectively, according to the manufacturer's instructions. Finally, the cells were washed with staining buffer and stored in the same buffer for data collection.

ELISA

Cytokines detection and quantification were performed with Ready-SET-Go! ELISA kits purchased from ThermoFisher Scientific and used according to the manufacturer's instructions.

Data collection

Flow cytometry was performed using either a CyAnTM ADP (Beckman Coulter, Brea, CA USA) or a BD LSRFortessaTM (BD Biosciences, San Jose, CA, USA). The data obtained were analyzed with FlowJo (v.10, FlowJo LLC, Ashland, OR, USA). Graphs and statistical analysis were done using the GraphPad Prism 7 Software (GraphPad Software Inc, La Jolla, CA, USA). Synergistic effect was defined as an effect higher than the sum of the individual adjuvant and noted with a *. Statistical significance between the different groups *in vivo* was determined with a one-way analysis of variance (ANOVA) followed by a Bonferroni post-test correction. * and ** indicate P values less than 0.05 and 0.01, respectively.

3.4. Results

Based on our results in the previous chapter showing the efficacy of nanoparticle adjuvants to activate BMDCs *in vitro*, the next question was if combinatorial administration of multiple adjuvanted-nanoparticles might lead to synergistic effects in BMDC activation, and subsequently, T cell-mediated immune responses, *in vitro* and *in vivo*. Specifically, nanoparticle adjuvants targeting any pair of different TLR pathways were co-administered in order to characterize dose responses in an *in vitro* screen, followed by administration of the most efficacious combinations, *in vivo*, in an orthotopic aggressive melanoma model.

Combining PS-MPLA with PS-CL075 promotes synergistic effects on BMDC activation and cytokine production by CD4⁺ T cells in vitro

To investigate combinatorial activation of TLR-4 and TLR-7/8, PS-MPLA and PS-CL075 were co-administered, and BMDC activation was quantified based on their cytokine production and surface expression of co-stimulatory molecules. For both adjuvants, dosing was based on the dose response experiments performed in the previous chapter (Fig.2.5.B & Fig.2.6.B). BMDCs were incubated for 24 h or 6 h, before collecting the supernatant, for cytokines quantification by ELISA, and cells, for co-stimulatory detection by flow cytometry analysis, respectively (Fig.3.2.A-B). At a fixed dose of PS-MPLA, the addition of 0.4 μ M of PS-CL075 was sufficient to synergize in the production of TNF α , by 2-fold, and IL12p70, between 2- to 4-fold, depending on the PS-MPLA dose (Fig.3.2.A, *left & middle*). The secretion of IL10 was also increased at high doses of PS-CL075 (Fig.3.2.A, *right*). The activation of BMDCs showed no synergistic effect between combinations, except for an upregulation in the expression of CD40 for all treatments (Fig.3.2.B). Overall all proinflammatory cytokines tested were increased and 4 μ M PS-CL075 did not further increase it compared to the medium dose.

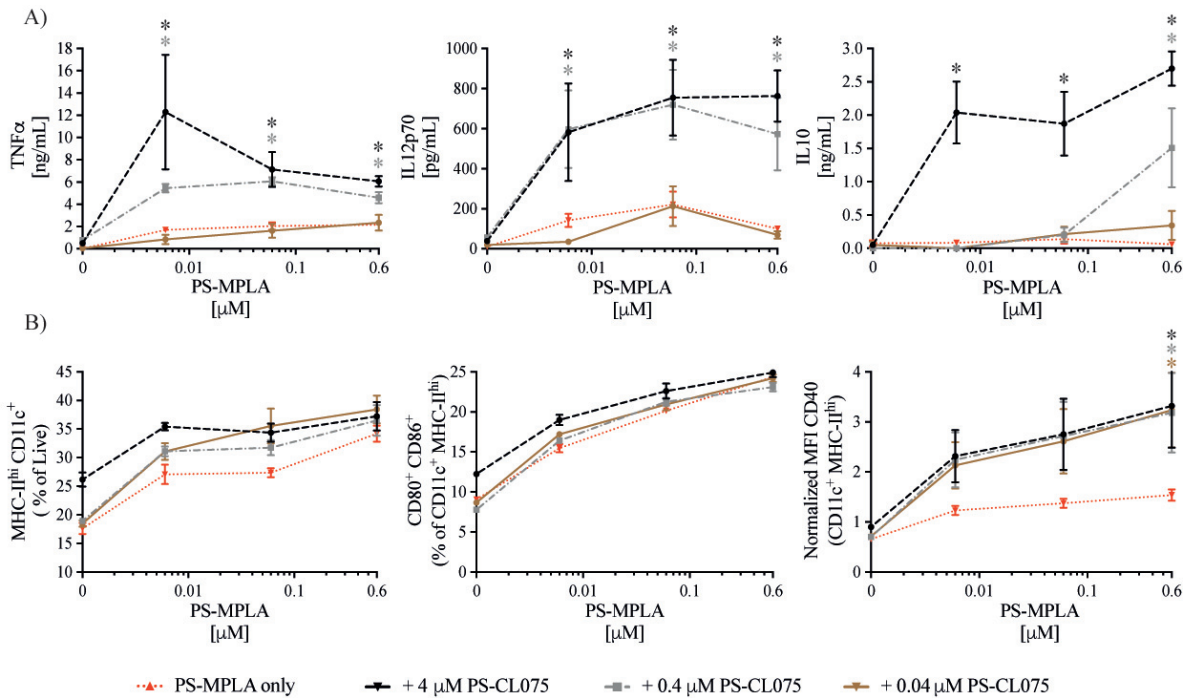


Figure 3.2 BMDCs activation with different PS-MPLA and PS-CL075 combinations showed synergistic effect for proinflammatory cytokines and CD40 expression. (A) Cytokine concentration. Cells were incubated with different doses of PS-MPLA and PS-CL075, for 24 h, before collecting the supernatant and quantifying the cytokines via ELISA. (B) BMDCs activation markers quantification by flow cytometry. Results are representative of two independent repeats, and * represent synergistic effects observed for that specific combination.

To test if the most efficacious combinations at triggering BMDC activation would also consequently induce optimal activation of CD8⁺ or CD4⁺ T cells, adjuvant-activated BMDCs were co-cultured with OVA-reactive OT-I or OT-II cells (Figure 3.3).

The three combinations used for co-cultures were the ones inducing the strongest synergistic effect with different adjuvant formulation ratio, 1:7 and 1:80 of PS-MPLA:PS-CL075. Generally, PS-MPLA and PS-CL075 did not synergize to promote enhanced CD8⁺ T cell activation, although a significant improvement in IL-2 secretion and a small but non-significant increase in proliferation was seen following co-administration at a 1:7 PS-MPLA:PS-CL075 (Fig.3.3.A-B). Focusing on the canonical CD8⁺ T cell effector cytokines, Granzyme B was not increased with the different conditions, and IFN γ was even decreased when a high dose of PS-CL075 was mixed with PS-MPLA, at any dose (Fig.3.3.A). On the other hand, combining PS-MPLA and PS-CL075 contributed to additive effect on IFN γ secretion in CD4⁺ T cells at low doses (Fig.3.3.C, *left*), but not IL2 production since it followed the same curve as the PS-MPLA single adjuvant (Fig.3.3.C, *right*). The flow cytometry analysis showed no difference in proliferation between all conditions (Fig.3.3.D, *left*), but an increase in IL2⁺ and IFN γ ⁺ single positive CD4⁺ T_{EFF/EM} cells, when a high dose of PS-CL075, combined with a medium dose of PS-MPLA, was observed (Fig.3.3.D, *middle & right*).

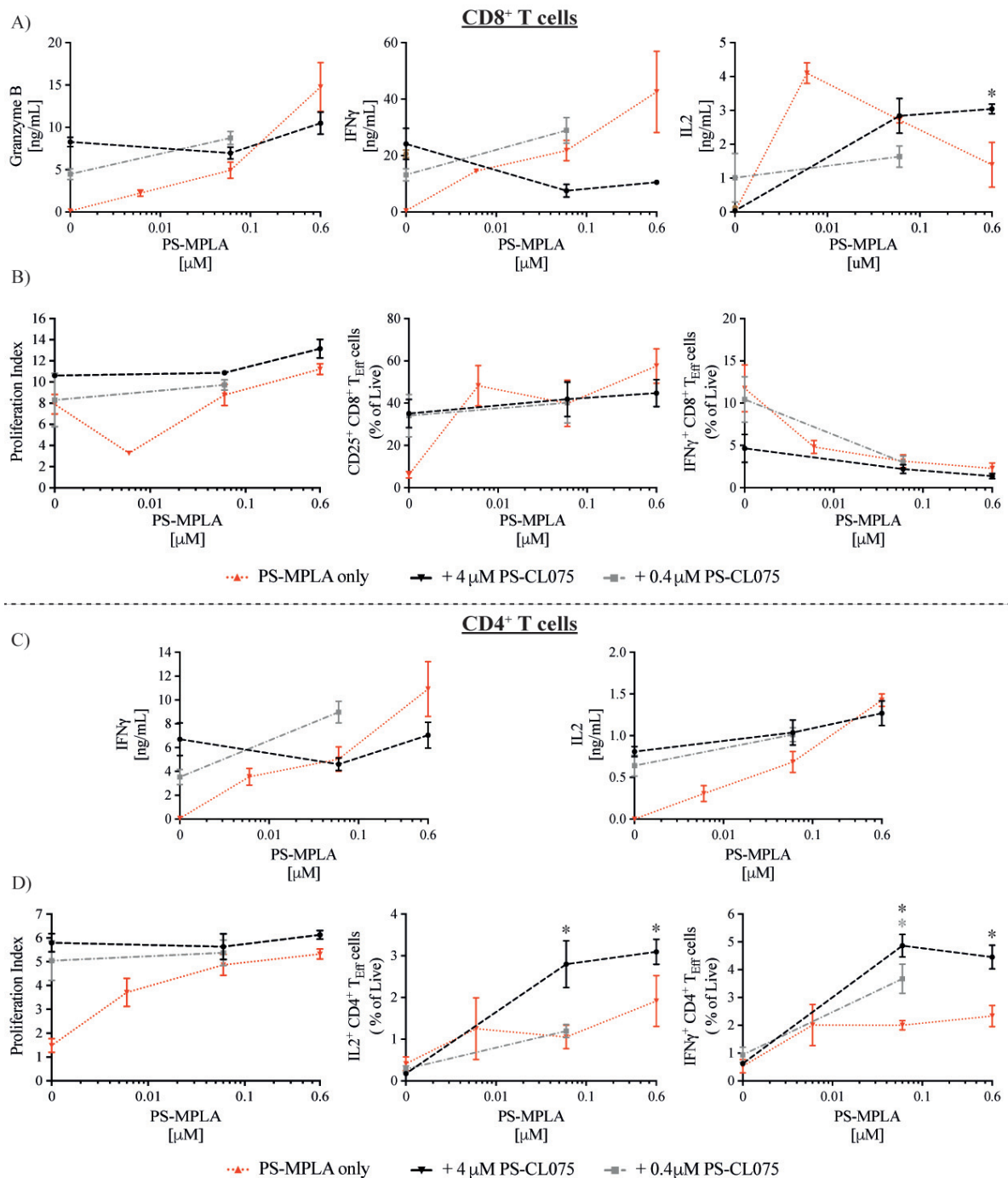


Figure 3.3 An increase in cytokine positive CD4⁺ T_{EFF/EM} but not CD8⁺ T_{EFF/EM} cells was observed. 15'000 BMDCs were activated overnight with OVA and different adjuvant combinations before removing the adjuvant formulation and adding CFSE labeled OT-I or OT-II. After three days, the supernatant was collected for cytokine quantification, by ELISA, and cells were staining for flow cytometry analysis. (A) Granzyme B, IFN γ and IL2 cytokines concentrations in the supernatant. (B) Flow cytometry of CD8⁺ T cells proliferation, activation marker and cytokine production. (C) IFN γ and IL2 concentrations in the supernatant. (D) Flow cytometry of CD4⁺ T cells proliferation and activation markers. Results are representative of three independent repeats, and * represent synergistic effects observed for that specific adjuvant combination.

The addition of PS-CL075 to PS-MPLA slightly increased the percentage of polyfunctional CD4⁺ & CD8⁺ T cells but did not reduce tumor growth

While the PS-MPLA/PS-CL075 combination synergized in BMDC activation, it only translated into an additive effect for T cell activation *in vitro*. On the other hand, in an *in vivo* setting, the limitation observed *in vitro* are less likely to occur and in addition, a multitude of other cells influence the activation of T cell-mediated immune response, which were not taken into account *in vitro*. Therefore, two different adjuvant formulations were tested in a therapeutic vaccine setting, wherein tumor-bearing mice were treated with a vaccine draining the same LN. The different factors considered when preparing the *in vivo* experiment were the vaccination strategy, the model used and the doses tested. Our lab had shown previously that although the TdLN was considered immunosuppressive, it was possible to reprogram it and still induce a cytotoxic CD8⁺ T cells response⁶³. Based on this study, B16-OVA cells were inoculated on the right dorsal scapular skin, and vaccinated, 7 days post tumor cell inoculation. The vaccine was administered i.d. in the forelimb draining the TdLN (Fig.3.4.A). 5 µg/mouse of PS-MPLA was used and two different doses of PS-CL075 were tested, 5 and 15 µg/mouse, which was already higher for the TLR-7/8 than what has been published with this adjuvant¹¹¹. PS-MPLA alone slightly slowed the tumor growth compared to the mock injection (Fig.3.4.B), and it correlated with an increase in the frequency of SIINFEKL-specific CD8⁺ T cells in both the tumor (49 ± 6.6 fold increase) and the spleen (Fig.3.4.C). On the other hand, PS-CL075 alone did not affect tumor growth despite a small increase in tumor antigen-specific CD8⁺ T cells in the tumor and spleen. When PS-MPLA and PS-CL075 were combined, no synergistic effects in terms of decrease tumor growth or increases in tumor antigen-specific CD8⁺ T cells was detected (Fig.3.4.B-C) but similar results to PS-MPLA alone were observed.

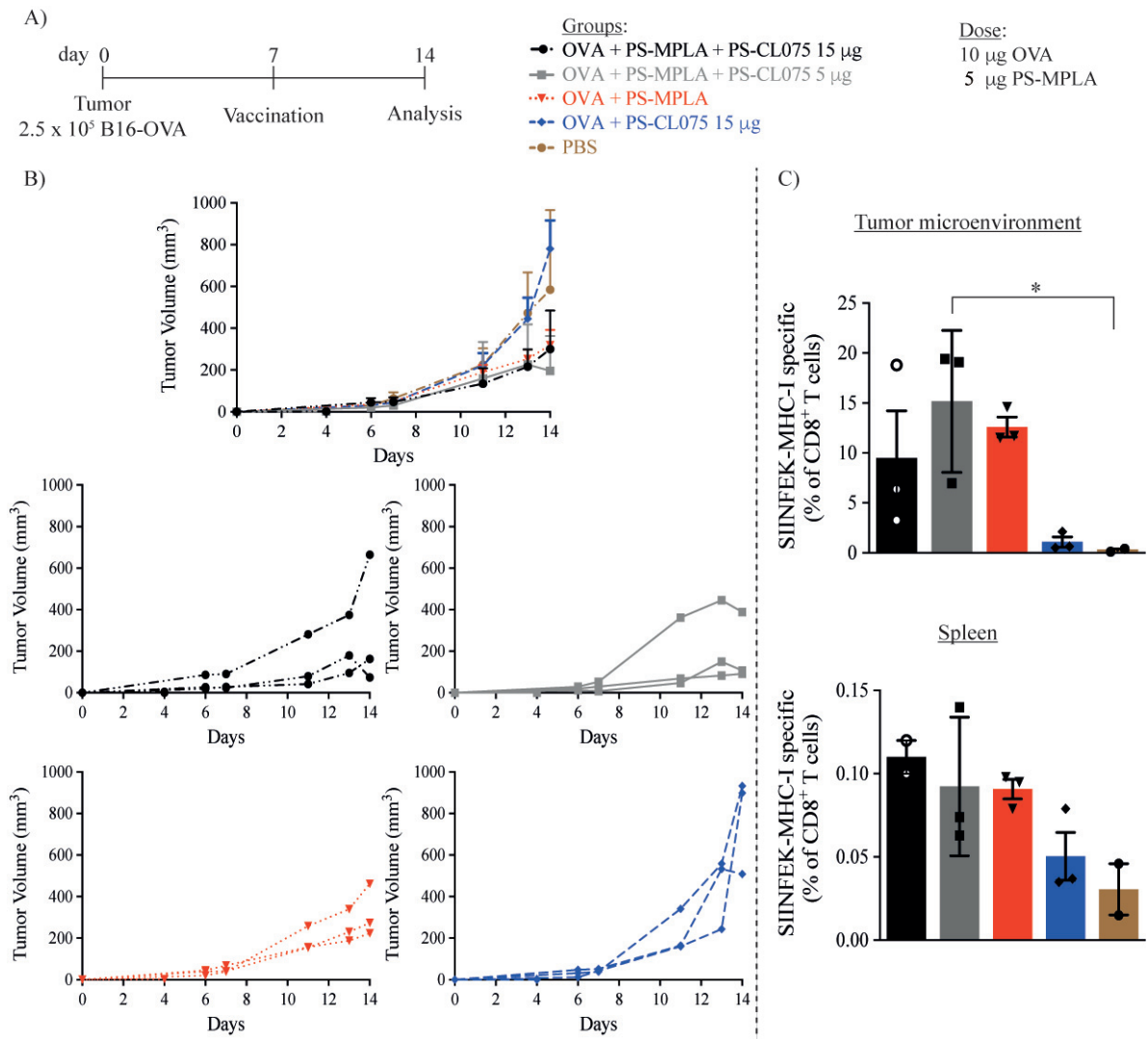


Figure 3.4 The addition of PS-CL075 to PS-MPLA did not delay tumor growth or increase antigen specific CD8^+ T cells. 2.5×10^5 B16-OVA cells were inoculated i.d. in the right dorsal scapular skin. Mice were vaccinated, i.d. in the forelimb draining to the same lymph node as the tumor, 7 days post tumor inoculation, before sacrificing the mice on day 14. (A) Experimental timeline, groups and dose. (B) Overall, and individual, tumor growth. (C) Percentage of SIINFEKL-specific CD8^+ T cells in the tumor microenvironment and the spleen quantified by SIINFEKL-MHC-I pentamer staining. Error bars indicate SEM for (B) and SD for (C) the other. N = 3 mice per groups. *P < 0.05.

To assess if the vaccination induced a T cell immune response, the spleen and the tumor-draining lymph node were restimulated with the MHC-I or MHC-II dominant tumor antigens (SIINFEKL and OVA₃₂₇₋₃₃₉). Following the experimental timeline shown previously (Fig.3.3.A), PS-MPLA alone increased the production of granzyme B and IFN γ relative to mock injected mice. These cytokines were all decreased when PS-CL075 was co-injected with PS-MPLA, independently of the dose (Fig.3.5.A). Inversely, a small increase in polyfunctional CD8^+ T cells were observed in the spleen for all vaccinated groups (Fig.3.5.B, *left*) and only the high dose of PS-CL075 with PS-MPLA induced a higher proportion of polyfunctional CD4^+ T cells compared to the other groups (Fig.3.5.B, *right*). In the tumor-draining lymph node, the granzyme B production was

similar to the one in the spleen between the different groups (Fig.3.5.C, *left*) whereas IFN γ was significantly increased in all treatments compared to mock injected mice (Fig.3.5.C, *right*). Finally, the proportion of polyfunctional CD8 $^{+}$ or CD4 $^{+}$ T cells were not significantly increased compared to the negative control group, but a trend for the combined adjuvants was observed in CD8 $^{+}$ T cells (Fig.3.5.D).

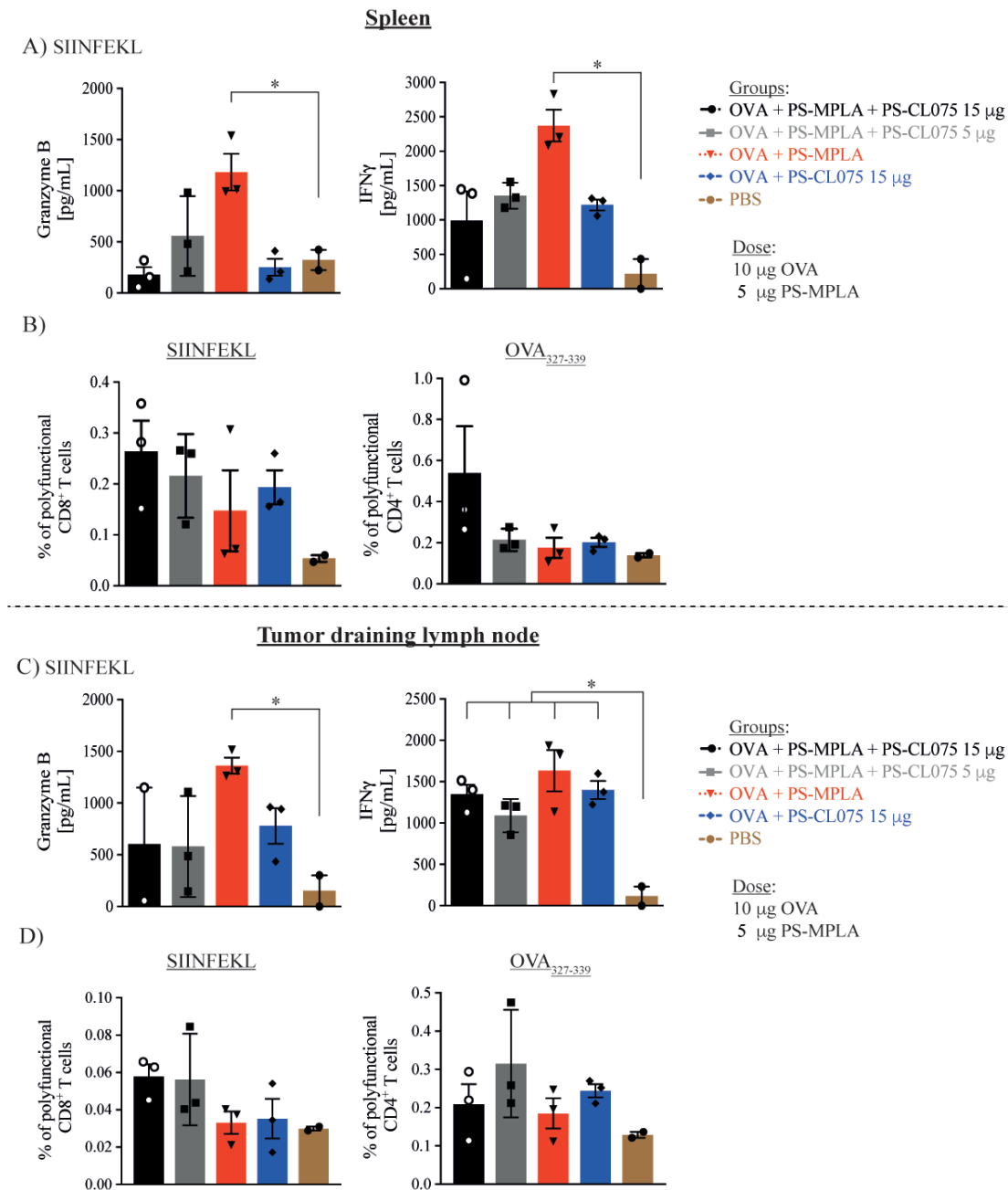


Figure 3.5 A decrease in granzyme B and IFN γ secretion were observed for co-administered adjuvant compared to PS-MPLA only. 2.5×10^5 B16-OVA cells were inoculated i.d. in the right scapular dorsal skin. Mice were vaccinated, i.d. in the forelimb draining to the TdLN, 7 days post tumor inoculation before sacrificed on day 14. (A & C) Granzyme B and IFN γ concentration in the supernatant after SIINFEKL reactivation in the spleen and TdLN, respectively. (B & D) Polyfunctional T cells in the spleen and TdLN, respectively. Polyfunctional cells were T cell secreting two or three of the cytokine: IL2, IFN γ or TNF α . Error bars are SD and N = 3 mice per groups. *P < 0.05.

Combining PS-CL075 with NP-CpG-B induced synergistic effects for TNF α secretion in BMDCs activation as well as CD4⁺ T cell cytokine expression, in vitro

Synergy between targeting of TLR-7/8 and TLR-9 via the nanoparticle adjuvants PS-CL075 and NP-CpG-B, respectively, was evaluated in assays for DC activation and T cell activation in similar fashion as for the previous adjuvant combination (Fig.3.6.A). First of all, the optimal dose of NP-CpG-B for the secretion of cytokines was 0.1 μ M independently of the presence of PS-CL075. Secondly, a synergistic effect was observed for the secretion of TNF α already when a small dose of the TLR-7/8 agonist was added to 0.1 μ M NP-CpG-B but an increase in PS-CL075 concentration did not correlate with higher synergistic effect (Fig.3.6.A, *left*). The highest dose of NP-CpG-B, alone or combined, induced lower concentration of all three cytokines quantified. The flow cytometry analysis showed additive effect in percentage of MHC-II^{hi} DCs as well as CD80⁺ CD86⁺ co-expression and CD40 when 0.01 μ M NP-CpG-B was combined to PS-CL075 at any concentration (Fig.3.6.B, *left*). The addition of the TLR-7/8 agonist to the two other doses of NP-CpG-B did not increase the DC activation or co-stimulatory molecules

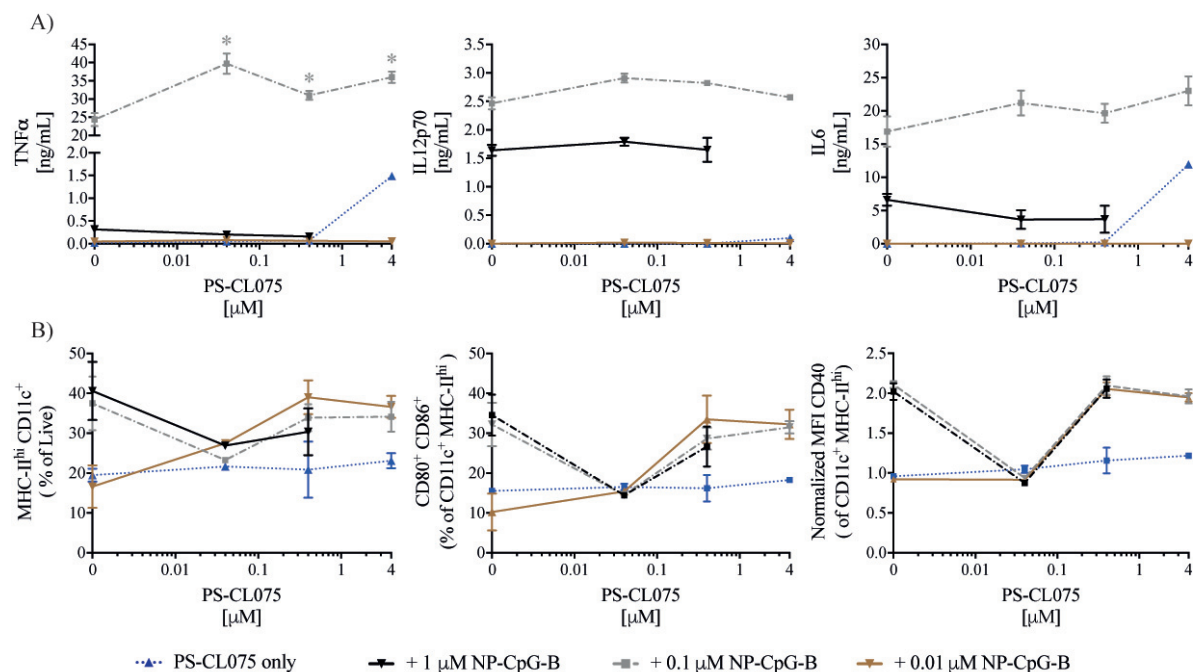


Figure 3.6 Only TNF α production was synergistically increased when 0.1 μ M NP-CpG-B was incubated with PS-CL075. (A) Cytokines concentration in supernatant after 24 h activation quantified by ELISA (B) BMDCs activation markers quantification by flow cytometry. Results are representative of two independent repeats and * represent synergistic effects observed for that specific dose

Based on the results obtained for the BMDC activation experiment, the most promising treatments were tested for their efficacy to indirectly induce CD4⁺ or CD8⁺ T cells activation through DCs with co-culture experiments. The combination tested were all three doses of PS-CL075 with 0.1μM NP-CpG-B. The three different cytokines quantified showed very different trends within the same treatment for CD8⁺ T cell co-culture (Fig.3.7.A). For example, the same combination of PS-CL075 and NP-CpG-B induced a lowered concentration of granzyme B, had no effect on the production of IFNγ compared to NP-CpG-B only, but increased significantly the secretion of IL2. CD8⁺ T cell analysis showed no synergistic effect in proliferation index (Fig.3.7.B, *left*) or the percentage of CD25⁺ CD8⁺ T cells (Fig.3.7.B, *right*), but a small increase in IFNγ⁺ CD8⁺ T cells (Fig.3.7.B, *middle*), when both adjuvants were combined. The CD4⁺ T cell co-culture showed a slight decrease in IFNγ secretion but no variation in the IL2 for the combination of both adjuvants (Fig.3.7.C). The CD4⁺ T cell analysis showed no differences in the proliferation index, the proportion of IFNγ cells and the fluorescence of IL2 between the different combinations (Fig.3.7.D).

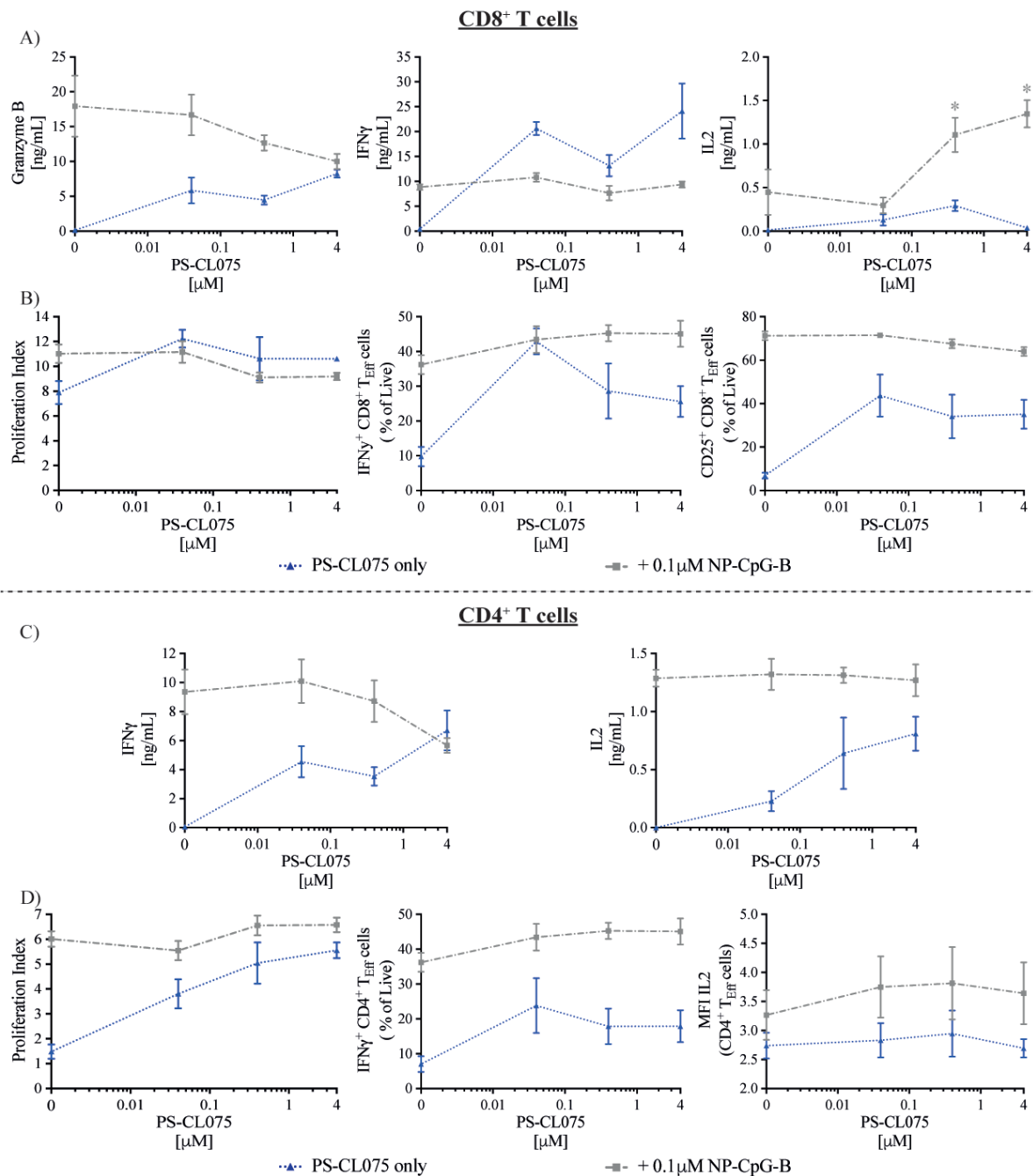


Figure 3.7 Synergistic effect for IL2 secretion in CD8⁺ T cells activation and a small increase in IFN γ + CD4⁺ T cells was detected when combining adjuvants. 15'000 BMDCs were activated overnight with OVA and different adjuvant combinations before removing the adjuvant formulation and adding CFSE labeled OT-I or OT-II. After three days, the supernatant was collected for cytokine quantification, by ELISA, and cells were staining for flow cytometry analysis. (A) Granzyme B, IFN γ and IL2 cytokines concentrations in the supernatant. (B) Flow cytometry of CD8⁺ T cells proliferation, activation marker and cytokine production. (C) IFN γ and IL2 cytokines concentrations in the supernatant. (D) Flow cytometry of CD4⁺ T cells proliferation and activation markers. Results are representative of three independent repeats, and * represent synergistic effects observed for that specific adjuvant combination.

At the dose tested, no enhance in the immune response was observed for the combination of PS-CL075 with NP-CpG-B, in tumor bearing mice

While the combination of these adjuvants synergized in BMDC activation, it only translated into a small increase in T cell activation, *in vitro*. These results demonstrated a stronger efficacy of NP-CpG-B alone to activate DCs compared to the TLR-7/8, and so, we wanted to determine if the addition of PS-CL075 would increase the efficacy of the TLR-9 vaccine in an orthotopical tumor model, *in vivo*. The dose of NP-CpG-B used for the vaccine was considered very low but unfortunately, the conjugation efficiency did not permit to inject a dose higher than 1 µg/mouse whereas the dose of PS-CL075 tested was 15 µg/mouse, which corresponds to what had been used previously in the combination of PS-MPLA + PS-CL075, *in vivo*. Briefly, mice were inoculated with B16-OVA in the right dorsal scapular skin before vaccination in the forelimb draining the TdLN 7 days post-inoculation (Fig.3.8.A). Although no significant difference in tumor growth was observed between treatments, a small delay, for the co-injected adjuvanted-particles, was detected (Fig.3.8.B). In addition three mice died for unknown reasons (red arrow), which, in the case of the PBS treated group, decreased its tumor growth curve, matching the other groups, which would not be the case if they had survive (Fig.3.8.B, *bottom left*). A significant increase in CD8⁺ T cells in addition to a decrease in CD4⁺ T_{reg} cells were observed, in the tumor microenvironment, when mice were vaccinated compared to the negative control group (Fig.3.8.C, *left & middle*). The ratio of activated CD8⁺ T cells over CD4⁺ T_{reg} cells was slightly increased when the treatment contained both adjuvants compared to NP-CpG-B alone but not significantly (Fig.3.8.C, *right*). Finally the percentage in SIINFEKL-specific CD8⁺ T cells, as well as CD25⁺ CD8⁺ T cells, showed similar results independently of the addition of PS-CL075 to NP-CpG-B (Fig.3.8.D).

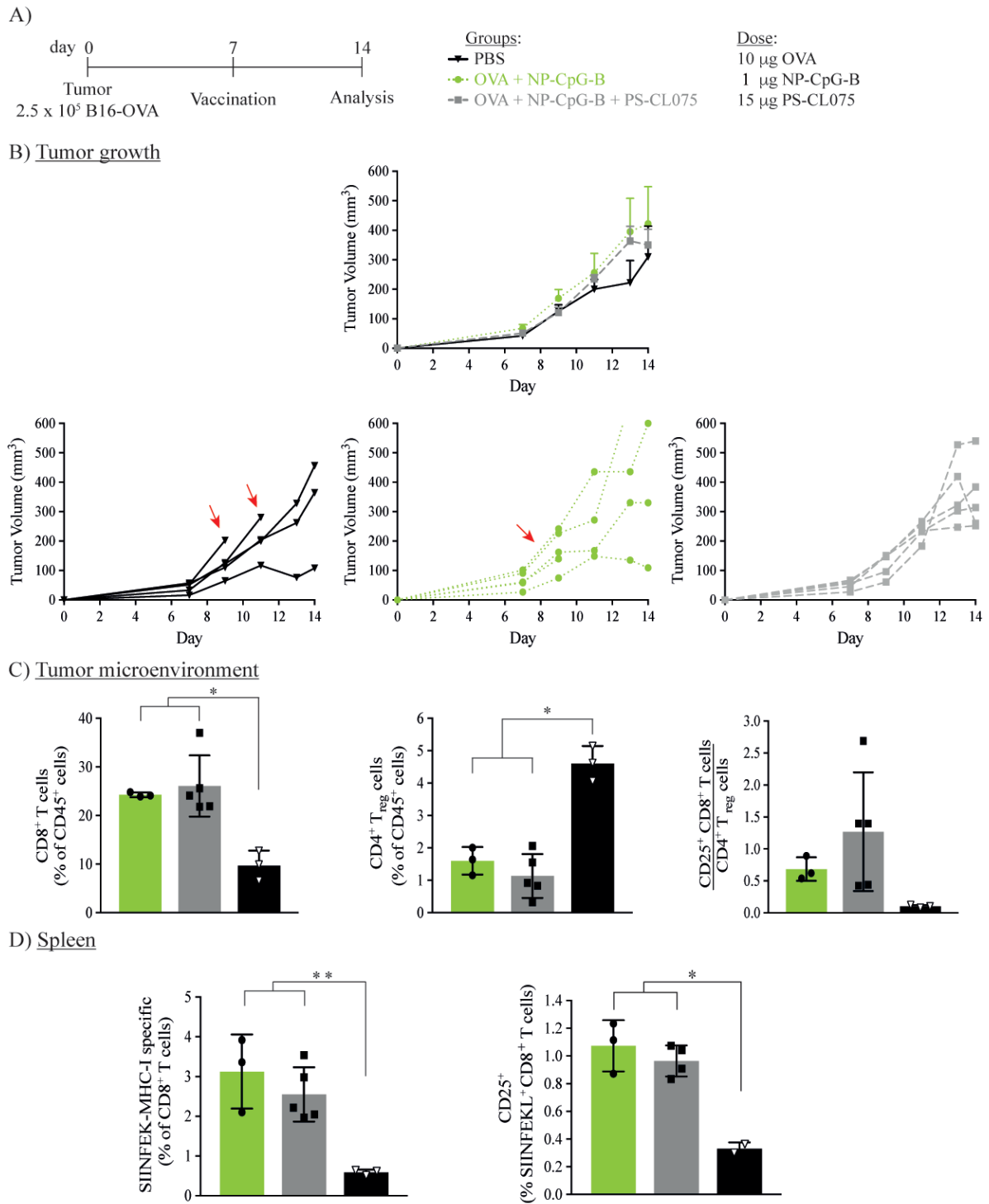


Figure 3.8 PS-CL075 addition to NP-CpG-B vaccine did not delay tumor growth or increase the T cell immune response. 2.5×10^5 B16-OVA cells were inoculated i.d. in the right dorsal scapular skin before vaccinating mice on day 7 i.d. in the forelimb draining to the same lymph node as the tumor (A) Experimental timeline, groups and dose. (B) Overall (*Top*), and individual (*Bottom*), tumor growth. (C) Proportion of CD8⁺ T cells, CD4⁺ T_{reg} cells and the ratio of both in the tumor microenvironments. (D) SIINFEKL-specific CD8⁺ T cells population in the spleen quantified by SIINFEKL-MHC-I pentamer staining. Error bars indicate SEM for (B) and SD for (C-D) the other. N = 3-5 mice per groups. *P < 0.05.

Finally, the T cell immune response was assessed by reactivating the spleen and the tumor-draining lymph nodes with MHC-I or MHC-II dominant tumor antigens. Although vaccinated mice had similar levels of granzyme B, independently of the treatment, a large decrease in IFN γ was observed when PS-CL075 was co-administered (Fig.3.9.A). The restimulation with the SIINFEKL peptide showed identical percentage of TNF α ⁺IFN γ ⁺ CD8⁺ T cells for both vaccines, which were significantly higher than the negative control group (Fig.3.9.B, *left*). A small increase in double positive CD4⁺ T cells was observed for vaccinated groups compared to PBS treated mice (Fig.3.9.B, *middle*) and in addition, the reactivation of CD8⁺ T cells with endogenous antigens, TRP-2 and gp100, showed no significant increase in TNF α positive cells compared to the PBS treated groups, but a small trend was observed (Fig.3.9.B, *right*). The TdLN showed no difference, in granzyme B secretion or polyfunctional T cells, between NP-CpG-B alone or combined to PS-CL075 (Fig.3.9.C-D). Inversely as seen in the spleen, the production of IFN γ was similar between both vaccines and significantly increased compared to PBS treated groups (Fig.3.9.C). Finally, no difference between vaccinated groups was observed when reactivated with endogenous B16-F10 peptides.

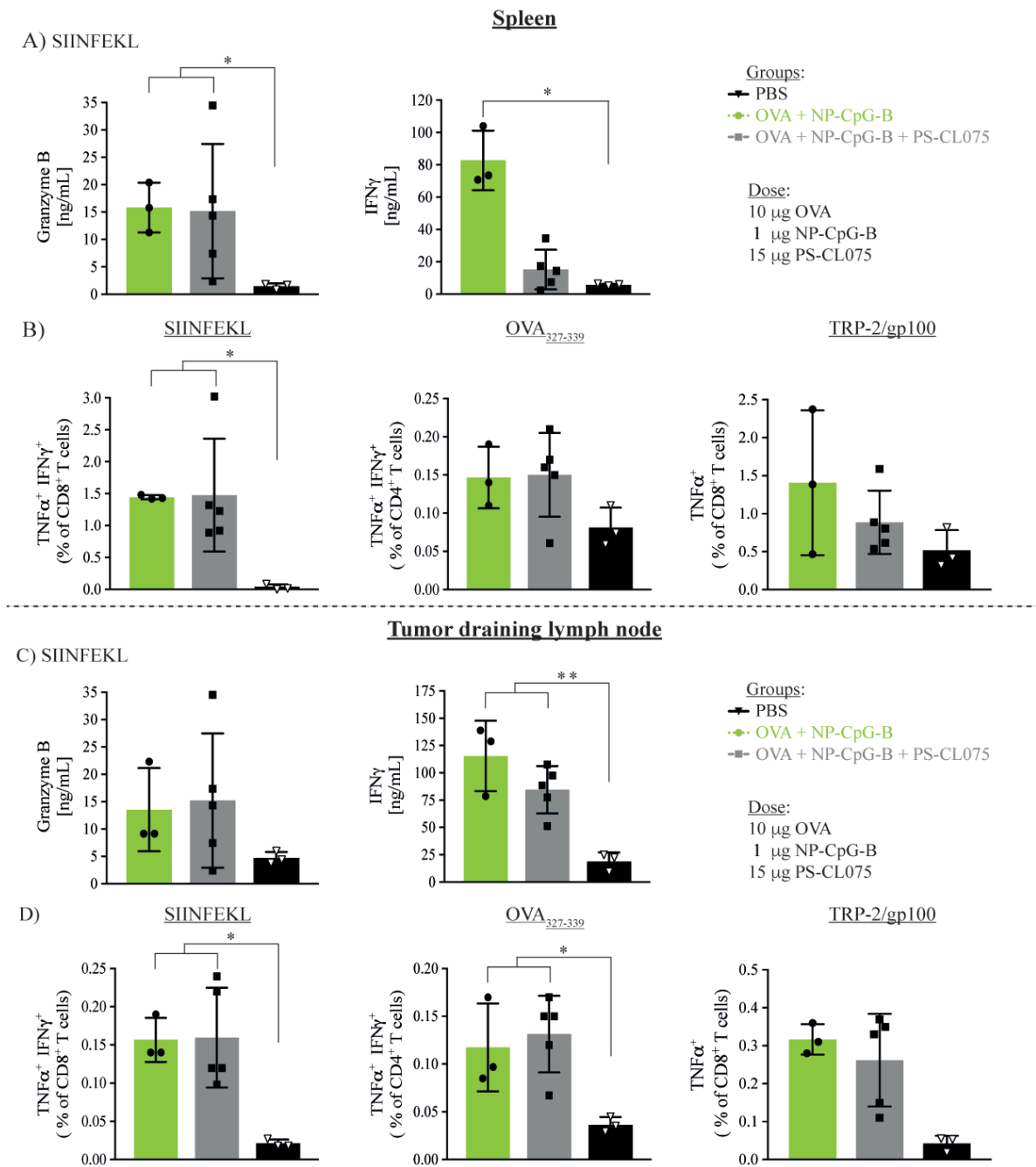


Figure 3.9 The addition of PS-CL075 to NP-CpG-B did not improve the T cells immune response in the spleen or TdLN. 2.5×10^5 B16-OVA cells were inoculated i.d. in the right scapular dorsal skin. Mice were vaccinated, i.d. in the forelimb draining TdLN, 7 days post tumor inoculation. The cytokine secretion quantification (A & C) was done after 4 days incubation before collecting the supernatant whereas polyfunctional T cells quantification by flow cytometry was performed after 6 h incubation (B & D). (A & C) Granzyme B and IFN γ concentration in the supernatant after SIINFEKL reactivation in the spleen and TdLN, respectively. (B & D) Polyfunctionality quantification in the spleen and TdLN. *Left*, was the proportion of TNF α ⁺ IFN γ ⁺ CD8⁺ T cells. *Middle*, was the proportion of TNF α ⁺ IFN γ ⁺ CD4⁺ T cells and *right* was TNF α ⁺ CD8⁺ T cells. Error bars are SD and N = 5 mice per groups. *P < 0.05 and **P < 0.01.

Although synergistic effects were observed for several PS-MPLA and NP-CpG-B combination in BMDCs activation, it did not translate in a strong T cell activation, in vitro

The final adjuvants combination tested for synergistic effect was NP-CpG-B with PS-MPLA, at different dose. As done in the previous adjuvant combination, the same three doses of each adjuvant were tested in combination with one another. As a reminder, NP-CpG-B concentrations tested was 1, 0.1 and 0.01 μM and PS-MPLA was 600, 60 and 6 nM. Interestingly, the highest dose of NP-CpG-B tested in combination with PS-MPLA induced synergistic effect for IL12p70 production but not for IL6 and was even almost inexistent for TNF α (Fig.3.10.A). The medium dose of NP-CpG-B also induced synergistic effect, with an increase effect at higher PS-MPLA dose, in all cytokines tested. Finally the low dose of NP-CpG-B only had an effect with a high dose of PS-MPLA for IL12p70 and IL6 secretion but not TNF α . Concerning the co-stimulatory markers, a small increase in expression was observed when combining the different adjuvants but the effect were not considered synergistic (Fig.3.10.B).

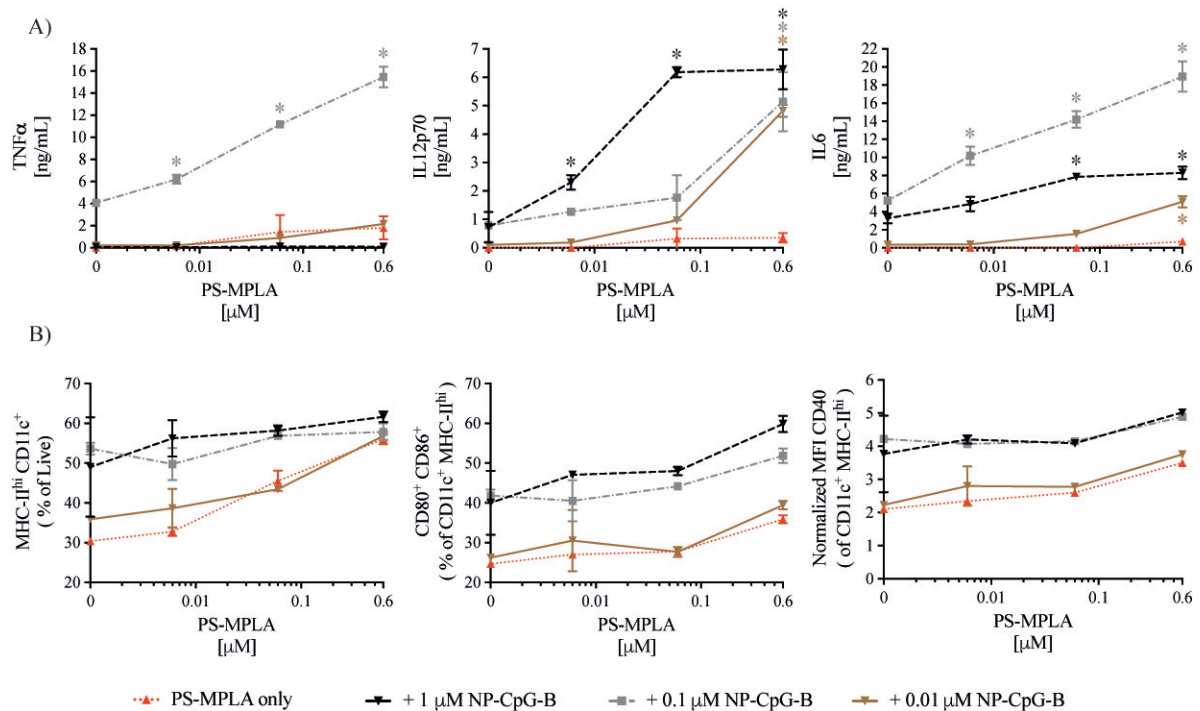


Figure 3.10 Synergistic effect was observed in cytokines secretion for several different adjuvant combinations. (A) Cytokines concentration after BMDCs activation. BMDCs were incubated in a 96-well plate, with different doses of NP-CpG-B and PS-MPLA, for 24 h before quantifying the supernatant by ELISA. (B) BMDCs activation and costimulatory expression. BMDCs were incubated with the same treatments as in (A) for 6 h before staining for flow cytometry analysis. Results are representative of two independent repeats, and * represent synergistic effects observed for that specific combination.

Based on the results obtained for the BMDC activation experiment, CD4⁺ and CD8⁺ T cells co-culture were performed to determine if the activation of DC increase the activation of T cells, *in vitro*. The dose tested were 0.1 μM NP-CpG-B mixed with any dose of PS-MPLA since they induced higher cytokines secretions than with a higher, or a lower, dose of NP-CpG-B. BMDCs were incubated overnight with different adjuvant treatments and 5 μM OVA before only removing the adjuvants and adding the OT-I or OT-II cells at a 1:10 ratio with BMDCs. Unfortunately, neither the CD8⁺ nor the CD4⁺ T cells co-culture showed an increase in activation when treated with the different adjuvant combinations. Interestingly, the addition of PS-MPLA to NP-CpG-B did not increase the production of granzyme B or IFN γ , even if PS-MPLA, alone, had an increase in the secretion at a dose dependent manner (Fig.3.10.A, *left & middle*). Inversely, the combination of both adjuvants followed the same curve as PS-MPLA alone for the secretion of IL2 (Fig.3.11.A, *right*). The proliferation index and expression of CD25 did not increase when both adjuvants were combined (Fig.3.11.B, *left & middle*) and it slightly decreased for the percentage of IFN γ ⁺ CD8⁺ T cells (Fig.3.11.B, *right*). The CD4⁺ T cell co-cultures showed the same trend as CD8⁺ T cells for IFN γ and IL2 cytokines secretion (Fig.3.11.C). Again, no differences were observed in proliferation index (Fig.3.11.D, *left*), the expression of IL2 (Fig.3.11.D, *right*) and only a slight increase in IFN γ ⁺ CD4⁺ T cells when adjuvants were combined (Fig.3.11.D, *middle*).

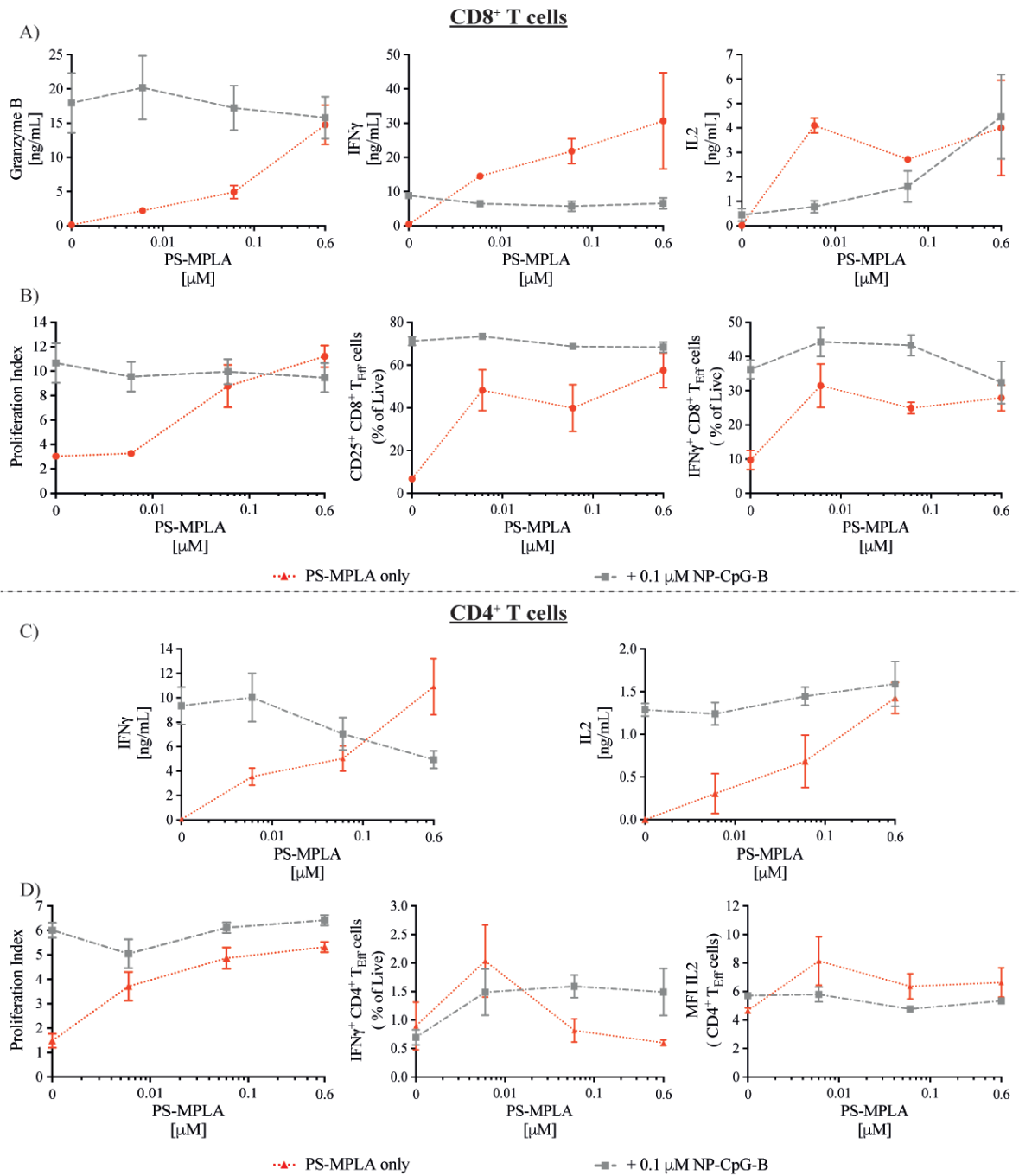


Figure 3.11 No synergistic effects were observed in CD8⁺ or CD4⁺ T cells co-cultures with the different adjuvant combinations tested. 15⁷000 BMDCs were activated overnight with OVA and different adjuvant combinations before removing the adjuvant formulation and adding CFSE labeled OT-I or OT-II. After three days, the supernatant was collected for cytokine quantification, by ELISA, and cells were staining for flow cytometry analysis. (A) Granzyme B, IFN γ and IL2 cytokines concentrations in the supernatant. (B) CD8⁺ T cells activation. The proliferation, activation markers and cytokine production was quantified by flow cytometry. (C) IFN γ and IL2 cytokines concentrations in the supernatant. (D) CD4⁺ T cells activation. Proliferation and activation markers quantification by flow cytometry. Results are representative of three independent repeats, and * represent synergistic effects observed for that specific combination.

A decrease in tumor growth was observed when both adjuvants were co-injected although the T cell immune response was similar

The *in vitro* experiment showed synergistic effect for several different adjuvant combinations, but the one inducing the most effect in BMDCs cytokine production was 0.1 μM NP-CpG-B with 0.6 μM PS-MPLA. This combination represents a 1:6 ratio between the two adjuvants, which was used for the following *in vivo* experiment in a tumor model setting. Briefly, mice were inoculated with B16-OVA cells on the upper right side of the back and 7 days post-inoculation, they were vaccinated with the different treatments (Fig.3.12.A). The tumor growth for the mice co-injected with both adjuvants clearly showed a decrease compared to NP-CpG-B alone (Fig.3.12.B). Unfortunately, two mice in the control groups died for unknown reason explaining the lower tumor growth curve than usual. Although a decrease in tumor growth was observed when both adjuvants were administered, a higher percentage of CD8⁺ T cells were present, in the tumor microenvironment, (Fig.3.12.C, *left*) and SIINFEKL-specific CD8⁺ T cells, in the spleen, were detected when only NP-CpG-B was injected (Fig.3.12.D). Vaccination also induced lower proportion of CD4⁺ T_{reg} and a higher ratio of activated CD8⁺ T cell versus CD4⁺ T_{reg} cells, in the tumor, compared to the PBS treated group (Fig.3.12.C, *middle & right*).

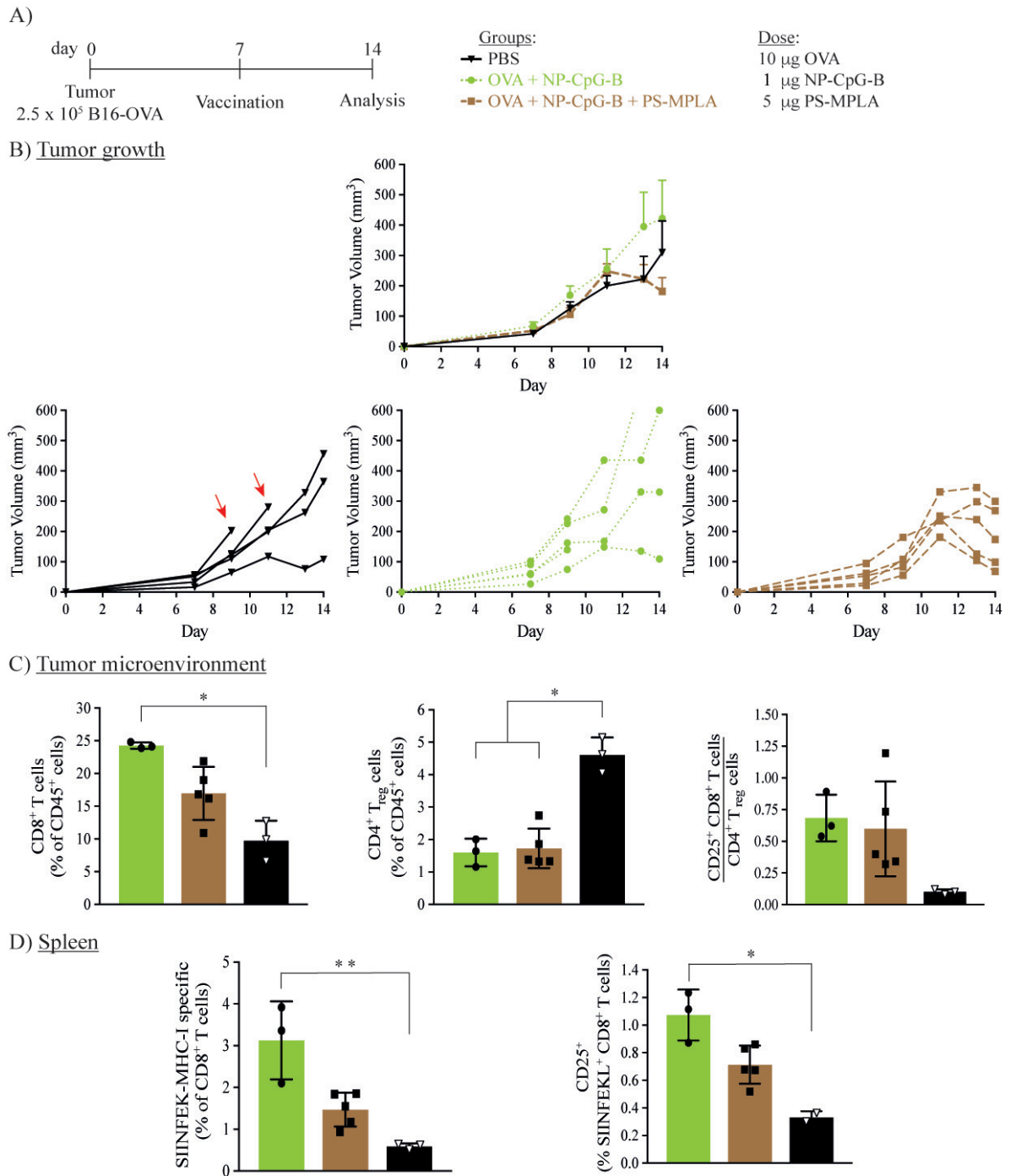


Figure 3.12 PS-MPLA addition to NP-CpG-B vaccine delayed tumor growth but did not increase SIINFEKL-specific CD8⁺ T cells. 2.5×10^5 B16-OVA cells were inoculated i.d. in the right dorsal scapular skin. Mice were vaccinated, i.d. in the hock draining to the same lymph node as the tumor, 7 days post tumor inoculation, before sacrificing the mice on day 14. (A) Experimental timeline, groups and dose. (B) Overall (*Top*), and individual (*Bottom*), tumor growth. (C) Proportion of CD8⁺ T cells, CD4⁺ T_{reg} cells and the ratio of both in the tumor microenvironments. (D) SIINFEKL-specific CD8⁺ T cells population in the spleen quantified by SIINFEKL-MHC-I pentamer staining. Error bars indicate SEM for (A) and SD for all the other. N = 5 mice per groups. *P < 0.05 and **P < 0.01.

The T cell immune response was quantified into more detail for the spleen and tumor-draining lymph node by reactivating CD8⁺ or CD4⁺ T cells with different MHC-I/II peptides. The spleen showed similar trends as in the tumor microenvironment where, mice vaccinated with only NP-CpG-B induced higher T cells response compared to the co-injected vaccine or the PBS treated control. Granzyme B and IFN γ concentration in the supernatant were slightly lower when both adjuvants were injected compared to NP-CpG-B alone but was still higher than the negative control (Fig.3.13.A). Finally, the vaccination increased the proportion of polyfunctional T cells compared to PBS treated mice (Fig.3.13.B, *left & middle*) but only a small trend was detected when cells were reactivated with endogenous CD8⁺ T cell specific antigens (Fig.3.13.B, *right*). Concerning the tumor-draining lymph node, similar trends as in the spleen were observed but in a lower proportion. A significant difference was detected between NP-CpG-B vaccine and PBS for the concentration of granzyme B concentration and IFN γ (Fig.3.13.C). Interestingly, both vaccines tested were significantly increased compared to the negative control for TNF α ⁺IFN γ ⁺ CD8⁺ and CD4⁺ T cells but not when endogenous antigens were used for the restimulation (Fig.3.13.D).

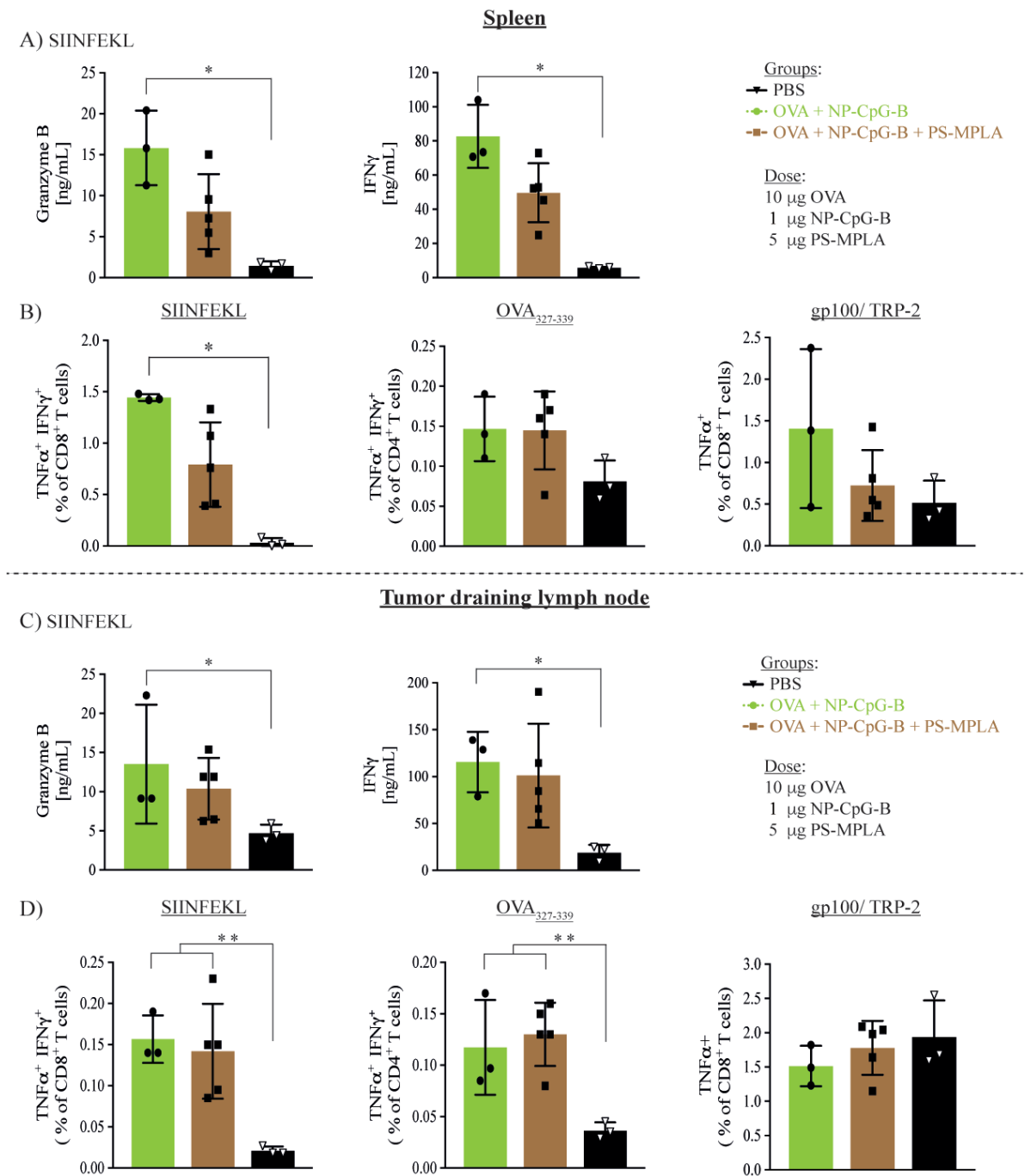


Figure 3.13 The addition of PS-MPLA to NP-CpG-B did not increase the T cells immune response. 2.5×10^5 B16-OVA cells were inoculated i.d. in the right scapular dorsal skin. Mice were vaccinated, i.d. in the hock draining TdLN, 7 days post tumor inoculation. The cytokine secretion quantification (A & C) was done after 4 days incubation before collecting the supernatant whereas polyfunctional T cells quantification by flow cytometry was performed after 6 h incubation (B & D). (A & C) Granzyme B and IFN γ concentration in the supernatant after SIINFEKL reactivation in the spleen and TdLN, respectively. (B & D) Polyfunctionality quantification in the spleen and TdLN. *Left*, was the proportion of TNF α^+ IFN γ^+ CD8 $^+$ T cells. *Middle*, was the proportion of TNF α^+ IFN γ^+ CD4 $^+$ T cells and *right* was TNF α^+ CD8 $^+$ T cells. Error bars are SD and N = 5 mice per groups. *P < 0.05 and **P < 0.01.

3.5. Discussion

Overall, we were able to determine which adjuvant combination synergize to increase BMDCs activation, *in vitro*, as well as some insight on T cell maturation, *in vitro* and *in vivo*. The ideas of combining different adjuvants to increase the immune response, while lowering the dose, was a very appealing strategy but since a multitude of pathways are involved for the upregulation of cytokines, it was very difficult to obtain a clear response in synergistic effect for the T cell response¹¹².

The first combination tested was the TLR-4 agonist, PS-MPLA, with the TLR-7/8 agonist, PS-CL075. Several different combinations tested induced a 2- to 4-fold synergistic effect in TNF α , and IL12p70 production, and up to a 24-fold increase for IL10 secretion when BMDCs were activated. Surprisingly, at a fixed concentration of PS-MPLA, the highest dose of PS-CL075 tested had similar levels of proinflammatory cytokines compared to a lower dose of the TLR-7/8 agonist and a strong increase in IL10 production, which correlates with an overactivation of BMDCs (Fig.3.2.A). Indeed, this cytokine is an immunosuppressive molecule that can inhibit proinflammatory response in order to prevent tissue damage due to inflammation^{113,114}. With this information, it was possible to assume that the highest dose of PS-CL075 with PS-MPLA overstimulated BMDCs leading to the secretion of IL10 to control the inflammatory response. Costimulatory molecules were increased in a dose dependent manner when both adjuvants were combined but not in a synergistic way. The decrease in granzyme B and IFN γ cytokines for the CD8⁺ T cell co-culture, as well as, the absence of difference in activation markers correlated with the increase in IL10 secretion produced by BMDCs (Fig.3.3.A)¹¹⁵. Interestingly, the CD4⁺ T cells co-culture showed a small increase in IFN γ ⁺ and IL2⁺ T cells, which was not the case for the CD8⁺ T cells. It has been demonstrated that IL10 can directly inhibit CD8⁺ T cells antigen sensitivity, thus dampening its activation, which is a possible explanation for the decrease IFN γ secretion observed^{115,116}. In addition, a subset of CD4⁺ T_H1 cells is known to be capable of producing not only IFN γ but also IL10, indicating the possibility of having IFN γ as well as IL10 secreted simultaneously¹¹⁷. For the *in vivo* setting, the injection of PS-MPLA alone produced the highest magnitude of activated T cells, in term of granzyme B and IFN γ (Fig.3.5), while adding PS-CL075 reduced their productions. Surprisingly, the percentage of SIINFEKL-specific CD8⁺ T cell was similar or slightly higher when the TLR-7/8 was added to PS-MPLA (Fig.3.4.C). This would suggest that either the restimulation induced the exhaustion of T cells or the combination itself overactivated them, thereby causing them to go into exhaustion or senescence too quickly. In addition, CD4⁺ T cells are known to express TLR-7/8 which when activated induce the secretion of IFN γ ¹¹⁸, increasing furthermore the immune activation of T cells. A solution to determine if the system was

overactivated would be to reduce the amount of PS-MPLA in combination with PS-CL075 and see if the immune response is increased since only one dose of PS-MPLA was tested. This demonstrates the fine equilibrium between activation and exhaustion when creating a vaccine.

The second combination tested was NP-CpG-B, a TLR-9 agonist, with PS-CL075, a TLR-7/8 agonist and the only synergistic effects observed were in the production of TNF α by BMDCs, *in vitro* (Fig.3.6.A). A possible explanation for the small synergistic effect (only 2-fold) would be that they both activate the NF- κ B pathway removing the advantage of activating several pathways. The decrease in cytokine secretion for PS-CL075 with 1 μ M NP-CpG-B, without increasing the production of IL10 (data not shown) could be due to a toxicity effect from the dose of the NP-CpG-B used. Indeed, the same concentration of free CpG-B also induced lower cytokine secretion compared to a lower dose. In the previous chapter, the flow cytometry analysis did not show an increase in cell death, which would indicate toxicity of the treatment, compared to the other groups (data not shown) but these results were obtained after only 6 h activation compared to the 24 h experiments for cytokine quantification. Surprisingly, the addition of PS-CL075, to 0.01 μ M NP-CpG-B, had an additive effect on the co-stimulatory expression, in a dose dependent manner but did not induce higher cytokine secretion (Fig.3.6.B). This suggested that a stronger activation was needed for cells to secrete cytokines whereas only a small one was required for the expression of co-stimulatory molecules. This would also explain why the other adjuvant combination did not show synergistic effect for BMDC by flow cytometry since they already showed stronger synergistic effect than the present combination. The co-culture experiments only showed an enhance IL2 secretion by CD8⁺ T cells (Fig.3.7.A, *right*) but no increase for the other cytokine. It was shown by Shannon et al that IL2 producing CD8⁺ T cells preferentially survive and develop memory traits, which is an important factor for the development of a long lasting immune response¹¹⁹. Overall, the dose of NP-CpG-B used for the treatments were generally enough to induce a strong activation of CD4⁺ and CD8⁺ T cells and, only a small increase in IL2 secretion when PS-CL075 was added to the TLR-9 agonist. A possible explanation was that CpG-B had a stronger inherent activation property than CL075. *In vivo* vaccination of both adjuvants did not significantly delay tumor growth and the addition of PS-CL075 had no visible effect on the immune response for antigen-specific CD8⁺ T cells (Fig.3.8.B). The CD4⁺ and CD8⁺ T cells restimulation, in the spleen and TdLN showed identical trend, with an increase in polyfunctional T cells when mice were vaccinated but no differences within them (Fig.3.9.B-C). As seen in the previous adjuvant combination, a decrease in IFN γ secretion was observed in the spleen when PS-CL075 was co-administered with NP-CpG-B (Fig.3.9.A, *right*). Overall no strong synergistic effect or increase in the immune response was detected when combining both adjuvants.

The final combination tested was PS-MPLA with NP-CpG-B and similar synergistic effects were observed in BMDCs activation for proinflammatory cytokines as when the PS-MPLA/PS-CL075 combination was tested. The increase of IL10 was also detected in a dose dependent manner when adjuvants were combined, which would explain the absence of TNF α secretion when 0.1 μ M NP-CpG-B was combined with PS-MPLA (Fig.3.10.A). As for the previous combination, no synergistic effects were observed for BMDCs co-stimulatory molecules (Fig.3.10.B) and co-culture experiments showed again a decrease in IFN γ secretions, as well as no significant differences between the different formulations tested. *In vivo*, a delay in tumor growth as well as a decrease in tumor size was observed when mice were vaccinated with both adjuvants (Fig.3.12.B). Surprisingly, these results did not translate in an increased percentage of antigen-specific CD8⁺ T cells, in the spleen, or CD8⁺ T cells infiltrate in the tumor (Fig.3.12.C), which was even lower than the mice receiving only NP-CpG-B in the vaccine. The restimulation of the spleen and the tumor-draining lymph node showed similar trends as previously, were a higher proportion of cytokine production (Fig.3.13. A & C) was detected when only the TLR-9 agonist was used. Even so no difference in T cell immune response was observed, a clear decrease in tumor growth was present.

In this study, we showed that combinatorial delivery of adjuvanted-nanoparticles targeting the TLR-4, TLR-7/8, and TLR-9 pathways can lead to synergistic effects in terms of DC activation and subsequently, T cell activation. *In vitro* screens identified promising formulations that optimized these measures, which are thought to generally correlate well with tumor killing, but in an orthotopic implantable model of aggressive melanoma, this was not always the case. In these studies, only the combination of TLR-4 with TLR-9 agonist achieved synergistic effects for BMDCs activation, *in vitro*, as well as a decrease in tumor growth, *in vivo*. It was notable that during *in vitro* screening, the TLR-4/TLR-9 co-targeting strategy was the only one among the three tested that produced strong synergistic effects in improving granzyme B and IFN γ expression by CD8⁺ T cells. On the other hand, all three combinations produced similar trends in terms of increasing TNF α and IL-12p70 secretion by BMDCs and small additive but insignificant effects on BMDC surface expression of co-stimulatory molecules. This suggests that future screening of adjuvant combinations for optimal formulations used for therapeutic tumor vaccination should continue to use granzyme B and IFN γ upregulation as a predictive marker for therapeutic efficacy.

Chapter 4

Radiotherapy in combination with an adjuvant-based
vaccine delays tumor growth

4.1. Abstract

Over the past decades an increasing number of studies were focused on understanding the effects of radiotherapy on the tumor microenvironment and the tumor-specific immune response. Since it has now been established that ionizing radiation does not only directly affect tumor cell proliferation and survival but can also promote the anti-tumor immune response, researchers are testing the effect of combining radiation with different forms of cancer immunotherapy.

We hypothesized that a reduction in tumor growth, as well as an increase in survival, could be obtained when combining localized tumor radiotherapy with our adjuvanted-nanoparticulate vaccine, since it is known that the tumor-draining lymph node (TdLN) is a primary site of T cell priming following tumor irradiation. Before testing our hypothesis, different parameters, such as the vaccination schedule, the injection site and the organ targeted by the vaccine were tested to determine their effect on the immune response when combined with radiotherapy. We first demonstrated that, although, the vaccine was administered in the forelimb draining the TdLN and not intratumorally, an enhance T cell immune response was obtained. In addition, a single vaccination induced a stronger response compared to a fractionated vaccine schedule. Interestingly, the vaccination of free CpG-B subcutaneous injected in the forelimb draining to a non-TdLN induced a strong IFN γ secretion in the spleen and a decrease of tumor growth compared to the targeting of the TdLN, it did not increase the percentage of antigen-specific CD8⁺ T cells, or increase the immune response in the tumor microenvironment and the draining lymph node. The last parameter tested was the difference in tumor growth and survival when mice were vaccinated with NP-CpG-B intradermally or intratumorally. The results demonstrated no difference between both injection sites, although some complications, due to the ulceration of the tumor which occurred for the intratumoral injection. Finally, the combination with radiotherapy and the co-injection of PS-MPLA and NP-CpG-B induced a decrease in tumor growth and an increase in survival. Consistently, CD8⁺ and CD4⁺ T cells were increased in the tumor site and secreted higher levels of IL2 in the TdLN following *ex vivo* reactivation. Overall the addition of adjuvant vaccine increased the survival of tumor-bearing mice with a trend towards increased IL2 and IFN γ secretion, but the exact mechanism by which the tumor growth was decreased has to be further studied.

4.2. Introduction

Although radiotherapy is traditionally used to directly kill tumor cells, more recent studies have shown that irradiation also has immunomodulatory properties and affects different cell populations in the tumor microenvironment¹²⁰. Indeed, it was demonstrated that not only tumor cells die, but antigen-presenting cells (APCs), T cells, endothelial cells and stromal cells undergo apoptosis after local irradiation¹²¹. Due to the radiosensitivity of lymphocytes and antigen-presenting cells to ionizing radiation, radiotherapy was thought to induce a suppressive effect on the immune system¹²². However, over the past two decades, several studies have shown the ability of irradiation to induce an immune response, depending on the dose, the frequency and the irradiated volume^{120, 123, 124}.

It was thought that a high dose of radiation induces enhanced double-stranded breakage, which leads to increased tumor cell death, release of tumor antigens, and IFN γ secretions, thus promoting activation of cytotoxic CD8⁺ T cells. Lugade et al compared a single dose of 15 Gy radiations with a fractionated radiotherapy, 3 x 5 Gy, and showed higher APCs and CD8⁺ T cells activation in the tumor-draining lymph node, as well as an increase in IFN γ -secreting cells when irradiated with the high dose¹²⁵. It has also been demonstrated that a 20 Gy dose induced tumor rejection of B16-F10 in immunocompetent mice but not immunodeficient, proving the ability of irradiation to mount an anti-tumor response⁵⁹. Furthermore, depending on the tumor type, the efficacy of the dose and schedule can influence the immune response. Indeed a single high-dose radiation induced a better immune response than fractionated in B16-F10 melanoma and, inversely, a fractionated dose (3 x 8 Gy) combined to CTLA-4 antibody treatment was more potent in murine breast cancer than an ablative dose¹²⁶. It was postulated that T cell priming occurred in the tumor draining lymph node after DC-mediated cross-presentation of tumor antigens. Moreover, radiotherapy treatment induces the secretion of a multitude of cytokines, an important one for radiation-induced T cell priming being IFN γ ¹²⁷. The presence of radiotherapy-induced IFN γ secretion in the tumor microenvironment was shown to increase the percentage of T cells trafficking to the tumor through the upregulation of VCAM-1 in the tumor vasculature and chemoattractant MIG and IP-10, thus reducing tumor growth¹²⁸.

Although radiotherapy is able to naturally induce an immune response against tumors, immune-mediated abscopal responses (i.e. regression of secondary tumors distant from the treated primary tumor site) remain rare. Therefore, combination with immunotherapy could be a promising option to improve the outcome of the patient¹². Several clinical trials demonstrated the efficacy of increasing the pool of dendritic cells in the tumor after radiotherapy by injecting up to 10⁷ cells

intratumorally and showed higher percentage of tumor-infiltrated CD8⁺ T cells as well as antigen-specific T cells in prostate cancer¹²⁹, carcinoma¹³⁰ and refractory hepatoma¹³¹. The activation of DCs can also be done with the use of TLR agonist. Brody et al reported a 27% increase response rate when patients with low-grade B cell lymphoma were irradiated with a fractionated low-dose (2 x 4 Gy) combined to CpG-B (30 mg), injected intratumorally¹³². A follow-up of this study, in mycosis fungoides showed a 33% response rate with a reduction of CD25⁺ T cells¹³³. An ongoing clinical trial using TLR-4, glycopyranosyl lipid A, with six fractions of radiotherapy for metastatic sarcoma (ClinicalTrials.gov identifier: NCT02180698) as well as a TLR-7 agonist in breast cancer metastases in the skin (ClinicalTrials.gov identifier: NCT01421017) are also being tested to determine their effect when added to ionizing radiation. Other approaches combining radiotherapy with checkpoint blockade (CTLA-4 or PD-1), co-stimulation (OX40 agonist), chemotherapy (cyclophosphamide) or even cytokines (IL2, IFN α) are being investigated in clinical trials after successfully demonstrating synergistic effect in mice.

Overall, an increase response rate was observed when radiotherapy was combined with immunotherapy. However, in most of these studies, TLR agonists were either applied topically on the tumor site or injected intratumorally. We hypothesized that combining PS-MPLA and NP-CpG-B with a single high dose of localized ionizing radiation would result in an enhanced therapeutic efficacy compared to either irradiation or vaccination alone. The advantage of our vaccine would be the targeting of the lymph node rather than the tumor, since DCs prime the immune response mainly in the TdLNs. In addition, while antigen presenting cells and lymphocytes within the tumor site may undergo apoptosis and reduced proliferation following localized tumor radiotherapy (due to their radiosensitivity), the pool of DCs and lymphocytes in the TdLNs is protected from the direct effects of radiation and thus represents an ideal target for vaccination in this context.

4.3. Materials and Methods

Mice

All mice used in experiments were C57BL/6 female 8-12 weeks old, purchased from Harlan (France) or Jackson laboratory (USA). All procedures were performed in compliance with the Veterinary Authority of the Canton of Vaud (Switzerland) according to Swiss laws and the Institutional Animal Care and Use Committee at the University of Chicago (USA)

Cell line

The melanoma B16-F10 expressing ovalbumin (B16-OVA) cells line was gifted from Bertrand Huard (University of Geneva, Switzerland) and was maintained in high glucose DMEM (Gibco, Waltham, Massachusetts, USA; Catalog # 11995) supplemented with 10% FBS.

Materials, reagents and antibodies

Reagent grade chemicals were purchased from Sigma-Aldrich (Saint Louis, MO, USA) unless noted otherwise. All adjuvants, except for CpG-B, were purchased from InvivoGen (San Diego, CA, USA). The modified 5'SPO₃-CpG-B (5'-TCCATGACGTTTCCTGACGTT-3') was purchased from Microsynth (Balgach, Switzerland) or TriLink Biotechnologies (San Diego, CA, USA).

Anti-mouse antibodies CD80 (clone 16-10A1), CD86 (clone GL1), CD40 (clone 3/23), CD8 (clone 53-6.7), CD4 (clone RM4-5), IFN γ (XMG1.2), CD25 (clone PC61), IL2 (clone JES6-5H4), CD45 (clone 30-F11), CD3 (clone 145-2C11), FoxP3 (clone MF23), TNF α (MP6-XT22), CD62L (clone MEL-14), CD44 (clone IM7) and fixable live/dead were purchased from ThermoFisher Scientific (Waltham, MA, USA). The SIINFEKL-specific pentamer, PE-labeled H-2Kb/OVA₂₅₇₋₂₆₄ was purchased from Proimmune (Oxford, UK).

Tumor inoculation and immunizations

An orthotopic injectable melanoma model was employed through the intradermal injection of B16-OVA tumor cells. To expose the injection site, healthy adult wild-type C57BL/6 mice were anesthetized with isoflurane (3.5%), and dorsal scapular skin on the mouse's right side after shaving and disinfecting the area. 2.5×10^5 B16-OVA tumor cells in 30-45 μ L of 0.9% saline solution were delivered intradermally at this site. All nanoparticle adjuvants were prepared as explained in the previous chapter, and conformed for low endotoxins levels by HEK-blueTM TLR-4 assay. The formulations were mixed right before the vaccination, which was administered i.d. in the forelimb, draining the same lymph node as the tumor. The maximum volume injected was 30 μ L.

Starting on day 4 post-inoculation, tumors were measured every other day with digital calipers and the volume was calculated using an ellipsoidal equation: $V = \frac{4}{3}\pi \times \frac{L}{2} \times \frac{W}{2} \times \frac{H}{2}$, where L is the length, W is the width and H is the height.

In vivo tumor irradiation

Mice were irradiated with 15 Gy using the RadSource Technologies X-ray RS-2000 biological irradiator operating at 160 kVp and 25 mA. Mice were anesthetized with a solution of ketamine/xylazine administered intraperitoneal and their entire body, except for the tumor, was placed under a lead shield to protect from irradiation. If necessary, the process was repeated 7 days after the first irradiation.

Whole organ/tumor processing into single-cell suspensions

To analyze immune responses within specific anatomic compartments, the tumor-draining lymph node, the spleen and the tumor were harvested and processed into single-cell suspensions for flow cytometry. For the TdLN and the spleen, cell suspensions were obtained by mechanically disrupting the organ and rinsing with PBS, or IMDM, through a 0.7 μm cell strainer (CorningTM, NY, USA), and then centrifuging the resulting cell suspension at 1500 rpm for 5 min. The TdLN was then resuspended in IMDM supplemented with 10% FBS, 10^2 U/mL penicillin, 10^2 $\mu\text{g}/\text{mL}$ streptomycin and 20 μM 2-mercaptoethanol (Full media) and counted. Splenocytes were first washed in a hypotonic solution of ammonium chloride-potassium bicarbonate (ACK) for 2 min to remove red blood cells, prior to centrifugation at 1500 rpm for 5 min, resuspension in full media and counting. The tumor cell suspension was obtained by adapting a protocol from Broggi et al ¹¹⁰. Briefly, the tumor was minced, and then digested in digestion media (DMEM + 2% FBS + 1.2 mM CaCl_2 + 10^2 U/mL penicillin + 10^2 $\mu\text{g}/\text{mL}$ streptomycin) supplemented with 1 mg/mL Collagenase IV and 40 $\mu\text{g}/\text{mL}$ DNase I (Worthington Biochemical Corp, Lakewood, New Jersey, USA). This suspension was stirred at 37°C for 30 min, further disrupted by repetitively pipetting 100x, and then filtered through a 70 μm strainer. The remaining undigested tumor fragments were further digested at 37°C for 1 h in a second digestion mix consisting of digestion buffer supplemented with 3.5 mg/mL Collagenase D and 40 $\mu\text{g}/\text{mL}$ DNase I. The tumor fragments were further mechanically disrupted through repetitive pipetting them 100x. The enzymes were quenched through the addition of EDTA to a final concentration of 2.5 mM, and then the cell suspensions were filtered through a 70 μm strainer and combined with the cells from the first digestion step. As tumors may contain a significant amount of blood, the resulting cell suspensions were treated similarly to the splenocytes described above before they were resuspended in full media and counted. As for the spleen, red blood cells were lysed using the same protocol. Finally, the cell suspension was resuspended in full media and counted.

Blood processing

Blood were collected in EDTA coated tubes and centrifuged at 1500 rpm for 5 min. The plasma was stored at -20°C and red blood cells were lysed with an ACK solution and resuspended in full media before staining them for flow cytometry.

Ex vivo restimulation

For the reactivation of antigen-specific T cells in TdLNs and spleens, these organs were processed into single-cell suspensions as described above, and then plated in U-bottom 96-well plates at up to 2×10^6 cells/well. The cells were incubated at 37°C in a 5% CO₂ incubator with 2 µg/mL of antigenic peptide in full medium. For cytokine quantification by ELISA, supernatants were collected following 4 days of incubation, whereas for flow cytometry analysis, cells were incubated for 3 h prior to halting cytokine export through the addition of brefeldin A to a final concentration of 5 µg/mL, followed by incubation for an additional 3h before harvest. To restimulate antigen-specific CD8⁺ T cells, the MHC-I-dominant peptides OVA₂₅₇₋₂₆₄ (SIINFEKL), whereas CD4⁺ T cells were reactivated with OVA₃₂₃₋₃₃₉.

Flow cytometry

Cell suspensions were centrifuged and washed with 1x PBS, and then incubated with a fixable live/dead at 4°C for 15 min before washing again once with PBS. Antigen-specific T cells were detected via pentamer staining, which was performed by incubating cells at room temperature in a solution of 1x PBS supplemented with 2% FBS (staining buffer), for 20-30 min. For surface staining, a cocktail of antibody was diluted in staining buffer and incubated at 4°C for 15 min. Intracellular staining and intranuclear staining were performed with the BD cytofix/cytoperm™ Kit or FoxP3 staining kit, respectively, according to the manufacturer's instructions. Finally, the cells were washed with staining buffer and stored in the same buffer for data collection.

ELISA

Cytokines detection and quantification were performed with Ready-SET-Go! ELISA kits purchased from ThermoFisher Scientific and used according to the manufacturer's instructions.

Flow cytometry

Flow cytometry was performed using either a CyAn™ ADP (Beckman Coulter, Brea, CA USA) or a BD LSRFortessa™ (BD Biosciences, San Jose, CA, USA). The data obtained were analyzed with FowJo (v.10, FlowJo LLC, Ashland, OR, USA). Graphs and statistical analysis were done using the GraphPad Prism 7 Software (GraphPad Software Inc, La Jolla, CA, USA).

Statistical significance between the different groups were determined with a one-way analysis of variance (ANOVA) followed by a Bonferroni post-test correction. * and ** indicate P values less than 0.05 and 0.01, respectively.

4.4. Results

As said previously, the final goal of this study was to test the combination of our adjuvanted-nanoparticle vaccine with radiotherapy and, in order to obtain the strongest immune response against B16-OVA with our treatment, different parameters were tested, beforehand.

The combination of adjuvant vaccination with radiotherapy enhance the T cell immune response and delayed tumor growth

The main purpose of this experiment was to determine if the immune response could be enhanced when vaccination in the forelimb draining the TdLN was added to radiotherapy and, in a second time, if the vaccination schedule influenced the response. Since all the studies mentioned previously injected the treatment intratumorally, it was important to determine if similar results could be obtained when injecting in the forelimb draining the TdLN. As discussed in the first chapter, the ionizing radiation can induce immunogenic cell death through several different mechanisms, which increase the uptake of antigens by DCs. The time for dendritic cells to reach the tumor-draining lymph node is not exactly known and so two different vaccination schedules were tested. The first group was vaccinated only once with 20 μg CpG-B whereas the second group received two injections of 10 μg CpG-B, with a 3 days gap between the first and second injection (Fig.4.1.A). This experiment was performed with free CpG-B, rather than with NP-CpG-B, to have the possibility to inject a higher dose. The overall tumor growth curve did not show any significant difference between groups (Fig.4.1.B, *top & bottom left*). Mice treated 4 times with CpG-B had similar tumor growth for most of the experiment but on day 17, the tumor grew much faster, than the other treatments (Fig.4.2, *bottom middle*). The isolated cell suspension from the spleen showed similar percentage of SIINFEKL-specific CD8^+ T cell in all three groups (Fig.4.1.C, *left*) but a significant increase in $\text{CD44}^+\text{CD62L}^- \text{CD8}^+$, and CD4^+ , T cells were observed for the vaccinated mice, independently of the schedule (Fig.4.1.C, *middle & right*). Concerning the tumor microenvironment, similar trends in CD8^+ (Fig.4.1.D) and CD4^+ T cells (Fig.4.1.E) were observed. No difference in the percentage of T cells (Fig.4.1.D & E, *left*) or effector (Fig.4.1.D & E, *middle*) were detected between treatments but a decrease in PD-1^+ T cells were present when mice were vaccinated with a single dose compared to the PBS-treated group (Fig.4.1.D & E, *right*).

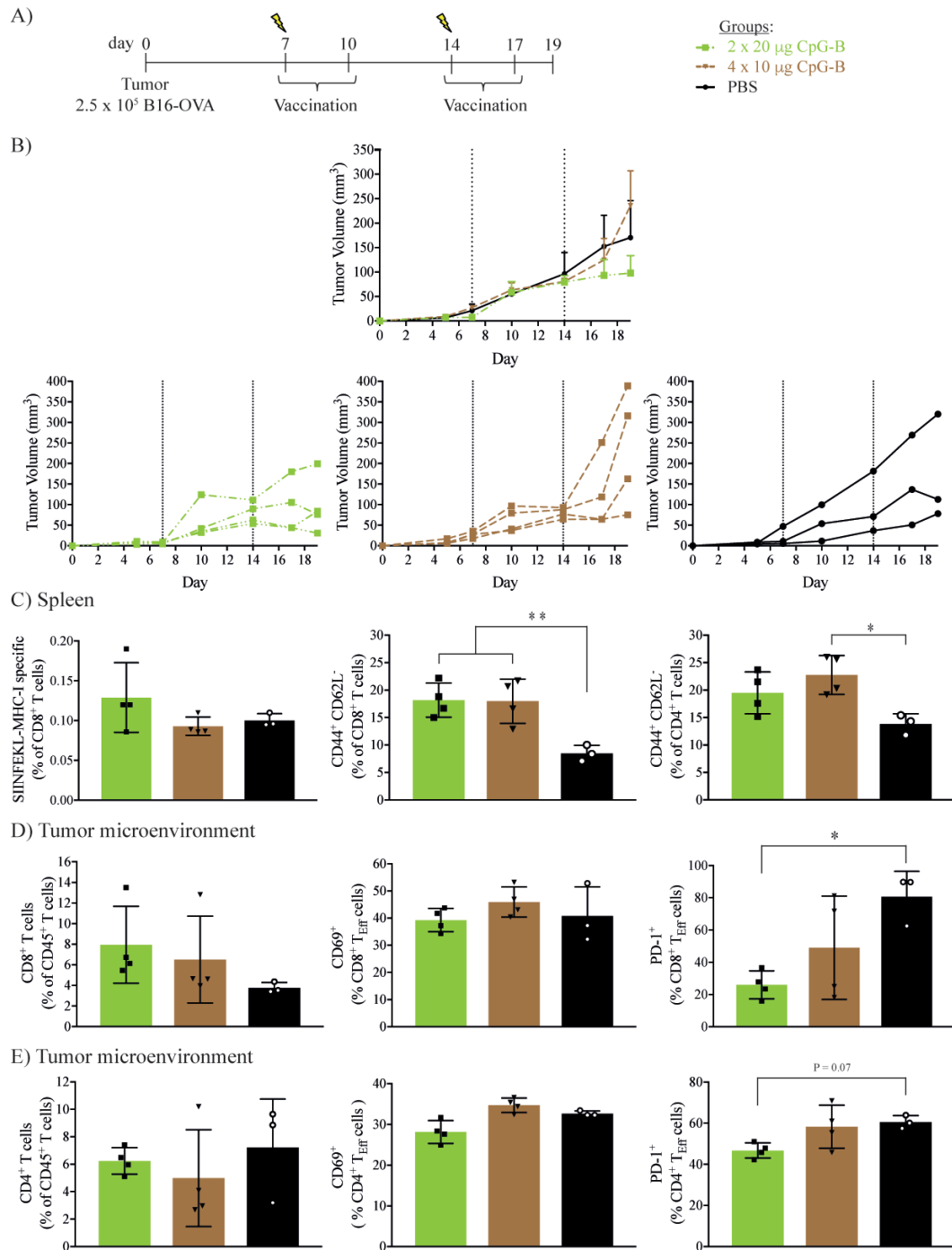


Figure 4.1 The T cell population was similar in the tumor microenvironment between both schedules. 2.5 x 10⁵ B16-OVA tumor cells were inoculated in the right scapular dorsal skin before irradiating them with 15 Gy on day 7. The “2 x 20 µg CpG-B” group was vaccinated on days 7 and 14 whereas the “4 x 10 µg CpG-B” were injected on days 7, 10, 14 and 17. Finally, mice were sacrificed on day 19 post-tumor inoculation to quantify the immune response. (A) Timeline and treatment groups. (B) Average, *top*, and individual, *bottom*, tumor growth. (C) T cell population in the spleen. *Left* is the percentage of SIINFEKL-specific CD8⁺ T cells. *Middle & right graph* was the CD8⁺ and CD4⁺ T_{EFFEM} cells, respectively. (D-E) CD8⁺ and CD4⁺ T cells population in the tumor microenvironment, respectively. Error bars indicate SEM for tumor growth curves and SD for all other graphs. N = 3-4 mice per groups. *P < 0.05 and **P < 0.01.

The reactivation *ex vivo*, of the tumor-draining lymph node and the spleen, was done to assess the T cell immune response after vaccinations. Although no significant differences in IFN γ ⁺ or TNF α ⁺IFN γ ⁺ CD8⁺ T cells in the TdLN were observed between treatment groups (Fig 4.2.A, *left & middle*), a trend towards an increased activation was detected when mice were vaccinated 4 times. The same trends between treatments were observed by flow cytometry and by ELISA for IFN γ expression (Fig 4.2.A, *right*). In the spleen, the percentage of TNF α ⁺IFN γ ⁺ CD8⁺ (Fig.4.2.B, *left*) and CD4⁺ T cells (Fig.4.2.B, *middle*) were similar between the two vaccination groups and both were increased compared to irradiation only. As in the TdLN, IFN γ secretion, assessed by ELISA, seemed to be increased in the 4x10 μ g CpG-B group compared to the 2x20 μ g CpG-B group (Fig 4.2.B, *right*).

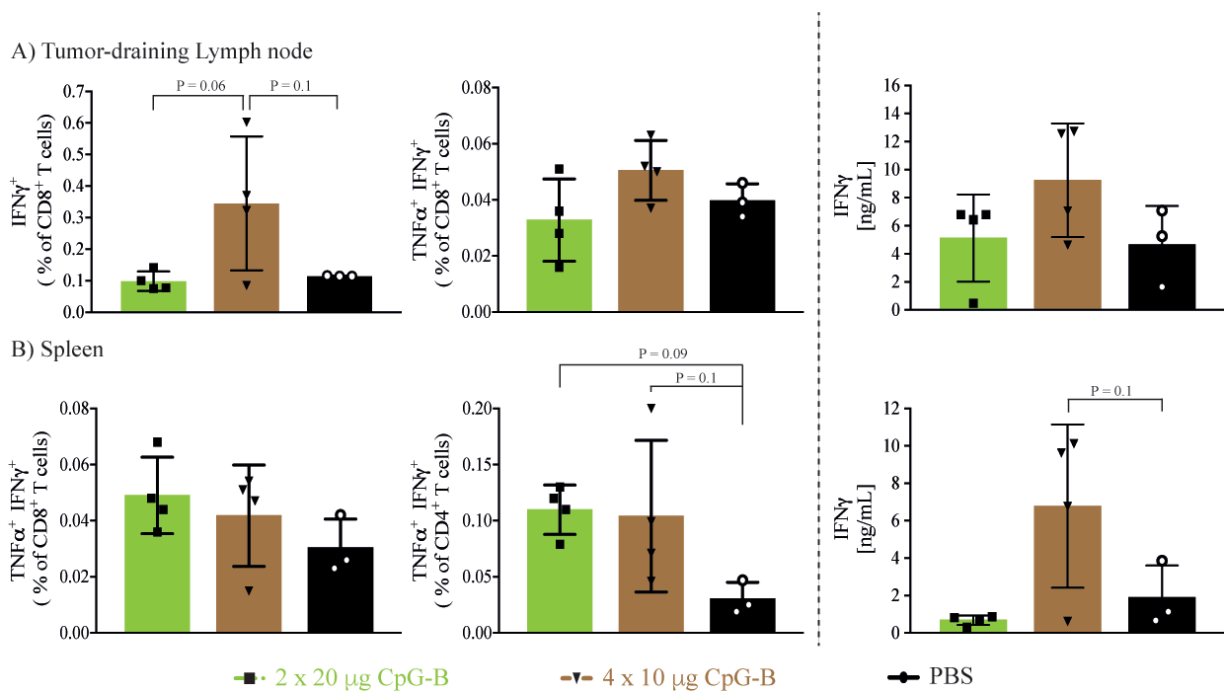


Figure 4.2 A trend in favor of an increased immune activation was detected when mice were vaccinated. 2.5×10^5 B16-OVA tumor cells were inoculated in the right scapular dorsal skin before irradiating them with 15 Gy on day 7. The “2 x 20 μ g CpG-B” group was vaccinated on days 7 and 14 whereas the “4 x 10 μ g CpG-B” were injected on days 7, 10, 14 and 17. Finally, mice were sacrificed on day 19 post-inoculation to quantify the immune response. (A) Tumor-draining lymph node restimulation with SIINFEKL assessed by flow cytometry (*Left & middle graph*) and by ELISA (*right graph*). (B) T cells immune response in the spleen after reactivation *ex vivo*. Polyfunctional CD8⁺ and CD4⁺ T cells quantified by flow cytometry (*left & middle graph*) and IFN γ production in the supernatant by ELISA (*right*). Error bars indicate SD for all graphs. N = 3-4 mice per groups. *P < 0.05.

Overall, this experiment showed an enhance T cell activation when CpG-B vaccination was combined to radiotherapy and a small incline towards delay of the tumor growth when a single dose of CpG-B was used. In addition, the reactivation of the spleen and the TdLN showed no significant enhance immune activation when mice were vaccinated.

A decrease in tumor growth and increase in polyfunctional CD8⁺ T cells was observed when targeting the non-TdLN

The next parameter tested was the variation in the T cell immune response when targeting the tumor-draining lymph node compared to a non-tumor draining lymph node. We hypothesized that the immune response would be increased when targeting the TdLN versus non-TdLN since tumor antigens, and activated APCs, would be drained to the TdLN. However, since the TdLN can be immunosuppressed, a dampening of the immune response can occur. This was tested by inoculating 2.5×10^5 B16-OVA tumor cells in the right dorsal scapular skin before irradiating and vaccinating mice on day 7 post-inoculation (Fig.4.3.A). At day 18, a significant difference in tumor volume was observed when mice were vaccinated intradermally in the forelimb of the non-TdLN ($30 \pm 8 \text{ mm}^3$) compared to the irradiated “only” group, $170 \pm 131 \text{ mm}^3$ (Fig.4.3.B). The decrease in tumor growth was not associated to an increase in SIINFEKL-specific CD8⁺ T cells in the spleen (Fig.4.3.C, *left*). The proportions of effector CD8⁺ and CD4⁺ T cells were increased for the vaccinated groups compared to irradiation only (Fig.4.3.C, *middle & right*) but no difference was observed between the two vaccine groups. The analysis of the immune infiltrate in the tumor microenvironment showed an increase in the frequency of CD8⁺ T cells (Fig.4.3.D, *left*) but no differences in CD4⁺ T cells (Fig.4.3.E, *left*). All three treatments showed no differences in CD69⁺ T cells and a decrease in PD-1⁺ CD8⁺ and CD4⁺, T cells when mice were vaccinated (Fig.4.3.D & E, *middle & right*).

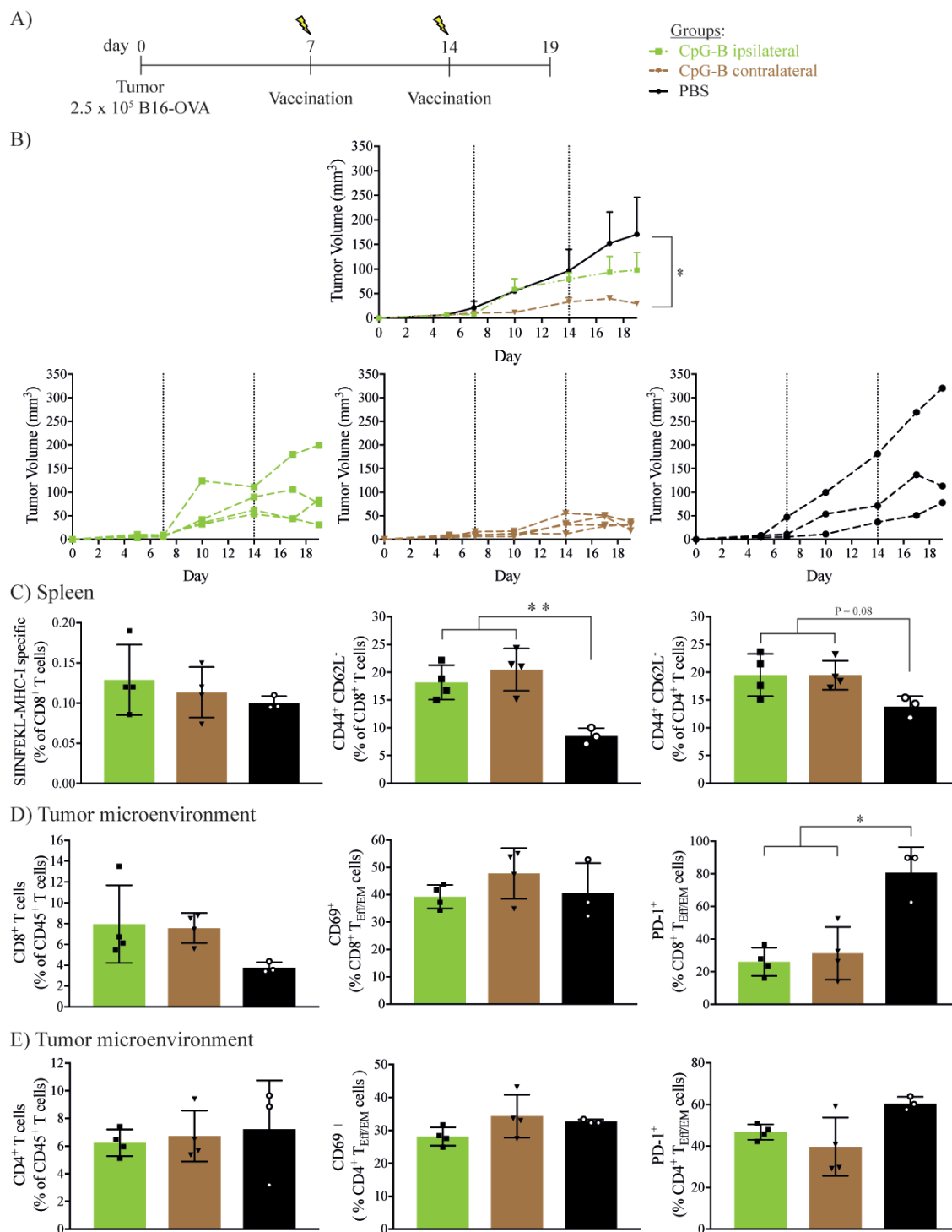


Figure 4.3 Targeting the non-TdLN results in a more marked delay of tumor growth compared to the TdLN, without significant changes in T cell frequencies. 2.5×10^5 B16-OVA tumor cells were inoculated in the right scapular dorsal skin before irradiating them with 15 Gy on day 7 and 14. Both vaccinated groups received $20 \mu\text{g}$ CpG-B, per injection, intradermally in the hock draining, or not the TdLN. (A) Timeline and treatments. (B) Average, *top*, and individual, *bottom*, tumor growth. (C) T cell immune activation in the spleen. *Left* were the percentage of SIINFEKL-specific CD8^+ T cells. *Middle & right graph* was the CD8^+ and CD4^+ T_{EFFEM} cells, respectively. (D-E) CD8^+ and CD4^+ T cells population in the tumor microenvironment, respectively. Error bars indicate SEM for tumor growth curves and SD for all other graphs. $N = 3-4$ mice per groups. * $P < 0.05$ and ** $P < 0.01$.

CD8⁺ T cells from the spleen, TdLN and non-TdLN were reactivated *ex-vivo* with the MHC-I dominant OVA epitope, SIINFEKL. The TdLN did not show any difference in polyfunctional CD8⁺ T cells or IFN γ secretion between all groups (Fig.3.4.A & B, *left*) and the non-TdLN had similar percentage in TNF α ⁺IFN γ ⁺ CD8⁺ T cells ($0.023 \pm 0.02\%$), compared to the TdLN ($0.03 \pm 0.02\%$). However, we observed a significantly increased IFN γ production in the non-TdLN in mice receiving the vaccine contralaterally to the tumor. This was explained by the fact that this specific lymph node was not targeted at all in the other two groups (Fig.4.4.A & B, *middle*). Finally, the spleen showed a significant increase in polyfunctional CD8⁺ T cells but no differences in IFN γ secretion when targeting the non-TdLN (Fig.4.4.A & B, *right*).

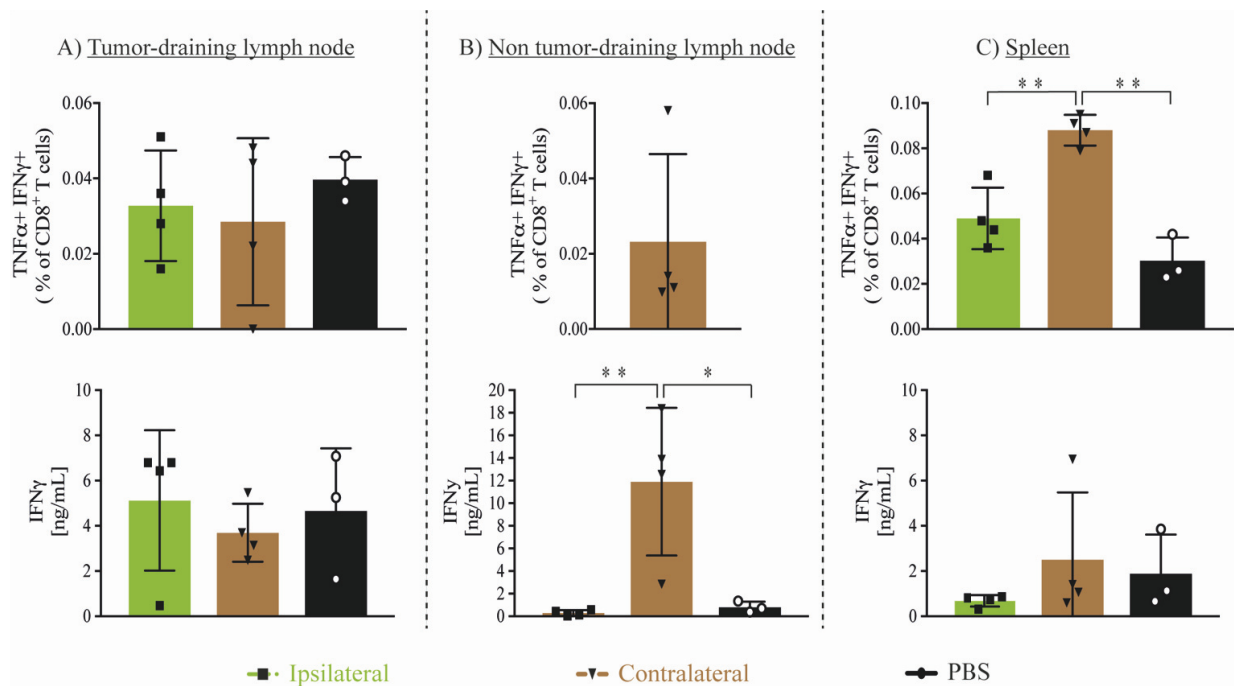


Figure 4.4 A significant increase in polyfunctional CD8⁺ T cells, in the spleen but not in the TdLN was observed when the non-TdLN was targeted. 2.5×10^5 B16-OVA tumor cells were inoculated in the right scapular dorsal skin before irradiating them with 15 Gy on day 7 and 14. Both vaccinated groups received 20 μ g CpG-B, per injection, intradermally in the hock draining, or not the TdLN. (A-C) TNF α ⁺IFN γ ⁺ CD8⁺ T cells after SIINFEKL reactivation (*Top*) and IFN γ quantification (*bottom*), by ELISA, in the tumor-draining lymph node, the non-TdLN and the spleen. Error bars indicate SD for all graphs. N = 3-4 mice per groups. *P < 0.05 and **P < 0.01.

In summary, a decrease in tumor growth was observed when targeting the non-TdLN, which was associated to a higher percentage of polyfunctional OVA-specific CD8⁺ T cells in the spleen.

Intradermal and intratumoral injection induced similar tumor growth and survival

The final parameter tested was the injection site. Although the advantage of our adjuvanted-particles was their capability to drain through the lymphatic system to reach the lymph node, we wanted to determine the difference in immune response and survival when vaccines were injected intradermally, in the forelimb draining to the TdLN compared to intratumorally. Although the previous experiment showed a stronger T cell activation when targeting the non-TdLN compared the TdLN, we decided to target to TdLN since both injection route would cause the adjuvants to drain to the same lymph node. When the tumor reached a size ranging between 50 and 150 mm³ mice received a 15 Gy radiation dose localized to the tumor area and the first adjuvant vaccinations before waiting 3 more days to vaccinate a second time. Seven days after the first irradiation, a second cycle of treatment was performed using the same schedule as the first round (Fig.4.5.A). The dose of NP-CpG-B being rather low, it was thought important to vaccinate a second time 3 days after to increase the immune response. The average tumor growth showed a slight decrease when mice were vaccinated compared to PBS-treated (Fig.4.5.B, *top*). In addition, two out of five mice in the intratumorally-administered group did not response to the first boost given on day 13. As observed in the tumor growth curve, the survival reflected no difference between the two vaccinated groups but was increased compared to the negative control (Fig.4.5.C). The proportion of SIINFEKL-specific CD8⁺ T cells was only slightly higher compared to the negative control and the percentage of CD44⁺CD62L⁻ as well as CD25⁺ CD8⁺ T cell population was unchanged (Fig.4.5.D, *top & bottom*).

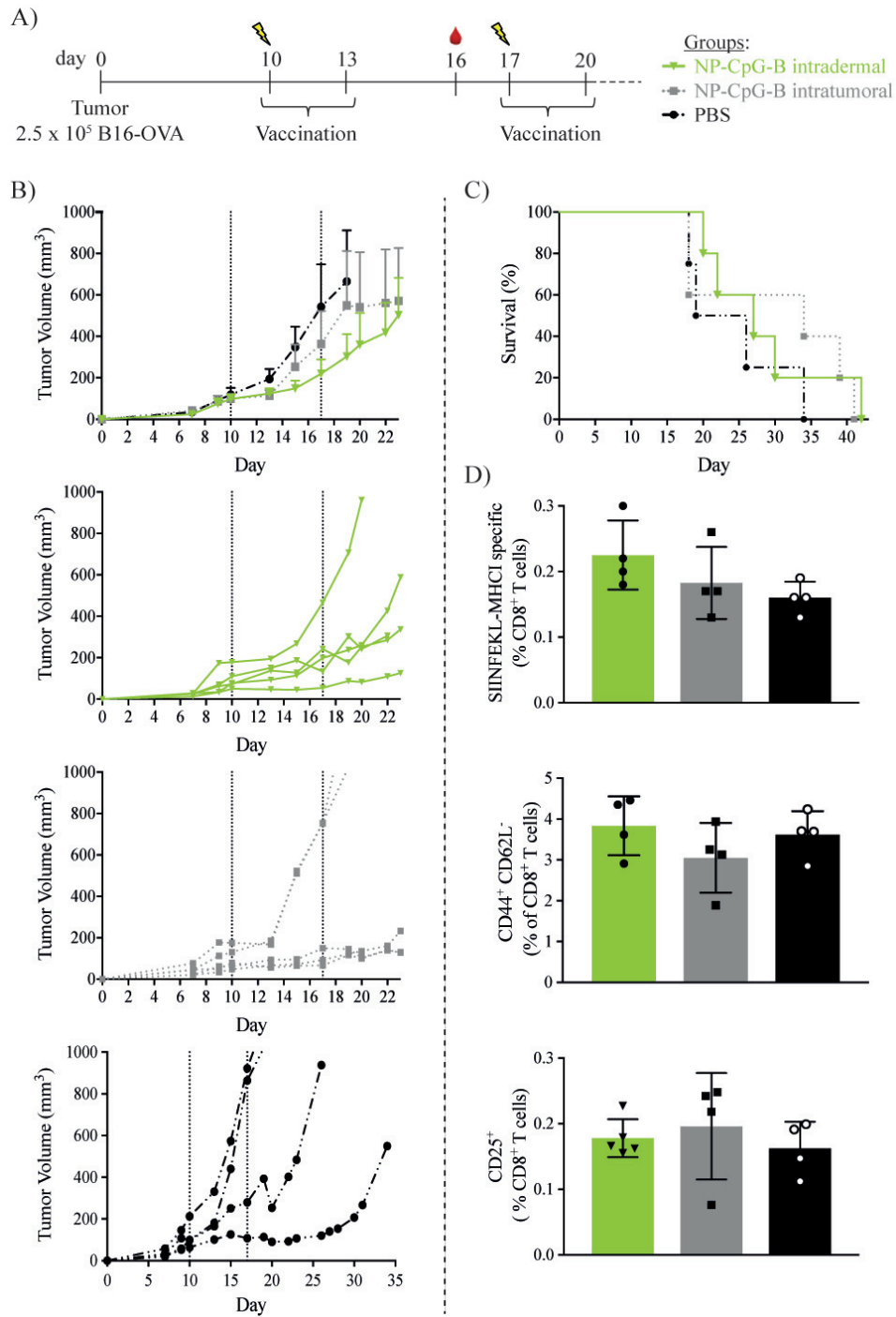


Figure 4.5 Intratumoral and intradermal NP-CpG-B injection have similar effects on tumor growth and mouse survival. 2.5×10^5 B16-OVA tumor cells were inoculated in the right scapular dorsal skin before irradiating them with 15 Gy on day 10 and 17. Both vaccinated groups received 1 μg NP-CpG-B, per injection, intradermally or intratumorally. (A) Timeline and treatment groups. (B) Average (top) and individual tumor growth. (C) Survival curves. (D) Percentage of SIINFEKL-specific and CD25⁺ CD8⁺ T cells in the blood. Error bars indicate SEM for tumor growth curves and SD for all other graphs. N = 4-5 mice per group. *P < 0.05 and **P < 0.01.

Increased production of IL2 in the TdLN was detected when PS-MPLA & NP-CpG-B were co-injected but similar tumor growth was observed for all vaccinated groups

After determining the optimal injection route and vaccine schedule, PS-MPLA and NP-CpG-B vaccine was tested, in combination with radiotherapy, to quantify the immune response. This combination was chosen based on the results obtained on the previous chapter. As a reminder, *in vitro* experiments showed strong synergistic effect in cytokines secretion after BMDC activation and, although, the immune response was similar to the single adjuvant, *in vivo*, a small decrease in tumor growth was detected. The PS-MPLA + PS-CL075 had similar *in vitro* results but the *in vivo* data did not induce as strong CD8⁺ T cells response compared to when NP-CpG-B was present in the treatment. Finally, PS-CL075 and NP-CpG-B combination did not show much synergistic effect *in vitro* and *in vivo*. For this experiment, only one cycle of irradiation and vaccination was performed in this chapter (Fig.4.6.A). The tumor growth curve did not show any differences between all vaccinated treatments but they were reduced compared to the non-vaccinated group (Fig.4.6.B). The staining of the spleen with SIINFEKL-specific CD8⁺ T cells did not show any significant difference between vaccinated mice and the negative control (Fig.4.6.C). The tumor microenvironment had an increased percentage of total CD8⁺ T cells, CD44⁺CD62L⁻ CD8⁺ T cells for NP-CpG-B alone, or combined, and CD25⁺ CD8⁺ T cells was upregulated in all vaccinated groups similarly (Fig.4.6.D). The CD4⁺ T cell response, in the tumor microenvironment, also showed similar trends as the CD8⁺ T cells (Fig.4.6.E, *left & middle*). The percentage of CD4⁺ T_{reg} was similar for all groups, with a slight increase for vaccinated mice (Fig.4.6.E, *right*).

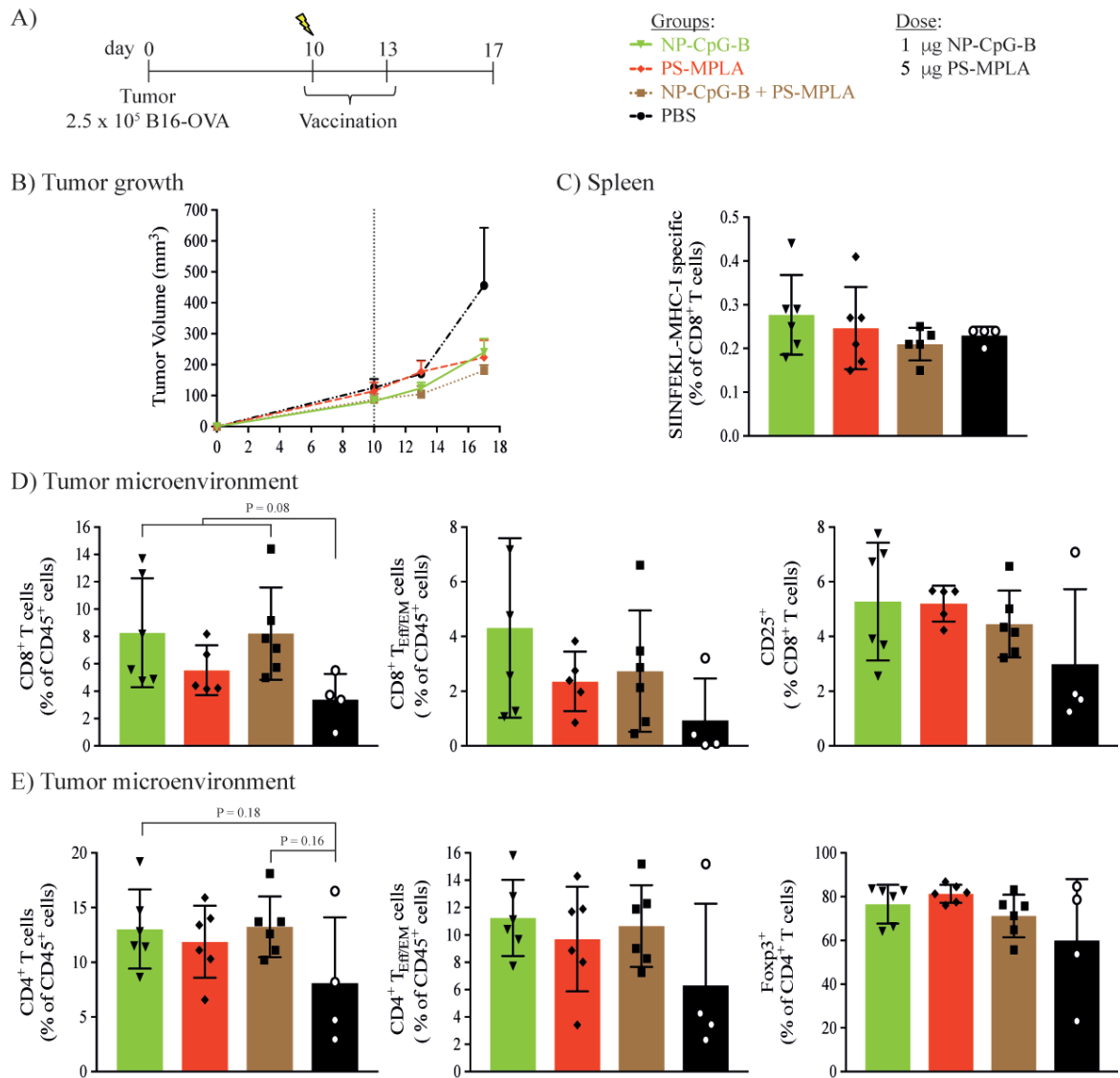


Figure 4.6 Vaccination with single or combined adjuvants resulted in a delayed tumor growth and an increased T cell response. 2.5 x 10⁵ B16-OVA tumor cells were inoculated in the right scapular dorsal skin before irradiating them with 15 Gy when tumor size reached 50-150 mm³. All vaccinated mice received two dose of vaccine, at day 10 and 13, by intradermal injection in the forelimb draining to the TdLN. (A) Timeline, treatment groups and adjuvant doses. (B) Average tumor growth. (C) SIINFEKL-specific CD8⁺ T cells in the spleen, without restimulation. (D) CD8⁺ T cells immune response in the tumor microenvironment. (E) CD4⁺ T cells immune response in the tumor microenvironment. Error bars indicate SEM for tumor growth curves and SD for all other graphs. N = 4-6 mice per groups. *P < 0.05 and **P < 0.01.

The *ex vivo* CD8⁺ T cells reactivation for the TdLN showed no differences in the percentage of TNFα⁺IFNγ⁺IL2⁺ positive cells (Fig.4.8.A, *top left*) but an increase in IL2 secretion was observed when both adjuvants were co-injected (277 ± 142 pg/mL) compared to all other treatments. A small trend in granzyme B production for all vaccinated groups was also detected (Fig.4.7.A, *middle & bottom left*). CD4⁺ T cells restimulation had an increase in triple positive cells when mice were vaccinated either with NP-CpG-B alone or combined (Fig.4.7.A, *top right*). In addition, a significant increase in IL2 and granzyme B secretion was observed when mice were vaccinated with PS-MPLA and NP-CpG-B and an even higher concentration of granzyme B was detected when NP-CpG-B alone was used to vaccinate the mice. Finally, no significant differences

were observed in cytokines secretion (Fig.4.7.B, *middle & bottom*) and polyfunctional cells (Fig.4.7.B, *top*) for all treatments when the spleen was reactivated with the SIINKEKL.

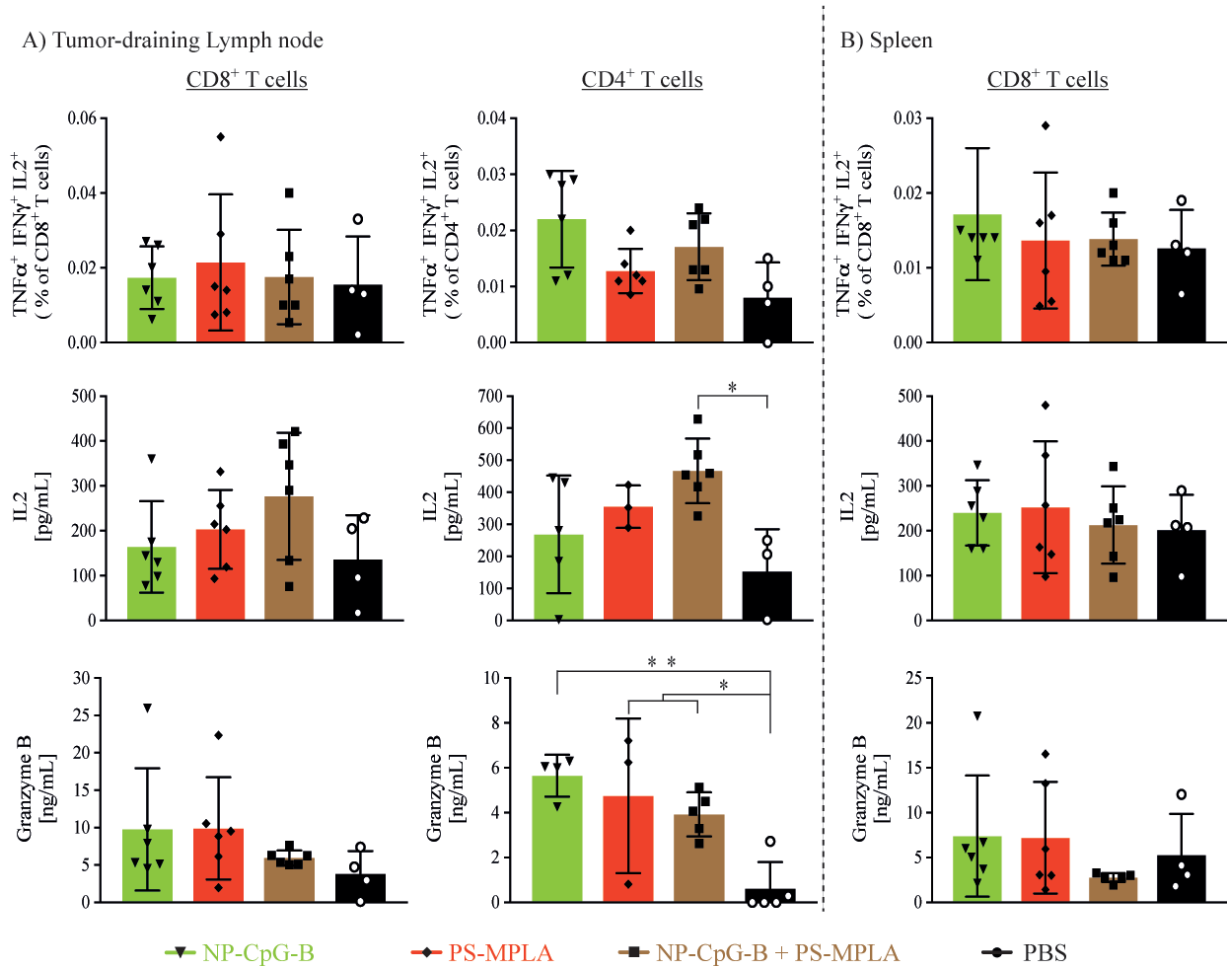


Figure 4.7 NP-CPG-B, alone or in combination, induced a slightly higher T cell activation in the TdLN. 2.5×10^5 B16-OVA tumor cells were inoculated in the right scapular dorsal skin before irradiating them with 15 Gy when tumor size reached 50-150 mm³. All vaccinated mice received two dose of vaccine, at day 10 and 13, by intradermal injection in the forelimb draining to the TdLN. (A) CD8⁺ and CD4⁺ T cells restimulation in the tumor-draining lymph node with SIINFEKL (*left column*) or OVA₃₂₇₋₃₃₉ (*right column*), respectively. *Top* graphs were TNF α^+ IFN γ^+ IL2⁺ T cells. *Middle* and *bottom* graphs were IL2 and granzyme B quantification by ELISA, respectively. (B) CD8⁺ T cell reactivation in the spleen. *Top* was the percentage of polyfunctional CD8⁺ T cells after 6 h restimulation. *Middle & bottom* graphs, indicated the IL2 and granzyme B concentration in the supernatant after 4 days restimulation. Error bars indicate SD for all other graphs. N = 4-5 mice per groups. *P < 0.05 and **P < 0.01

Overall the strongest immune response was observed when either NP-CpG-B alone, or in combination with PS-MPLA, was used. In addition the production of IL2 was increased compared to the other treatments when both TLRs agonist were co-injected.

Co-injection of PS-MPLA & NP-CpG-B reduced tumor growth and increased overall survival compared to radiotherapy only or NP-CpG-B.

Finally, an experiment was performed to determine if the adjuvant combination, together with tumor irradiation, increased the overall survival of tumor-bearing mice. The same vaccination schedule, and dose, as the previous experiment was used (Fig.4.9.A). Blood was sampled on day 16, before the start of the second treatment cycle, to quantify the presence of SIINFEKL-specific CD8⁺ T cells as well as their activation. As observed in the previous experiments, the vaccinated mice had a delay in tumor growth with a stronger effect when both adjuvants were co-injected (Fig.4.8.B, *top*). Indeed, since the tumor grew slower, mice co-injected with both adjuvants had a delay in the tumor growth after the two rounds of radiotherapy (Fig.4.8.B, *3rd graph*). The survival was increased by 5 and 17 days for the NP-CpG-B and PS-MPLA + NP-CpG-B, respectively, compared to irradiated mice only (Fig.4.8.C). A small increase in antigen-specific CD8⁺ T cells was detected when mice were only vaccinated with the TLR-9 agonist CpG-B ($0.22 \pm 0.05\%$) and the adjuvant combination had similar values ($0.16 \pm 0.04\%$) then the negative control, $0.16 \pm 0.02\%$ (Fig.4.8.D, *top*). On the other hand, PS-MPLA + NP-CpG-B injection induced a slightly higher percentage of CD25⁺ CD8⁺ T cells, compared to the two other groups (Fig.4.8.D, *middle & bottom*) but no differences in CD44⁺CD62L⁻ CD8⁺ T cells.

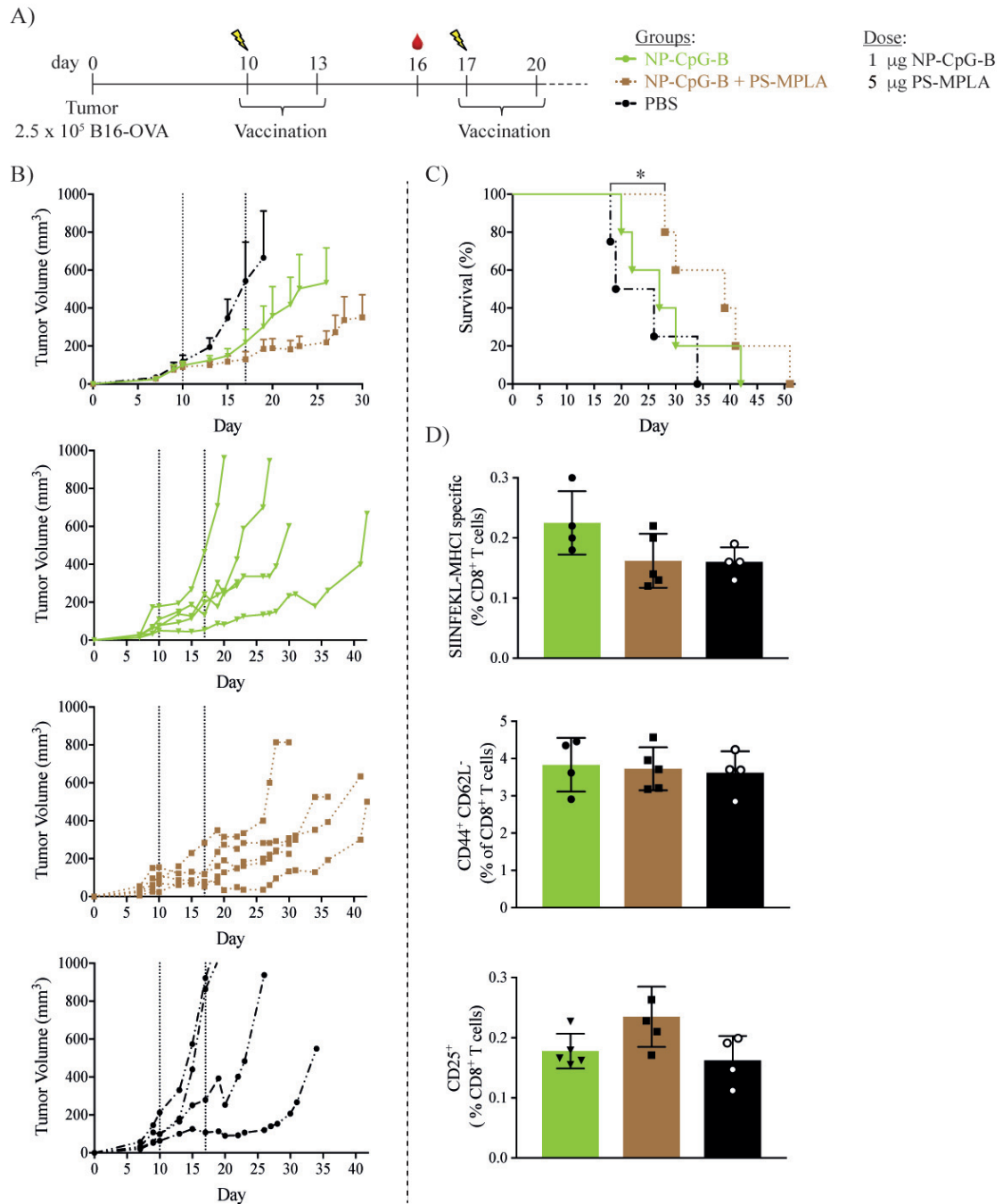


Figure 4.8 Survival was increased when mice were co-injected with both adjuvants. 2.5×10^5 B16-OVA tumor cells were inoculated in the right scapular dorsal skin before irradiating them with 15 Gy when tumor size reached 50-150 mm^3 . All vaccinated mice received two doses of vaccine, at day 10 and 13, by intradermal injection in the forelimb draining the tumor-draining lymph node. (A) Timeline, treatment groups and adjuvant doses. (B) Average and individual tumor growth. (C) Survival curve. (D) SIINFEKL-specific CD8⁺ T cells in the spleen, without restimulation and T cell immune activation. *Top graph*, SIINFEKL-specific CD8⁺ T cells. *Middle & bottom graph* were CD44⁺CD62L⁻ and CD25⁺ CD8⁺ T cells, respectively. Error bars indicate SEM for tumor growth curves and SD for all other graphs. N = 4-6 mice per group. *P < 0.05 and **P < 0.01.

4.5. Discussion

The main goal of this study was to determine the immune response and overall survival of B16-OVA tumor-bearing mice when radiotherapy was combined with an adjuvanted-nanoparticulate vaccination. We hypothesized that since the immune priming occurred in the tumor-draining lymph node after radiotherapy, the response would be increased if our vaccine would deliver TLR agonists to the same lymph node. In order to obtain to optimal immune response when combining adjuvant vaccination with ionizing radiation, several parameters were tested.

The purpose of the first experiment was to determine if the combination of TLR agonist vaccination and radiotherapy enhanced the immune response compared to ionizing radiation only since most of the studies inject intratumorally the vaccine whereas we target the tumor-draining lymph node. The results demonstrated a clear increase in T cells immune response when mice were vaccinated, in addition to an increase of T cells infiltrate in the tumor microenvironment. In a second time we also tested two different vaccination schedule since the process by which APCs phagocytize cancer cells and drain to the lymph node is not instantaneous. We hypothesized that the immune response would be increased if mice received a second vaccination 3 days after the 1st adjuvant injection, due to a higher percentage of activated APCs in the lymph node. Surprisingly, following the two vaccination schedules the tumor growth was no different from the negative control, which was only irradiated (Fig.4.1.B). First of all the lack of differences with the negative control group could be due the time at which the first irradiation occurred. Indeed, the average tumor size for all three groups were between 5-30 mm³, which was considered rather small and, in addition, the irradiation used was considered ablative, thus the tumor growth delay could simply be due to the radiation and not because of the vaccination. The reasoning for using B16-OVA cell line was to be able to quantify the amount of SIINFEKL-specific CD8⁺ T cells but unfortunately, the percentage between all three treatments was not significantly different, although a small trend was detected when mice were vaccinated with 2 x 20 µg CpG-B compared to the other groups (Fig.4.1.C, *left*). Of course, since radiotherapy induces the release of a broad range of antigens, it was possible to have differences for other tumor antigens, such as TRP-2, gp100 or other neoantigens, which was not tested here. The adjuvant vaccination, independently of the schedule, increased the percentage of effector CD8⁺ T cells, in addition to having higher CD8⁺ T cells in the tumor microenvironment, which indicate an overall increased immune activation compared to the mice only irradiated (Fig.4.1.D, *left*). The small increase of PD-1+ T cells when mice were only irradiated, in addition to the decrease in cytokine secretion, after restimulation, would suggests an exhaustion of T cell or a lower immune activation. Indeed it is known that exhausted T cell express activation markers as well as PD-1 but induce less cytokine secretion^{134,135}. Although both vaccine

schedules induced similar response in the tumor microenvironment, the reactivation of specific peptide showed higher cytokine production, especially IFN γ , when a vaccination boost was administered to the mice. The increased secretion observed during restimulation for the 4 x 10 μ g CpG-B group could simply be due to the timing of the boost, which was 4 days before collecting the organs and so the increase was due to the activation caused by the vaccine rather than the reactivation itself. The slightly higher T cell activation observed for the 2 x 20 μ g CpG-B compared to the other vaccine could be explained by the fact that the higher dose at an earlier time point was better at inducing an anti-tumor response. Overall, vaccinating mice with a TLR agonist enhanced the immune response compared to radiotherapy only and a small trend in increased activation was detected when for the group not receiving a boost.

The second parameter tested was the choice of the lymph node to target. Indeed the most logical choice would be to target the tumor-draining lymph node since this is the location where tumor antigens and APCs would drain but there was a risk of it being immunosuppressive, which would dampen the immune response. The significant decrease in tumor growth when the non-TdLN was targeted was likely due to the initial size of the tumor (< 30 mm³) and the increased T cell response (as evidenced by the higher antigen-specific IFN γ secretion in the spleen) compared to the other two treatments. Indeed both of these parameters were shown to be important at inducing a tumor growth reduction and immune response. Surprisingly, the reduced tumor size was not associated with an increased T cell population in the tumor compared to the negative control (Fig.4.3.C). The comparison of IFN γ secretion in both lymph nodes indicated a small dampening of the immune response in the TdLN since it was decreased compared to the non-TdLN. Finally, the absence of IFN γ in the non-TdLN in the two other treatment groups (Fig.4.4.B, *bottom*) demonstrate that the activation of the immune system occurs only in the adjuvant targeted lymph node, which would be important to reduce the risk of toxicity due to systemic activation as well as autoimmune disease. Indeed radiotherapy will induce the release of not only tumor antigens but also self-antigens, thus potentially activating the immune response in the lymph node against all of them. We hypothesized that if the activation happened in only a specific organ and not the entire system, the risk of adverse effect would be decreased. Overall, although results showed a decreased tumor growth and increased immune response, when targeting the non-TdLN, these experiments should be repeated with a later irradiation starting point to reduce the effect induced by radiotherapy in addition to using NP-CpG-B as vaccine.

The last parameter tested was the injection site. As discussed in the introduction, most of the TLR agonist treatments currently tested in combination with radiotherapy are, for the most part, injected intratumorally. We were interested in comparing both injection routes to determine if one

was preferred to the other in term of T cell response when using nanocarriers to deliver the adjuvant. In general, mice vaccinated, independently from the injection site, showed a reduced tumor growth in addition to increased survival compared to irradiated only (Fig.4.5.B & C). 2 out of 5 mice in the intratumoral injection groups did not responded after the first boost administered because, not only their size were close to the limit (700 mm^3), the tumor ulcerated, thus preventing the second vaccination to be effective (Fig.4.5.B, 3rd graph). In addition due to the multiple vaccination (4x) and the technique used to irradiate mice, most tumors ulcerated at one point and if the vaccine was administered intratumorally, part of the injection was lost. As observed in the previous experiments, a trend was observed in the proportion of SIINFEKL-specific CD8⁺ T cells (Fig.4.5.C, top) and no difference in percentage (data not shown) of T cells, or activation (Fig.4.5.C, middle & bottom), were detected in the blood. Overall, the two different injection sites did not modify of the T cell immune response or the survival but due to the risk of losing the vaccination efficacy due to tumor ulceration, it was considered safer to inject mice intradermally in the forelimb draining to the TdLN for the following experiments.

The induction of the immune response was quantified after combining radiotherapy with PS-MPLA + NP-CpG-B adjuvant vaccination. All vaccinations tested decreased the tumor growth, similarly, but the tumor microenvironment had an increase in CD8⁺ and CD4⁺ T cells when mice were vaccinated with NP-CpG-B alone or in combination. In addition, the same vaccine induced a trend in increase CD44⁺CD62L⁻ T cells, which suggested higher immune activation. Unfortunately, most of the CD4⁺ T cells present in the tumor were regulatory cells, which is known to induce an immunosuppressive environment, but the difference between vaccinated and the negative control were small, indicating no strong increase in suppression when the vaccination was added to the treatment. The increase in IL2 secretion after CD8⁺ or CD4⁺ T cell reactivation in the TdLN when both adjuvants were co-injected indicate a strong immune activation. This cytokine induces not only the activation and proliferation of CD8⁺ T cell, it also activates NK cells, which are important for a strong anti-tumor¹³⁶. It has been demonstrated that CD4⁺ T cells can also be cytotoxic and secrete granzyme B after recognition of the MHC-II antigen¹³⁷. The expression of granzyme B in CD4⁺ T cells restimulation condition was caused by an increase of secretion in IL2. Indeed it was shown that IL2 induced the expression of granzyme B, as well as perforin¹³⁸. Overall the co-injection of PS-MPLA with NP-CpG-B, as well as NP-CpG-B to a lesser extent, induced a stronger immune response in the tumor-draining lymph node, which translated in an increase percentage in CD8⁺ or CD4⁺ T cells populations. The survival experiment with NP-CpG-B, with or without PS-MPLA, demonstrated a strong reduction in tumor growth when mice were vaccinated with both adjuvants, which increased the survival of mice compared to the negative control group. Some studies had shown that an antibody response was able to reduce tumor growth but unfortunately, no

OVA-specific antibodies were detected in any of the treatment tested (data not shown). The exact mechanism by which the adjuvant combination induced a reduce tumor growth was not yet found but the increase in IL2 secretion in the tumor draining lymph node could be an reasonable option since it not only induce the activation of CD8⁺ T cells, it also activated NK cells.

Chapter 5

Conclusion, Implication and Future prospect

5.1. Conclusion

The purpose of this thesis was to develop a nano-adjuvant vaccine, which will target the tumor-draining lymph node (TdLN), and evaluate its efficacy in melanoma, alone or in combination with radiotherapy.

We have started this project by synthesizing the different components of the two nanocarriers, previously developed in our laboratory, and characterizing the loading of the different Toll-like receptors (TLRs) agonists on either of them. The adjuvants MPLA and CL075 were successfully encapsulated in polymersomes (PSs) whereas CpG-B was conjugated onto nanoparticles (NPs). A small decrease in dendritic cells (DCs) activation, *in vitro*, was observed when MPLA was loaded in polymersomes compared to the free adjuvant whereas no difference was detected for PS-CL075 or NP-CpG-B compared to their free counterpart. Finally, we have also demonstrated that both particulates are internalized by DCs through macropinocytosis.

Once we had characterized the different nano-adjuvants, we determined if synergistic effect could be detected when combining them together using a combinatorial approach. A strong increase in pro-inflammatory cytokine (IL2p70, TNF α and IL6) was observed when PS-MPLA was incubated with either PS-CL075 or NP-CpG-B with DCs, *in vitro*. In addition, it appeared that the highest dose tested induced exhaustion of the cells through the secretion of IL10. The third adjuvant combination, PS-CL075 and NP-CpG-B, only induced a synergy for the secretion of TNF α but not the other cytokines. Afterwards, we verified if the results obtained on DCs would translate into an enhanced T cell activation, *in vitro* and *in vivo*. Overall small increases in activations were detected in proliferation or cytokine production, *in vitro*, but none were synergistic. All three nano-adjuvant combinations were tested *in vivo* in a B16-OVA implantable melanoma model and although they all induced similar T cell immune responses, only PS-MPLA and NP-CpG-B was able to delay the tumor growth compared to the single adjuvant.

Finally, we studied the combination of radiotherapy with our adjuvant-nanoparticulate vaccine as well as different parameters for the vaccine injection, such as the injection route, the lymph node targeted and the vaccine schedule. Most of the ongoing clinical trials and studies combining radiotherapy with adjuvant vaccine administer the treatment intratumorally and so we wanted to determine if the immune system could also be enhanced when injecting intradermally to target the tumor-draining lymph node. We have demonstrated an enhance T cell response when adjuvants were injected intradermally compared to ionizing radiation only. In addition, intradermal or intratumoral administration of NP-CpG-B induced similar tumor growth and survival. The

administration of PS-MPLA + NP-CpG-B, in combination with 15 Gy radiotherapy increased significantly the survival compared to NP-CpG-B vaccination or ionizing radiation only.

5.2. Implication and future directions

Development of an adjuvanted-cancer vaccine

One of the major goals of this thesis was to develop a cancer vaccine composed only of adjuvants, which were delivered to the tumor-draining lymph node thanks to the different particles produced in our laboratory. A majority of the studies published with these nanocarriers have used CpG-B as the adjuvants without testing other TLR agonist. Here we were able to produce, in addition to NP-CpG-B, two other nano-adjuvants, PS-MPLA and PS-CL075. In addition, the combination of the different adjuvants induced an enhanced DCs activation, *in vitro*. This research showed that although the adjuvants were on different particles, synergistic effect could still be observed *in vitro*. Indeed, most of the studies combining different TLRs agonists deliver them all on the same carrier, and so doses of each TLR cannot be varied. In our case, different doses could be used for the vaccine, making it a much more flexible and tunable approach. In addition, if someone would like to add another nano-adjuvant or antigen to our vaccine, it would be easy to do so without having to modify the pre-existing components of the vaccines.

Although synergistic effects were detected for the combination of PS-MPLA with PS-CL075 or NP-CpG-B, when activating BMDCs *in vitro*, it did not translate in strong differences in T cells activation. In addition, some of the doses tested induced the production of IL10, indicating an overstimulation and exhaustion of DCs¹³⁹. A solution for this issue would be to decrease the incubation time in order to quantify cytokines secretion at an earlier stage of cell maturation, before it reaches exhaustion. In addition, only pro-inflammatory cytokines as well as IL10 have been quantified but MPLA is also supposed to induce the expression of type I IFN, which is known to initiate an anti-tumor response¹⁴⁰. A deeper understanding of the DCs activation in terms of cytokines and chemokines would help understanding the findings observed when testing the different nano-adjuvants combination in an orthotopical implantable melanoma model. Indeed, PS-MPLA co-administered with NP-CpG-B decreased tumor growth but the T cell immune response was not different compared to the injection of only NP-CpG-B. It would also be interesting to assess the activation of other antigen-presenting cells in the lymph node in addition to natural killer cells and B cells which play a role in tumor growth. This could be done *in vitro*, thanks to co-cultures, as well as *in vivo*.

Radiotherapy combination with adjuvanted vaccine

Although radiotherapy was initially thought to only induce cell death and an immunosuppressive environment, it has since then been demonstrated that this treatment was able to induce an anti-tumor response depending on the irradiation dose, frequency and the type of cancer. Since radiotherapy is one of the first-line of treatment for many cancers, several clinical trials are testing the efficacy of adding intratumoral injection of adjuvants to it. In addition, it has been reported that following radiotherapy, the priming of the immune system occurs in the tumor-draining lymph node ¹⁴¹. The advantage of combining our nano-adjuvant vaccine with radiotherapy was to take advantage of the targeting properties of the carriers for the tumor-draining lymph node to enhance the immune response taking place due to radiotherapy. In addition, several immune cells, as well as endothelial, are radiosensitive, and so rather than activating the immune system in the tumor microenvironment, which reduces the immune response within it, the lymph node immune population is not affected by the treatment. Finally, the induction of immunogenic cell death of cancerous cells will release a broad range of antigens, tumor-associated and tumor-specific, which in turn will educate the immune system against a broad range of molecules decreasing the chance of tumor evasions ¹⁴².

Overall, we were able to enhance the immune response when both treatments were used and even increase survival when PS-MPLA + NP-CpG-B was used compared to only radiotherapy. We had previously shown that the immunosuppressive environment in the lymph node could be overturned into a more immunopermissive state when NP-CpG-B was administered ⁶³. It would be interesting to quantify the immune suppression in the TdLN after radiotherapy by itself and how it changes after the different vaccination were administered. In addition, the response of other immune cells, such as natural killers (NK), NK T cells and macrophages should be assessed since we did not see clear differences in the T cell immune activation between the different vaccinations.

An increasing number of studies show the advantage of combining different cancer treatments in order to fight the disease from all possible sides, and our approach has the advantage of being easily tunable and versatile depending on the vaccine requirement. Furthermore, our treatment targets the tumor-draining lymph node rather than the tumor directly, which when combined to radiotherapy is an important aspect due to the radiosensitivity of certain cells. One characteristic that our vaccine does not take into account is the immunosuppressive microenvironment generated by the tumor, which is a known mechanism for tumor evasion. Therefore, it would be important to assess how the tumor and the tumor-draining lymph node environments are modified after radiotherapy and vaccination, to further improve our treatment.

References

- 1 World Health Organization. Cancer: Key facts. www.who.int/en/news-room/fact-sheets/detail/cancer (2018). Available at: (Accessed: 20 May 2018)
- 2 **National Health Institute of the USA. Cancer Facts & Figures 2018. 1–76 (2018).**
- 3 Mehlen, P. & Puisieux, A. Metastasis: a question of life or death. *Nat Rev Cancer* **6**, 449–458 (2006).
- 4 Hanahan, D., & Weinberg, R. A. (2000). The hallmarks of cancer. *cell*, *100*(1), 57-70.
- 5 Dunn, G. P., Old, L. J., & Schreiber, R. D. (2004). The immunobiology of cancer immunosurveillance and immunoediting. *Immunity*, *21*(2), 137-148.
- 6 Quail, D. F., & Joyce, J. A. (2013). Microenvironmental regulation of tumor progression and metastasis. *Nature medicine*, *19*(11), 1423.
- 7 Teng, M. W., Galon, J., Fridman, W. H., & Smyth, M. J. (2015). From mice to humans: developments in cancer immunoediting. *The Journal of clinical investigation*, *125*(9), 3338-3346.
- 8 Mittal, D., Gubin, M. M., Schreiber, R. D., & Smyth, M. J. (2014). New insights into cancer immunoediting and its three component phases—elimination, equilibrium and escape. *Current opinion in immunology*, *27*, 16-25.
- 9 Bracci, L., Schiavoni, G., Sistigu, A., & Belardelli, F. (2014). Immune-based mechanisms of cytotoxic chemotherapy: implications for the design of novel and rationale-based combined treatments against cancer. *Cell death and differentiation*, *21*(1), 15.
- 10 Chen, G., & Emens, L. A. (2013). Chemoimmunotherapy: reengineering tumor immunity. *Cancer Immunology, Immunotherapy*, *62*(2), 203-216.
- 11 Deloch, L., Derer, A., Hartmann, J., Frey, B., Fietkau, R., & Gaipl, U. S. (2016). Modern radiotherapy concepts and the impact of radiation on immune activation. *Frontiers in oncology*, *6*, 141.
- 12 Formenti, S. C., & Demaria, S. (2013). Combining radiotherapy and cancer immunotherapy: a paradigm shift. *JNCI: Journal of the National Cancer Institute*, *105*(4), 256-265.
- 13 Koury, J., Lucero, M., Cato, C., Chang, L., Geiger, J., Henry, D., ... & Tran, A. (2018). Immunotherapies: Exploiting the Immune System for Cancer Treatment. *Journal of immunology research*, 2018.
- 14 Rosenberg, S. A. (2014). Decade in review—Cancer immunotherapy: Entering the mainstream of cancer treatment. *Nature Reviews Clinical Oncology*, *11*(11), 630
- 15 Palucka, K., & Banchereau, J. (2013). Dendritic-cell-based therapeutic cancer vaccines. *Immunity*, *39*(1), 38-48.
- 16 Whilding, L. M., & Maher, J. (2015). CAR T cell immunotherapy: The path from the byroad to the freeway?. *Molecular oncology*, *9*(10), 1994-2018.
- 17 Pierce, R. H., Campbell, J. S., Pai, S. I., Brody, J. D., & Kohrt, H. E. (2015). In-situ tumor vaccination: bringing the fight to the tumor. *Human vaccines & immunotherapeutics*, *11*(8), 1901-1909.
- 18 Hammerich, L., Binder, A., & Brody, J. D. (2015). In situ vaccination: Cancer immunotherapy both personalized and off the shelf. *Molecular oncology*, *9*(10), 1966-1981.
- 19 Kakimi, K., Karasaki, T., Matsushita, H., & Sugie, T. (2017). Advances in personalized cancer immunotherapy. *Breast Cancer*, *24*(1), 16-24.
- 20 Zhang, X., Sharma, P. K., Goedegebuure, S. P., & Gillanders, W. E. (2017). Personalized cancer vaccines: Targeting the cancer mutanome. *Vaccine*, *35*(7), 1094-1100.
- 21 Yang, Y. (2015). Cancer immunotherapy: harnessing the immune system to battle cancer. *The Journal of clinical investigation*, *125*(9), 3335-3337.
- 22 Ilyas, S., & Yang, J. C. (2015). Landscape of tumor antigens in T cell immunotherapy. *The Journal of Immunology*, *195*(11), 5117-5122.

- 23 Coulie, P. G., Van den Eynde, B. J., Van Der Bruggen, P., & Boon, T. (2014). Tumour antigens recognized by T lymphocytes: at the core of cancer immunotherapy. *Nature Reviews Cancer*, *14*(2), 135.
- 24 Lennerz, V., Fatho, M., Gentilini, C., Frye, R. A., Lifke, A., Ferel, D., ... & Wölfel, T. (2005). The response of autologous T cells to a human melanoma is dominated by mutated neoantigens. *Proceedings of the National Academy of Sciences of the United States of America*, *102*(44), 16013-16018.
- 25 Baitsch, L., Fuertes-Marraco, S. A., Legat, A., Meyer, C., & Speiser, D. E. (2012). The three main stumbling blocks for anticancer T cells. *Trends in immunology*, *33*(7), 364-372.
- 26 Chiang, C. L. L., Coukos, G., & Kandalafi, L. E. (2015). Whole tumor antigen vaccines: where are we?. *Vaccines*, *3*(2), 344-372.
- 27 Spiotto, M., Fu, Y. X., & Weichselbaum, R. R. (2016). The intersection of radiotherapy and immunotherapy: mechanisms and clinical implications. *Science immunology*, *1*(3).
- 28 Chacon, J. A., Schutsky, K., & Powell, D. J. (2016). The impact of chemotherapy, radiation and epigenetic modifiers in cancer cell expression of immune inhibitory and stimulatory molecules and anti-tumor efficacy. *Vaccines*, *4*(4), 43.
- 29 Ma, Y., Adjemian, S., Mattarollo, S. R., Yamazaki, T., Aymeric, L., Yang, H., ... & Martins, I. (2013). Anticancer chemotherapy-induced intratumoral recruitment and differentiation of antigen-presenting cells. *Immunity*, *38*(4), 729-741.
- 30 Benvenuti, F. (2016). The dendritic cell synapse: a life dedicated to T cell activation. *Frontiers in immunology*, *7*, 70.
- 31 Thaiss, C. A., Semmling, V., Franken, L., Wagner, H., & Kurts, C. (2011). Chemokines: a new dendritic cell signal for T cell activation. *Frontiers in immunology*, *2*, 31.
- 32 Malissen, B., Grégoire, C., Malissen, M., & Roncagalli, R. (2014). Integrative biology of T cell activation. *Nature immunology*, *15*(9), 790.
- 33 Lizée, G., Overwijk, W. W., Radvanyi, L., Gao, J., Sharma, P., & Hwu, P. (2013). Harnessing the power of the immune system to target cancer. *Annual review of medicine*, *64*, 71-90.
- 34 Palm, N. W., & Medzhitov, R. (2009). Pattern recognition receptors and control of adaptive immunity. *Immunological reviews*, *227*(1), 221-233.
- 35 Tatsumi, T., Kierstead, L. S., Ranieri, E., Gesualdo, L., Schena, F. P., Finke, J. H., ... & Storkus, W. J. (2002). Disease-associated bias in T helper type 1 (Th1)/Th2 CD4+ T cell responses against MAGE-6 in HLA-DRB10401+ patients with renal cell carcinoma or melanoma. *Journal of Experimental Medicine*, *196*(5), 619-628.
- 36 Dowling, J. K., & Mansell, A. (2016). Toll-like receptors: the swiss army knife of immunity and vaccine development. *Clinical & translational immunology*, *5*(5).
- 37 Ammi, R., De Waele, J., Willemen, Y., Van Brussel, I., Schrijvers, D. M., Lion, E., & Smits, E. L. (2015). Poly (I: C) as cancer vaccine adjuvant: knocking on the door of medical breakthroughs. *Pharmacology & therapeutics*, *146*, 120-131.
- 38 Einstein, M. H., Baron, M., Levin, M. J., Chatterjee, A., Edwards, R. P., Zepp, F., ... & Dubin, G. (2009). Comparison of the immunogenicity and safety of Cervarix™ and Gardasil® human papillomavirus (HPV) cervical cancer vaccines in healthy women aged 18–45 years. *Human vaccines*, *5*(10), 705-719.
- 39 Neidhart, J., Allen, K. O., Barlow, D. L., Carpenter, M., Shaw, D. R., Triozzi, P. L., & Conry, R. M. (2004). Immunization of colorectal cancer patients with recombinant baculovirus-derived KSA (Ep-CAM) formulated with monophosphoryl lipid A in liposomal emulsion, with and without granulocyte-macrophage colony-stimulating factor. *Vaccine*, *22*(5-6), 773-780.
- 40 Awasthi, S. (2014). Toll-like receptor-4 modulation for cancer immunotherapy. *Frontiers in immunology*, *5*, 328.
- 41 Narayan, R., Nguyen, H., Bentow, J. J., Moy, L., Lee, D. K., Greger, S., ... & Konishi, T. (2012). Immunomodulation by imiquimod in patients with high-risk primary melanoma. *Journal of Investigative Dermatology*, *132*(1), 163-169.

- 42 Pashenkov, M., Goëss, G., Wagner, C., Hörmann, M., Jandl, T., Moser, A., ... & Tantcheva-Poor, I. (2006). Phase II trial of a Toll-like receptor 9-activating oligonucleotide in patients with metastatic melanoma. *Journal of Clinical Oncology*, 24(36), 5716-5724.
- 43 Bode, C., Zhao, G., Steinhagen, F., Kinjo, T., & Klinman, D. M. (2011). CpG DNA as a vaccine adjuvant. *Expert review of vaccines*, 10(4), 499-511.
- 44 Vonderheide, R. H., Flaherty, K. T., Khalil, M., Stumacher, M. S., Bajor, D. L., Hutnick, N. A., ... & Green, S. J. (2007). Clinical activity and immune modulation in cancer patients treated with CP-870,893, a novel CD40 agonist monoclonal antibody. *Journal of Clinical Oncology*, 25(7), 876-883.
- 45 Schwartzentruber, D. J., Lawson, D. H., Richards, J. M., Conry, R. M., Miller, D. M., Treisman, J., ... & Kendra, K. L. (2011). gp100 peptide vaccine and interleukin-2 in patients with advanced melanoma. *New England Journal of Medicine*, 364(22), 2119-2127.
- 46 Huckriede, A., Bungener, L., Stegmann, T., Daemen, T., Medema, J., Palache, A. M., & Wilschut, J. (2005). The virosome concept for influenza vaccines. *Vaccine*, 23, S26-S38.
- 47 Swartz, M. A. (2001). The physiology of the lymphatic system. *Advanced drug delivery reviews*, 50(1-2), 3-20.
- 48 Reddy, S. T., Rehor, A., Schmoekel, H. G., Hubbell, J. A., & Swartz, M. A. (2006). In vivo targeting of dendritic cells in lymph nodes with poly (propylene sulfide) nanoparticles. *Journal of Controlled Release*, 112(1), 26-34.
- 49 Hauert, S., & Bhatia, S. N. (2014). Mechanisms of cooperation in cancer nanomedicine: towards systems nanotechnology. *Trends in biotechnology*, 32(9), 448-455.
- 50 Adjei, I. M., Sharma, B., & Labhasetwar, V. (2014). Nanoparticles: cellular uptake and cytotoxicity. In *Nanomaterial* (pp. 73-91). Springer, Dordrecht.
- 51 Behzadi, S., Serpooshan, V., Tao, W., Hamaly, M. A., Alkawareek, M. Y., Dreaden, E. C., ... & Mahmoudi, M. (2017). Cellular uptake of nanoparticles: journey inside the cell. *Chemical Society Reviews*, 46(14), 4218-4244.
- 52 Petros, R. A., & DeSimone, J. M. (2010). Strategies in the design of nanoparticles for therapeutic applications. *Nature reviews Drug discovery*, 9(8), 615.
- 53 Orth, M., Lauber, K., Niyazi, M., Friedl, A. A., Li, M., Maihöfer, C., ... & Belka, C. (2014). Current concepts in clinical radiation oncology. *Radiation and environmental biophysics*, 53(1), 1-29.
- 54 Prasanna, A., Ahmed, M. M., Mohiuddin, M., & Coleman, C. N. (2014). Exploiting sensitization windows of opportunity in hyper and hypo-fractionated radiation therapy. *Journal of thoracic disease*, 6(4), 287.
- 55 Galluzzi, L., Kepp, O., & Kroemer, G. (2013). Immunogenic cell death in radiation therapy.
- 56 Golden, E. B., & Apetoh, L. (2015, January). Radiotherapy and immunogenic cell death. In *Seminars in radiation oncology* (Vol. 25, No. 1, pp. 11-17). Elsevier.
- 57 Perez, C. A., Fu, A., Onishko, H., Hallahan, D. E., & Geng, L. (2009). Radiation induces an antitumour immune response to mouse melanoma. *International journal of radiation biology*, 85(12), 1126-1136.
- 58 Cummings, R. J., Gerber, S. A., Judge, J. L., Ryan, J. L., Pentland, A. P., & Lord, E. M. (2012). Exposure to ionizing radiation induces the migration of cutaneous dendritic cells by a CCR7-dependent mechanism. *The Journal of Immunology*, 189(9), 4247-4257.
- 59 Lee, Y., Auh, S. L., Wang, Y., Burnette, B., Wang, Y., Meng, Y., ... & Weichselbaum, R. R. (2009). Therapeutic effects of ablative radiation on local tumor require CD8+ T cells: changing strategies for cancer treatment. *Blood*, 114(3), 589-595.
- 60 Gameiro, S. R., Jammed, M. L., Wattenberg, M. M., Tsang, K. Y., Ferrone, S., & Hodge, J. W. (2014). Radiation-induced immunogenic modulation of tumor enhances antigen processing and calreticulin exposure, resulting in enhanced T-cell killing. *Oncotarget*, 5(2), 403.

- 61 Van Der Vlies, A. J., O'Neil, C. P., Hasegawa, U., Hammond, N., & Hubbell, J. A. (2010). Synthesis of pyridyl disulfide-functionalized nanoparticles for conjugating thiol-containing small molecules, peptides, and proteins. *Bioconjugate chemistry*, *21*(4), 653-662.
- 62 Thomas, S. N., Vokali, E., Lund, A. W., Hubbell, J. A., & Swartz, M. A. (2014). Targeting the tumor-draining lymph node with adjuvanted nanoparticles reshapes the anti-tumor immune response. *Biomaterials*, *35*(2), 814-824.
- 63 Jeanbart, L., Ballester, M., De Titta, A., Corthésy, P., Romero, P., Hubbell, J. A., & Swartz, M. A. (2014). Enhancing efficacy of anticancer vaccines by targeted delivery to tumor-draining lymph nodes. *Cancer immunology research*, *2*(5), 436-447.
- 64 De Titta, A., Ballester, M., Julier, Z., Nembrini, C., Jeanbart, L., Van Der Vlies, A. J., ... & Hubbell, J. A. (2013). Nanoparticle conjugation of CpG enhances adjuvancy for cellular immunity and memory recall at low dose. *Proceedings of the National Academy of Sciences*, *110*(49), 19902-19907
- 65 Scott, E. A., Stano, A., Gillard, M., Maio-Liu, A. C., Swartz, M. A., & Hubbell, J. A. (2012). Dendritic cell activation and T cell priming with adjuvant-and antigen-loaded oxidation-sensitive polymersomes. *Biomaterials*, *33*(26), 6211-6219.
- 66 Stano, A., Scott, E. A., Dane, K. Y., Swartz, M. A., & Hubbell, J. A. (2013). Tunable T cell immunity towards a protein antigen using polymersomes vs. solid-core nanoparticles. *Biomaterials*, *34*(17), 4339-4346.
- 67 Bagchi, A., Herrup, E. A., Warren, H. S., Trigilio, J., Shin, H. S., Valentine, C., & Hellman, J. (2007). MyD88-dependent and MyD88-independent pathways in synergy, priming, and tolerance between TLR agonists. *The Journal of Immunology*, *178*(2), 1164-1171.
- 68 Minor, P. D. (2015). Live attenuated vaccines: historical successes and current challenges. *Virology*, *479*, 379-392.
- 69 Draper, S. J., & Heeney, J. L. (2010). Viruses as vaccine vectors for infectious diseases and cancer. *Nature reviews Microbiology*, *8*(1), 62.
- 70 Karch, C. P., & Burkhard, P. (2016). Vaccine technologies: from whole organisms to rationally designed protein assemblies. *Biochemical pharmacology*, *120*, 1-14.
- 71 Kourtis, I. C., Hirosue, S., De Titta, A., Kontos, S., Stegmann, T., Hubbell, J. A., & Swartz, M. A. (2013). Peripherally administered nanoparticles target monocytic myeloid cells, secondary lymphoid organs and tumors in mice. *PloS one*, *8*(4), e61646.
- 72 Nembrini, C., Stano, A., Dane, K. Y., Ballester, M., Van Der Vlies, A. J., Marsland, B. J., ... & Hubbell, J. A. (2011). Nanoparticle conjugation of antigen enhances cytotoxic T-cell responses in pulmonary vaccination. *Proceedings of the National Academy of Sciences*, *108*(44), E989-E997.
- 73 Hirosue, S., Kourtis, I. C., van der Vlies, A. J., Hubbell, J. A., & Swartz, M. A. (2010). Antigen delivery to dendritic cells by poly (propylene sulfide) nanoparticles with disulfide conjugated peptides: Cross-presentation and T cell activation. *Vaccine*, *28*(50), 7897-7906.
- 74 Galan-Navarro, C., Rincon-Restrepo, M., Zimmer, G., Saphire, E. O., Hubbell, J. A., Hirosue, S., ... & Kunz, S. (2017). Oxidation-sensitive polymersomes as vaccine nanocarriers enhance humoral responses against Lassa virus envelope glycoprotein. *Virology*, *512*, 161-171.
- 75 Rincon-Restrepo, M., Mayer, A., Hauert, S., Bonner, D. K., Phelps, E. A., Hubbell, J. A., ... & Hirosue, S. (2017). Vaccine nanocarriers: Coupling intracellular pathways and cellular biodistribution to control CD4 vs CD8 T cell responses. *Biomaterials*, *132*, 48-58.
- 76 Sato, Y., Goto, Y., Narita, N., & Hoon, D. S. (2009). Cancer cells expressing toll-like receptors and the tumor microenvironment. *Cancer microenvironment*, *2*(1), 205-214.
- 77 Salem, M. L., Díaz-Montero, C. M., Al-Khami, A. A., El-Naggar, S. A., Naga, O., Montero, A. J., ... & Cole, D. J. (2009). Recovery from cyclophosphamide-induced lymphopenia results in expansion of immature dendritic cells which can mediate enhanced prime-boost vaccination antitumor responses in vivo when stimulated with the TLR3 agonist poly (I: C). *The Journal of Immunology*, *182*(4), 2030-2040.

- 78 Mehrotra, S., Britten, C. D., Chin, S., Garrett-Mayer, E., Cloud, C. A., Li, M., ... & Paulos, C. M. (2017). Vaccination with poly (IC: LC) and peptide-pulsed autologous dendritic cells in patients with pancreatic cancer. *Journal of hematology & oncology*, *10*(1), 82.
- 79 Iribarren, K., Bloy, N., Buqué, A., Cremer, I., Eggermont, A., Fridman, W. H., ... & Kroemer, G. (2016). Trial Watch: Immunostimulation with Toll-like receptor agonists in cancer therapy. *Oncoimmunology*, *5*(3), e1088631.
- 80 Vaure, C., & Liu, Y. (2014). A comparative review of toll-like receptor 4 expression and functionality in different animal species. *Frontiers in immunology*, *5*, 316.
- 81 Romanowski, B., Schwarz, T. F., Ferguson, L. M., Peters, K., Dionne, M., Schulze, K., ... & Schuind, A. (2011). Immunogenicity and safety of the HPV-16/18 AS04-adjuvanted vaccine administered as a 2-dose schedule compared to the licensed 3-dose schedule: Results from a randomized study. *Human vaccines*, *7*(12), 1374-1386.
- 82 Schwarz, T. F., Huang, L. M., Medina, D. M. R., Valencia, A., Lin, T. Y., Behre, U., ... & Descamps, D. (2012). Four-year follow-up of the immunogenicity and safety of the HPV-16/18 AS04-adjuvanted vaccine when administered to adolescent girls aged 10–14 years. *Journal of Adolescent Health*, *50*(2), 187-194.
- 83 Drachenberg, K. J., Wheeler, A. W., Stuebner, P., & Horak, F. (2001). A well-tolerated grass pollen-specific allergy vaccine containing a novel adjuvant, monophosphoryl lipid A, reduces allergic symptoms after only four preseasonal injections. *Allergy*, *56*(6), 498-505.
- 84 Boland, G., Beran, J., Lievens, M., Sasadeusz, J., Dentico, P., Nothdurft, H., ... & Van Hattum, J. (2004). Safety and immunogenicity profile of an experimental hepatitis B vaccine adjuvanted with AS04. *Vaccine*, *23*(3), 316-320.
- 85 Thoelen, S., De Clercq, N., & Tornieporth, N. (2001). A prophylactic hepatitis B vaccine with a novel adjuvant system. *Vaccine*, *19*(17-19), 2400-2403.
- 86 Cervantes, J. L., Weinerman, B., Basole, C., & Salazar, J. C. (2012). TLR8: the forgotten relative revindicated. *Cellular & molecular immunology*, *9*(6), 434.
- 87 Lu, C. C., Kuo, H. C., Wang, F. S., Jou, M. H., Lee, K. C., & Chuang, J. H. (2014). Upregulation of TLRs and IL-6 as a marker in human colorectal cancer. *International journal of molecular sciences*, *16*(1), 159-177.
- 88 Scheiermann, J., & Klinman, D. M. (2014). Clinical evaluation of CpG oligonucleotides as adjuvants for vaccines targeting infectious diseases and cancer. *Vaccine*, *32*(48), 6377-6389.
- 89 Hanagata, N. (2017). CpG oligodeoxynucleotide nanomedicines for the prophylaxis or treatment of cancers, infectious diseases, and allergies. *International journal of nanomedicine*, *12*, 515.
- 90 Liu, L., Yong, K. T., Roy, I., Law, W. C., Ye, L., Liu, J., ... & Prasad, P. N. (2012). Bioconjugated pluronic triblock-copolymer micelle-encapsulated quantum dots for targeted imaging of cancer: in vitro and in vivo studies. *Theranostics*, *2*(7), 705.
- 91 Rehor, A., Hubbell, J. A., & Tirelli, N. (2005). Oxidation-sensitive polymeric nanoparticles. *Langmuir*, *21*(1), 411-417.
- 92 Velluto, D., Demurtas, D., & Hubbell, J. A. (2008). PEG-b-PPS diblock copolymer aggregates for hydrophobic drug solubilization and release: cyclosporin A as an example. *Molecular pharmaceutics*, *5*(4), 632-642.
- 93 Lutz, M. B., Kukutsch, N., Ogilvie, A. L., Röbner, S., Koch, F., Romani, N., & Schuler, G. (1999). An advanced culture method for generating large quantities of highly pure dendritic cells from mouse bone marrow. *Journal of immunological methods*, *223*(1), 77-92.
- 94 Han, H. D., Byeon, Y., Jang, J. H., Jeon, H. N., Kim, G. H., Kim, M. G., ... & Lee, Y. J. (2016). In vivo stepwise immunomodulation using chitosan nanoparticles as a platform nanotechnology for cancer immunotherapy. *Scientific reports*, *6*, 38348.
- 95 Hafner, A. M., Corthésy, B., Textor, M., & Merkle, H. P. (2016). Surface-assembled poly (I: C) on PEGylated PLGA microspheres as vaccine adjuvant: APC activation and bystander cell stimulation. *International journal of pharmaceutics*, *514*(1), 176-188.

- 96 Wu, C. Y., Yang, H. Y., Monie, A., Ma, B., Tsai, H. H., Wu, T. C., & Hung, C. F. (2011). Intraperitoneal administration of poly (I: C) with polyethylenimine leads to significant antitumor immunity against murine ovarian tumors. *Cancer Immunology, Immunotherapy*, 60(8), 1085-1096.
- 97 Velluto, D., Thomas, S. N., Simeoni, E., Swartz, M. A., & Hubbell, J. A. (2011). PEG-b-PPS-b-PEI micelles and PEG-b-PPS/PEG-b-PPS-b-PEI mixed micelles as non-viral vectors for plasmid DNA: tumor immunotoxicity in B16F10 melanoma. *Biomaterials*, 32(36), 9839-9847.
- 98 Vartak, A., & Sucheck, S. J. (2016). Recent advances in subunit vaccine carriers. *Vaccines*, 4(2), 12.
- 99 Pulendran, B., & Ahmed, R. (2011). Immunological mechanisms of vaccination. *Nature immunology*, 12(6), 509.
- 100 Petrovsky, N. (2015). Comparative safety of vaccine adjuvants: a summary of current evidence and future needs. *Drug safety*, 38(11), 1059-1074.
- 101 Lei, C., Liu, P., Chen, B., Mao, Y., Engelmann, H., Shin, Y., ... & Hellstrom, K. E. (2010). Local release of highly loaded antibodies from functionalized nanoporous support for cancer immunotherapy. *Journal of the American Chemical Society*, 132(20), 6906-6907.
- 102 Kuai, R., Ochyl, L. J., Bahjat, K. S., Schwendeman, A., & Moon, J. J. (2017). Designer vaccine nanodiscs for personalized cancer immunotherapy. *Nature materials*, 16(4), 489.
- 103 Zhang, Z., Tongchusak, S., Mizukami, Y., Kang, Y. J., Ioji, T., Touma, M., ... & Sasada, T. (2011). Induction of anti-tumor cytotoxic T cell responses through PLGA-nanoparticle mediated antigen delivery. *Biomaterials*, 32(14), 3666-3678.
- 104 Xu, Z., Ramishetti, S., Tseng, Y. C., Guo, S., Wang, Y., & Huang, L. (2013). Multifunctional nanoparticles co-delivering Trp2 peptide and CpG adjuvant induce potent cytotoxic T-lymphocyte response against melanoma and its lung metastasis. *Journal of Controlled Release*, 172(1), 259-265.
- 105 Ries, C. H., Cannarile, M. A., Hoves, S., Benz, J., Wartha, K., Runza, V., ... & Jones, T. (2014). Targeting tumor-associated macrophages with anti-CSF-1R antibody reveals a strategy for cancer therapy. *Cancer cell*, 25(6), 846-859.
- 106 REED, Steven G., ORR, Mark T., et FOX, Christopher B. Key roles of adjuvants in modern vaccines. *Nature medicine*, 2013, vol. 19, no 12, p. 1597.
- 107 Kasturi, S. P., Skountzou, I., Albrecht, R. A., Koutsonanos, D., Hua, T., Nakaya, H. I., ... & Villinger, F. (2011). Programming the magnitude and persistence of antibody responses with innate immunity. *Nature*, 470(7335), 543.
- 108 Fox, C. B., Sivananthan, S. J., Duthie, M. S., Vergara, J., Guderian, J. A., Moon, E., ... & Carter, D. (2014). A nanoliposome delivery system to synergistically trigger TLR4 AND TLR7. *Journal of nanobiotechnology*, 12(1), 17.
- 109 Abhyankar, M. M., Noor, Z., Tomai, M. A., Elvecrog, J., Fox, C. B., & Petri Jr, W. A. (2017). Nanoformulation of synergistic TLR ligands to enhance vaccination against *Entamoeba histolytica*. *Vaccine*, 35(6), 916-922.
- 110 Broggi, M. A., Schmalzer, M., Lagarde, N., & Rossi, S. W. (2014). Isolation of murine lymph node stromal cells. *Journal of visualized experiments: JoVE*, (90).
- 111 Dowling, D. J., Scott, E. A., Scheid, A., Bergelson, I., Joshi, S., Pietrasanta, C., ... & Kats, D. (2017). Toll-like receptor 8 agonist nanoparticles mimic immunomodulating effects of the live BCG vaccine and enhance neonatal innate and adaptive immune responses. *Journal of Allergy and Clinical Immunology*, 140(5), 1339-1350.
- 112 Tan, R. S., Ho, B., Leung, B. P., & Ding, J. L. (2014). TLR cross-talk confers specificity to innate immunity. *International reviews of immunology*, 33(6), 443-453.
- 113 Ouyang, W., Rutz, S., Crellin, N. K., Valdez, P. A., & Hymowitz, S. G. (2011). Regulation and functions of the IL-10 family of cytokines in inflammation and disease. *Annual review of immunology*, 29, 71-109.

- 114 Wilbers, R. H., Van Raaij, D. R., Westerhof, L. B., Bakker, J., Smant, G., & Schots, A. (2017). Re-evaluation of IL-10 signaling reveals novel insights on the contribution of the intracellular domain of the IL-10R2 chain. *Plos One*, 12(10), e0186317.
- 115 Smith, L. K., Boukhaled, G. M., Condotta, S. A., Mazouz, S., Guthmiller, J. J., Vijay, R., ... & Richer, M. J. (2018). Interleukin-10 Directly Inhibits CD8⁺ T Cell Function by Enhancing N-Glycan Branching to Decrease Antigen Sensitivity. *Immunity*, 48(2), 299-312.
- 116 Cox, M. A., Kahan, S. M., & Zajac, A. J. (2013). Anti-viral CD8 T cells and the cytokines that they love. *Virology*, 435(1), 157-169.
- 117 Trinchieri, G. (2007). Interleukin-10 production by effector T cells: Th1 cells show self control. *Journal of Experimental Medicine*, 204(2), 239-243.
- 118 Kabelitz, D. (2007). Expression and function of Toll-like receptors in T lymphocytes. *Current opinion in immunology*, 19(1), 39-45.
- 119 Kahan, S. M., Bakshi, R. K., Luther, R., Harrington, L. E., Hendrickson, R. C., Lefkowitz, E. J., ... & Zajac, A. J. (2017). IL-2 producing and non-producing effector CD8 T cells phenotypically and transcriptionally coalesce to form memory subsets with similar protective properties.
- 120 Shiao, S. L., & Coussens, L. M. (2010). The tumor-immune microenvironment and response to radiation therapy. *Journal of mammary gland biology and neoplasia*, 15(4), 411-421.
- 121 Friedman, E. J.. 2002. Immune modulation by ionizing radiation and its implications for cancer immunotherapy. *Curr. Pharm. Design* 8: 1765-1780
- 122 Trowell, O. A. (1952). The sensitivity of lymphocytes to ionising radiation. *The Journal of Pathology*, 64(4), 687-704.
- 123 Ciernik, I. F., Romero, P., Berzofsky, J. A., & Carbone, D. P. (1999). Ionizing radiation enhances immunogenicity of cells expressing a tumor-specific T-cell epitope. *International Journal of Radiation Oncology• Biology• Physics*, 45(3), 735-741.
- 124 Filatenkov, A., Baker, J., Mueller, A. M., Kenkel, J., Ahn, G. O., Dutt, S., ... & Shizuru, J. A. (2015). Ablative tumor radiation can change the tumor immune cell microenvironment to induce durable complete remissions. *Clinical Cancer Research*, 21(16), 3727-3739.
- 125 Lugade, A. A., Moran, J. P., Gerber, S. A., Rose, R. C., Frelinger, J. G., & Lord, E. M. (2005). Local radiation therapy of B16 melanoma tumors increases the generation of tumor antigen-specific effector cells that traffic to the tumor. *The Journal of Immunology*, 174(12), 7516-7523.
- 126 Dewan, M. Z., Galloway, A. E., Kawashima, N., Dewyngaert, J. K., Babb, J. S., Formenti, S. C., & Demaria, S. (2009). Fractionated but not single-dose radiotherapy induces an immune-mediated abscopal effect when combined with anti-CTLA-4 antibody. *Clinical Cancer Research*, 15(17), 5379-5388.
- 127 Gerber, S. A., Sedlacek, A. L., Cron, K. R., Murphy, S. P., Frelinger, J. G., & Lord, E. M. (2013). IFN- γ mediates the antitumor effects of radiation therapy in a murine colon tumor. *The American journal of pathology*, 182(6), 2345-2354.
- 128 Lugade, A. A., Sorensen, E. W., Gerber, S. A., Moran, J. P., Frelinger, J. G., & Lord, E. M. (2008). Radiation-induced IFN- γ production within the tumor microenvironment influences antitumor immunity. *The Journal of Immunology*, 180(5), 3132-3139.
- 129 Finkelstein, S. E., Rodriguez, F., Dunn, M., Farmello, M. J., Smilee, R., Janssen, W., ... & Torres-Roca, J. F. (2012). Serial assessment of lymphocytes and apoptosis in the prostate during coordinated intraprostatic dendritic cell injection and radiotherapy. *Immunotherapy*, 4(4), 373-382.
- 130 Finkelstein, S. E., Iclozan, C., Bui, M. M., Cotter, M. J., Ramakrishnan, R., Ahmed, J., ... & Berman, C. (2012). Combination of external beam radiotherapy (EBRT) with intratumoral injection of dendritic cells as neo-adjuvant treatment of high-risk soft tissue sarcoma patients. *International Journal of Radiation Oncology• Biology• Physics*, 82(2), 924-932.

- 131 Chi, K. H., Liu, S. J., Li, C. P., Kuo, H. P., Wang, Y. S., Chao, Y., & Hsieh, S. L. (2005). Combination of conformal radiotherapy and intratumoral injection of adoptive dendritic cell immunotherapy in refractory hepatoma. *Journal of immunotherapy*, 28(2), 129-135.
- 132 Brody, J. D., Ai, W. Z., Czerwinski, D. K., Torchia, J. A., Levy, M., Advani, R. H., ... & Wapnir, I. (2010). In situ vaccination with a TLR9 agonist induces systemic lymphoma regression: a phase I/II study. *Journal of clinical oncology*, 28(28), 4324.
- 133 Kim, Y. H., Gratzinger, D., Harrison, C., Brody, J. D., Czerwinski, D. K., Ai, W. Z., ... & Tibshirani, R. J. (2012). In situ vaccination against mycosis fungoides by intratumoral injection of a TLR9 agonist combined with radiation: a phase 1/2 study. *Blood*, 119(2), 355-363.
- 134 Mognol, G. P., Spreafico, R., Wong, V., Scott-Browne, J. P., Togher, S., Hoffmann, A., ... & Trifari, S. (2017). Exhaustion-associated regulatory regions in CD8+ tumor-infiltrating T cells. *Proceedings of the National Academy of Sciences*, 114(13), E2776-E2785.
- 135 Jiang, Y., Li, Y., & Zhu, B. (2015). T-cell exhaustion in the tumor microenvironment. *Cell death & disease*, 6(6), e1792.
- 136 Liao, W., Lin, J. X., & Leonard, W. J. (2013). Interleukin-2 at the crossroads of effector responses, tolerance, and immunotherapy. *Immunity*, 38(1), 13-25.
- 137 Takeuchi, A., & Saito, T. (2017). CD4 CTL, a cytotoxic subset of CD4+ T cells, their differentiation and function. *Frontiers in immunology*, 8, 194.
- 138 Janas, M. L., Groves, P., Kienzle, N., & Kelso, A. (2005). IL-2 regulates perforin and granzyme gene expression in CD8+ T cells independently of its effects on survival and proliferation. *The Journal of Immunology*, 175(12), 8003-8010.
- 139 Kajino, K., Nakamura, I., Bamba, H., Sawai, T., & Ogasawara, K. (2007). Involvement of IL-10 in exhaustion of myeloid dendritic cells and rescue by CD40 stimulation. *Immunology*, 120(1), 28-37.
- 140 Diamond, M. S., Kinder, M., Matsushita, H., Mashayekhi, M., Dunn, G. P., Archambault, J. M., ... & Murphy, K. M. (2011). Type I interferon is selectively required by dendritic cells for immune rejection of tumors. *Journal of Experimental Medicine*, jem-20101158.
- 141 Herrera, F. G., Bourhis, J., & Coukos, G. (2017). Radiotherapy combination opportunities leveraging immunity for the next oncology practice. *CA: a cancer journal for clinicians*, 67(1), 65-85.
- 142 Neller, M. A., López, J. A., & Schmidt, C. W. (2008, October). Antigens for cancer immunotherapy. In *Seminars in immunology* (Vol. 20, No. 5, pp. 286-295). Academic Press.

Curriculum Vitae

Sylvie Hauert

2040 Rownham Hill Road
60451 New Lenox, IL, USA
+1 773 358 0838

20/02/1989
Swiss
sylvie.hauert@gmail.com

Education

- 2014 – Present **Ecole Polytechnique Fédérale de Lausanne (EPFL)**
PhD in Chemistry and chemical Engineering
Research area in cancer vaccines and nanoparticles
- 2012 – 2013 **Ecole Polytechnique Fédérale de Lausanne (EPFL)**
Master of Science MSc in molecular and biological chemistry
Project: “Hyaluronic acid decorated nanoparticle targeting lymphatic endothelium cells”
- 2013 Laboratory project (EPFL, 2 d/week)
“Generation of photoswitchable peptides ligand by phage display”
- 2009 – 2012 Bachelor of Science BSc in chemistry and chemical engineering
- 2004 – 2008 **Lycée Denis-de-Rougemont, Neuchâtel**
Scientific Baccalaureat, specific option: Biology - Chemistry
Bilingual maturity English - French

Teaching experience

- 2016 Master Project Supervisor, Chemistry and Chemical Engineering, EPFL
- 2014 – 2016 Teaching Assistant for Biochemistry course (BSc) in Life Sciences and Technology, EPFL
- 2014 – 2016 Teaching Assistant for Biomaterial course (MSc) in Life Science and Technology, EPFL
- 2015 – 2016 High School outreach: Immersion in Science
- 2008 – 2016 Ice Skating Coach (Neuchâtel, 4 h/week)

Publications

Vaccine nanocarriers: Coupling intracellular pathways and cellular biodistribution to control CD4 vs CD8 T cell responses. Rincon-Restrepo M.¹, Mayer A.¹, **Hauert S.**, Bonner D. K., Phelps E. A., Hubbell J. A., Swartz M. A., Hirose S.

Tumor lymphangiogenesis promotes T cell infiltration and potentiates immunotherapy in melanoma. Fankhauser M., Broggi M. A. S., Potin L., Bordry N., Jeanbart L., Lund A., Da Costa E., **Hauert S.**, Rincon-Restrepo M., Tremblay C., Cabello E., Homicsko K., Michielin O., Hanahan D., Speiser D. E., Swartz M. A.

Nanoparticle conjugation of human papillomavirus 16 E7-long peptides enhances therapeutic vaccination efficacy against well-established solid tumors in mice. Galliverti G., Tichet M., Domingos-Pereira S., **Hauert S.**, Nardelli-Haeffliger D., Swartz M. A., Wullschleger S. *In preparation*

Skills

Immunology Techniques :	Flow cytometry, ELISA, Primary cell isolation, <i>in vitro</i> cultures
Molecular biology :	RNA extraction, cDNA synthesis, RT-PCR, western blot, protein and DNA electrophoresis
Mouse <i>in vivo</i> techniques :	Anesthesia, intraperitoneal and intradermal injections, immunization, tumor inoculation, localize irradiation
Chemistry :	Strong synthesis understanding and background
Programming language :	C, Matlab
Software:	Microsoft Office, ChemDraw, Adobe Illustrator, GraphPad Prism, FlowJo

Language

French :	Mother tongue
English :	Second mother tongue Obtention of the First Certificate in English (FCE) in 2007
German :	High school understanding

Interests

Traveling, discover new cultures and plays all types of sports.